Control Flow Graphs for Real-Time System Analysis

Reconstruction from Binary Executables and Usage in ILP-Based Path Analysis

Dissertation

Zur Erlangung des Grades
Doktor der Ingenieurwissenschaften
(Dr.-Ing.)
der Naturwissenschaftlich-Technischen Fakultät I
der Universität des Saarlandes

von
Diplominformatiker
Henrik Theiling
aus Saarbrücken

Saarbrücken 2002

Tag des Kolloquiums:	4. Februar 2003
Dekan:	Prof. Dr.-Ing. Philipp Slusallek
Vorsitzender:	Prof. Dr.-Ing. Gerhard Weikum
Gutachter:	Prof. Dr. Reinhard Wilhelm
	Prof. Dr. Harald Ganzinger
als Vertretung im Kolloquium:	Prof. Dr. Andreas Podelski
Beisitzer:	Dr.-Ing. Ralf Schenkel

Abstract

Real-time systems have to complete their actions w.r.t. given timing constraints. In order to validate that these constraints are met, static timing analysis is usually performed to compute an upper bound of the worst-case execution times (WCET) of all the involved tasks.

This thesis identifies the requirements of real-time system analysis on the *control flow graph* that the static analyses work on. A novel approach is presented that extracts a control flow graph from binary executables, which are typically used when performing WCET analysis of real-time systems.

Timing analysis can be split into two steps: a) the analysis of the behaviour of the hardware components, b) finding the worst-case path. A novel approach to path analysis is described in this thesis that introduces sophisticated interprocedural analysis techniques that were not available before.

Zusammenfassung

Echtzeitsysteme müssen ihre Aufgaben innerhalb vorgegebener Zeitschranken abwickeln. Um die Einhaltung der Zeitschranken zu überprüfen, sind für gewöhnlich statische Analysen der schlimmsten Ausführzeiten der Teilprogramme des Echtzeitsystems nötig.

Diese Arbeit stellt die Anforderungen von Echtzeitsystem an den *Kontrollflußgraphen* vor, auf dem die statischen Analysen arbeiten. Ein neuartiger Ansatz zur Rückberechnung von Kontrollflußgraphen aus Maschinenprogrammen, die häufig die Grundlage der WCET-Analyse von Echtzeitsystemen bilden, wird vorgestellt.

WCET-Analysen können in zwei Teile zerlegt werden: a) die Analyse des Verhaltens der Hardwarebausteine, b) die Suche nach dem schlimmsten Ausführpfad. In dieser Arbeit wird ein neuartiger Ansatz der Pfadanalyse vorgestellt, der für ausgefeilte interprozedurale Analysemethoden ausgelegt ist, die vorher hier nicht verfügbar waren.

Extended Abstract

Real-time systems are computer systems that have to perform their actions with fulfilment of timing constraints. Additional to performing the actions correctly, their correctness also depends on the fulfilments of these timing constraints.

The validation of timing aspects is called a *schedulability analysis*. A real-time system often consists of many tasks. Existing techniques for schedulability analysis require that the worst-case execution time (WCET) of each task is known.

Since the real WCET of a program is in general not computable, an upper bound to the real WCET has to be computed instead. For real-time systems, these WCET predictions must be *safe*, i. e., the real WCET must never be underestimated. On the other hand, to increase the probability of a successful schedulability analysis, the predictions should be as *precise* as possible.

Most static analyses, including approaches to WCET analysis, examine the control flow of the program. Because the behaviour of the program is typically not known in advance, an approximation to the control flow is used as the basis of the analysis. This approximation is called a *control flow graph*.

For good performance, modern real-time systems use modern hardware architectures. These use heuristic components, like caches and pipelines, to speed up the program in typical situations. Neglecting these speed up factors in a WCET analysis would lead to a dramatic overestimation of the real WCET of the program.

For taking into account hardware components, the program usually has to be analysed at the hardware level. Therefore, *binary executables* are the bases of analyses. Further, the timing behaviour of typical modern hardware depends on the data that is processed, and in particular on the addresses that are used to access memory. Again, full information about addresses is available from binary executables.

The first part of this work presents a novel approach to extracting control flow graphs from binary executables. The general task is non-trivial, since often, the possible control flow is not obvious, e. g., when function pointers, switch tables or dynamic dispatch come into play. Further, it is often hard to predict what is the influence of a certain machine instruction on control flow, e. g., because its usage is ambiguous.

The reconstruction algorithms presented in this work are designed with real-time systems in mind. The requirements for a safe analysis also have to be considered during the extraction of control flow graphs from binaries, since analyses can only be safe if the underlying data structure is safe, too.

The reconstruction of control flow graphs from binary executables will be conceptually split into two separate tasks: a) given a stream of bytes from a binary executable and the address in the processor's code pointer, the precise classification of the instruction that will be executed by the machine, b) given a set of instruction classifications and possible program start nodes, the automatic composition of a safe and precise control flow graph.

For solving the first task, we will use very efficient *decision trees* to convert raw bytes into instruction classifications. An algorithm will be presented that computes the decision trees automatically from very concise specifications that can trivially be derived from the vendor's architecture documentation. This is a novel approach that extricates the user from error-prone programming that had to be done in the past.

For the reconstruction of control flow from a set of instruction classifications, a *bottom-up approach* will be presented. This algorithm overcomes problems that top-down approaches usually have. Top-down approaches are fine for producing disassembly listings and for debugging purposes, but static analysis poses additional requirements on safety and precision that top-down algorithms cannot fulfil. Our bottom-up approach meets these requirements. Furthermore, it is implemented very efficiently.

The second part of this work deals with the analysis of real-time systems itself. Timing analysis that is close to hardware can be split into two parts: a) the analysis of the behaviour of the components at all blocks of the program and b) the computation of a global upper bound for the WCET based on the results of the analysis of each block. The latter analysis is called the *path analysis*.

An established technique of path analysis uses Integer Linear Programming (ILP). The idea is as follows: the program's control flow is described by a set of constraints, and the execution times of the program's blocks are combined in an objective function. The task of finding an upper bound of the WCET of the whole program is solved by maximising the objective function under consideration of the control flow constraints.

Because of the complex behaviour of modern hardware, sophisticated techniques for WCET analysis must typically be used. For instance, routine invocations in the program should not be analysed in isolation, since their timing behaviour may be very different from invocation to invocation. This is because the state of the machine's hardware components is typically very different for each invocation and this state influences performance a lot.

For this reason, analyses usually perform better when they consider routine invocations in different execution *contexts*, where the contexts depend on the history of the program execution.

To make use of contexts, both parts of WCET analysis, the analysis of the hardware components and the path analysis must handle them. Up to now, it was not examined how path analysis can be done with arbitrary static assignment of execution contexts. This work will close this gap by presenting a new approach to ILP-based path analysis that can handle contexts, providing a high degree of flexibility to the user of the WCET analysis tool.

All algorithms presented in this thesis are implemented in tools that are now widely used in educational as well as industrial applications.

Ausführliche Zusammenfassung

Echtzeitsysteme sind Computersysteme, die ihre Aufgaben innerhalb vorgegebener Zeitschranken erfüllen müssen. Zu ihre Korrektheit gehört zusätzlich zur funktionalen Korrektheit die Einhaltung dieser Zeitschranken.

Die Überprüfung des korrekten Zeitverhaltens nennt man *Planbarkeitsanalyse* (engl.: *schedulability analysis*). Ein Echtzeitsystem besteht häufig aus mehreren Teilprogrammen. In allen bekannten Ansätzen zur Planbarkeitsanalyse wird vorrausgesetzt, daß die schlimmste Ausführzeit (WCET, von engl. *worst-case execution time*) jedes einzelnen Teilprogramms bekannt ist.

Da die wirkliche Maximallaufzeit eines Programmes im allgemeinen nicht berechenbar ist, wird stattdessen eine obere Schranke berechnet. Bei Echtzeitsystemen müssen diese Vorhersagen *sicher* sein, d. h. die wirkliche Maximallaufzeit des Programmes darf niemals unterschätzt werden. Weiterhin sollten die Vorhersagen möglichst *genau* sein, um die Wahrscheinlichkeit einer erfolgreichen Planbarkeitsanalyse zu erhöhen.

Die meisten statischen Analysen, die WCET-Analyse eingeschlossen, untersuchen den Kontrollfluß eines Programmes. Da aber das Verhalten normalerweise vor Ablauf des Programms nicht bekannt ist, müssen Analysen mit einer Annäherung an den Kontrollfluß vorliebnehmen. Diese Annäherung nennt man *Kontrollflußgraph*.

Heutige Echtzeitsystem benutzen moderne Hardware, um deren Leistungsvorteile auszunutzen. Die Architekturen benutzen häufig heuristische Bausteine, wie Caches oder Pipelines, die die Ausführungsgeschwindigkeit des Programmes in häufig vorkommenden Situationen erhöhen sollen. Um starke Überschätzungen der Laufzeit zu vermeiden, muß eine WCET-Analyse typischerweise das Verhalten dieser Bausteine mitberücksichtigen.

Zur Vorhersage des Verhaltens von Hardwarebausteinen ist es normalerweise erforderlich, das Programm hardwarenah zu analysieren. Daher benutzt man für die Analyse das *Maschinenprogramm*. Die Ausführgeschwindigkeit hängt auch von den verarbeiteten Daten ab, vor allem von den Adressen, die zum Zugriff auf den Speicher benutzt werden. Auch aus diesem Grund verwendet man Maschinenprogramme, denn die nötigen Informationen sind dort vorhanden.

Im ersten Teil dieser Arbeit wird ein neuartiger Ansatz zur Rückberechnung von Kontrollflußgraphen aus Maschinenprogrammen vorgestellt. Die allgemeine Aufgabe ist schwierig, denn oft ist der mögliche Kontrollfluß nicht offensichtlich, z. B. bei der Verwendung von Funktionszeigern, switch-Tabellen oder dynamischen Methodenaufrufen. Desweiteren ist es häufig schwierig, vorherzusagen, welchen Einfluß bestimmte Befehlen auf den Kontrollfluß haben, da diese mitunter in verschiedenen Situationen auftauchen.

Der in dieser Arbeit vorgestellte Algorithmus zur Rückberechnung von Kontrollflußgraphen wurde unter besonderer Beachtung der speziellen Anforderungen von Echtzeitsystemanalyse entwickelt, denn ohne eine sichere Rückberechnung von Kontrollflußgraphen können darauf arbeitende Analysen ebenfalls nicht sicher sein.

Die Rückberechnung läßt sich in zwei Phasen zerlegen: a) die Erstellung einer Klassifizierung eines Maschinenbefehls bei Eingabe eines Byte-Stroms und der Adresse des Befehls, b) die automatische Rückberechnung eines sicheren und genauen Kontrollflußgraphen bei Eingabe einer Menge von Befehlsklassifikationen.

Um die erste Aufgabe zu lösen, werde ich einen sehr effizienten *Entscheidungsbaum* vorstellen, mit dessen Hilfe sich eine Folge roher Bytes in eine Befehlsklassifikation umwandeln läßt. Ein Algorithmus zur automatischen Berechnung eines solchen Entscheidungsbaums wird vorgestellt werden, der als Eingabe einzig eine Spezifikation erhält, die sich leicht aus der Architekturbeschreibung des Herstellers erstellen läßt. Dieser Ansatz befreit den Benutzer von fehlerträchtiger Programmierarbeit, die bisher nötig war.

Zur Rückberechnung eines Kontrollflußgraphen aus einer Menge von Befehlsklassifikationen wird ein *Bottom-Up-Ansatz* vorgestellt werden. Dieser überwindet Probleme von Top-Down-Ansätzen, die sich zwar gut zum Programmieren von Disassemblern oder Debuggern eignen, aber keineswegs den Anforderungen von Echtzeitsystemen gerecht werden. Unser Bottom-Up-Ansatz hingegen wird diesen gerecht und ist zudem sehr effizient implementiert.

Der zweite Teil dieser Arbeit behandelt die Analyse von Echtzeitsystemen selbst. Hardwarenahe WCET-Analyse kann man in zwei Teile aufspalten: a) die Analyse des Verhaltens der Hardwarebausteine für jeden Block des Programmes, b) die Berechnung einer oberen Schranke der WCET des Programms basierend auf den Ergebnissen der Analyse in a). b) nennt man *Pfadanalyse*.

Eine verbreitete Methode der Pfadanalyse benutzt Ganzzahlige Lineare Programmierung (ILP von engl. *Integer Linear Programming*). Die Idee dabei ist, daß man den Kontrollfluß des Programmes durch Nebenbedingungen beschreibt und die Laufzeiten der einzelnen Blöcke des Programmes in einer Zielfunktion zusammenfaßt. Das Maximierungsproblem der Zielfunktion unter Beachtung der Nebenbedingungen löst dann das Problem der Suche nach einer oberen Schranke für die Maximallaufzeit des Programmes.

Weil moderne Hardware sich komplex verhält, müssen normalerweise ausgefeilte Methoden zur WCET-Analyse verwendet werden. Beispielsweise sollten Routinenaufrufe nicht isoliert behandelt werden, da sich ihr Verhalten von Aufruf zu Aufruf stark unterscheiden kann. Das liegt daran, daß der Zustand der Hardwarebausteine die Ausführzeiten stark beeinflussen.

Aus diesem Grunde verbessert man die Vorhersagen für gewöhnlich, indem man Routinenaufrufe in verschiedenen *Kontexten* analysiert, wobei die Kontexte davon abhängen, was im Programm vorher schon ausgeführt wurde.

Um von Kontexten Gebrauch zu machen, müssen beide Teile der WCET-Analyse, die der Bausteine und die Pfadanalyse, sie verarbeiten können. Bisher war es nicht untersucht, wie man auf ILP beruhende Pfadanalysen mit beliebigen statisch berechneten Kontextzuweisungen durchführen kann. Diese Arbeit schließt diese Lücke und stellt einen Ansatz vor, der dem Benutzer des Analysewerkzeugs einen hohen Grad an Freiheit überläßt.

Alle in dieser Arbeit vorgestellten Algorithmen sind in Werkzeugen implementiert, die inzwischen in universitärem wie industriellem Gebrauch sind.

Acknowledgements

First of all, I very much thank Reinhard Wilhelm for letting me have the opportunity to work and research at his chair and to write my thesis about this challenging and interesting topic. He was very helpful in discussions about this work and provided me with a lot of freedom for approaching my goals.

The research group provided a very pleasant working atmosphere. I would like to thank Michael Schmidt for our good team work with discussions about interfaces, implementation and algorithms. We implemented parts of the overall WCET framework together and Michael also contributed by writing some modules for exec2crl. Thanks are also due to Florian Martin and Christian Ferdinand for fruitfully discussing a lot of different topics with me. They often found peculiarities and had many hints and ideas. Thanks to Reinhold Heckmann for providing helpful thoughts and links to other peoples' research from most different areas of computer science. He was also a great help for me by proof-reading this thesis.

For excellent team work and discussions, I also thank Daniel Kästner, Marc Langenbach and Martin Sicks. Nico Fritz did a magnificent job implementing the ARM decoder module for exec2crl, despite his being a complete novice to its internal structure when he began.

During international conferences and other occasions, the whole real-time community constituted a nice atmosphere. Most notably, I had a lot of discussions with Sheayun Lee, Sungsoo Lim, Jan Gustafsson, Jakob Engblom and Andreas Ermedahl.

Thanks to Uta Hengst, Björn Huke, Daniel Kästner, Markus Löckelt and Nicola Wolpert for proof-reading parts of this work and giving valuable hints.

Last but not least, I would like to thank my family for their support during the time of my research and also Uta Hengst and Florian Martin for continuously reminding me to work hard.

Contents

Part I

Introduction

Chapter 1
Introduction

1.1 Timing Analysis of Real-Time Systems

The fundamental characteristic of real-time systems is that they are subject to timing constraints that determine when actions have to be taken. The fulfilment of these timing constraints, additional to the operational results, is part of the correctness of a real-time system.

In literature, real-time systems are usually divided into two types: hard and soft real-time systems, depending on whether their timing constraints are imperative or desirable. If not explicitly stated otherwise, the term *real-time system* will be used for a hard real-time system in this work. The imperative nature of the timing constraints makes static analysis particularly interesting for real-time system validation.

Real-time systems occur in many areas, e. g. in process control, nuclear power plants, avionics, air traffic control, medical devices, defence applications and controllers in automobiles.

A failure of a safety critical real-time system can lead to considerable damage or even a loss of lives. Therefore, the system must be validated. Among other properties, it has to be shown that it fulfils all its timing constraints. The validation of timing aspects is called a *schedulability analysis* (*see* [Liu and Layland., 1973; Stankovic, 1996]).

A real-time system is often composed of many tasks. All existing techniques for schedulability analysis require the worst-case execution time (WCET) of each task in the system to be known.

Since the exact WCET is in general not computable, estimations of the WCET have to be calculated. These estimations have to be *safe*, meaning they must never underestimate the actual WCET.

On the other hand, the WCET approximation should be *tight*, i. e., the overestimation should be as small as possible. This helps to reduce the costs for the hardware and increases the chances of a successful timing validation.

For simple hardware, i. e. for a processor with a fixed execution time for each instruction, estimation of the WCET is quite easy: if each instruction's execution time is known, the WCET can be computed by recursively combining execution times along the syntax tree of the program. This method was used in [Puschner and Koza, 1989] and in [Park and Shaw, 1991].

Modern hardware, however, becomes increasingly difficult to predict due to sophisticated heuristic components that increase execution speed of instructions for common special cases, which most likely make programs much faster on average, while single instructions may still be slow. This means that simple, conservative analysis techniques strongly overestimate the actual WCET.

The execution time of an instruction may depend on the internal state of the processor. This state gets more and more complex with the presence of the mentioned heuristic components. Therefore, predicting the relevant parts of the processor's internal state that influence the timing behaviour becomes more and more difficult. The following list shows some components of modern hardware that make predictions complicated.

Pipelines. Processing of a single instruction is usually split into several steps in a microprocessor: e. g., instruction fetch, instruction decode, compute, write-back, etc.. For one instruction, only one of these steps is used at the same time. Therefore, the idea is to use free components for other instructions in parallel.

This leads to *overlapping execution of instructions*, so-called *pipelining*. And because there might be dependencies between the instructions (e. g., a computed value is needed by a subsequent instruction), this means that interaction can occur between instructions that are executed after one another.

Caches. *Caches*, i. e. fast memory with limited size between the processor and the main memory of the computer, make execution times depend on execution history, because the access time of a cache depends on what was accessed before.

The degree of predictability of caches depends on various aspects, e. g. on the type of data stored in the cache (instructions or data, or even mixed) and on the cache design, in particular the cache replacement policy.

Speculative execution. To keep the pipeline filled at branches in the program, modern processors often implement a *branch prediction*, i. e. a heuristics to predict what is executed after a conditional branch when the condition is not yet known. These processors then speculatively fetch instructions from memory, which are discarded if the prediction is found to having been wrong. This mechanism often influences the cache behaviour in most complex ways.

The above list is not exhaustive.

Instructions not only interact with adjacent instructions w.r.t. their execution times, but also with very distant instructions in the program and even with themselves during subsequent executions. Additionally, the execution time depends on the input data for the instructions. Therefore, a simple method of recursively composing the run-time is usually not feasible for modern architectures.

1.2 Control Flow Graphs

Most static analyses work along the control flow of a program. The abstract concept of control flow has to be approximated by a data structure for analysis. One common structure is a *control flow graph*. In the following, the more precise term *interprocedural control flow graph* (ICFG) will be used. (The difference will be formally introduced later.)

Usually, the actual control flow is not fully known in general due to complex control transfers (e. g. computed branches, function pointers, dynamic dispatch, etc.). The more precise the approximating ICFG is, the more precise the analysis will be. Most importantly for real-time systems, it is vital that the approximating ICFG is *safe* under all circumstances.

Work about static analysis usually comes with the assumption that an ICFG is available. Even if it is, we must guarantee that the approximation is safe.

In order to estimate the WCET of a program, the analysis has to take the timing semantics of all hardware components into account. For this, it is vital on modern architectures to take all parts of hardware into account. Therefore, an analysis must typically consider the *machine code level*.

Further, for predicting their precise behaviour, all aspects that lead to different timing behaviour in any involved hardware component must be known. Any higher level than machine code might lack vital information. E. g., assembly code lacks information about addresses. Similarly, even compiled object files containing machine code sections lack the information about absolute location in memory, making predictions of memory accesses impossible. For these reasons, our framework performs WCET analysis on *statically linked binary executables*.

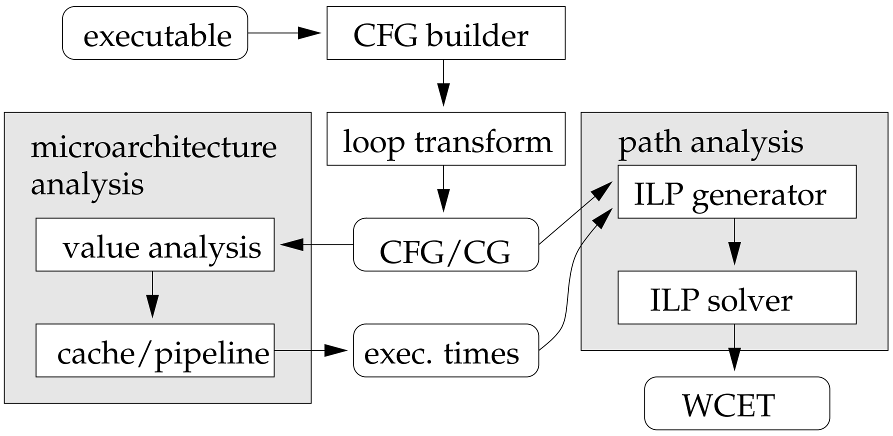

Figure 1.1: WCET Framework

Dealing with binary executables, the question arises whether an ICFG is really available and whether this ICFG is really safe. Compilers often generate debug code containing information about the ICFG of the program. Unfortunately, though, one usually cannot always assume that this information is correct. Due to code optimisations the compiler may have performed, the hints about the ICFG often only correspond vaguely with reality.

It is even more unfortunate that executables for real-time systems most likely have no debug information at all, at least not for all parts, since *hand-written assembly code* is often included. E. g., hand-written assembly code can certainly be found in the real-time operating system, which is part of the statically linked executable.

In this work, an approach to a safe and precise ICFG reconstruction for real-time system analysis will be presented. The reconstruction problem will be discussed in detail in Chapter 4.

1.3 Path Analysis

Our analysis framework for predicting the worst-case execution time (WCET) of binary executables for real-time systems is depicted in Figure 1.1. A WCET analysis can be split into two basic steps.

The first step is the *microarchitecture analysis*. The result of the first step is a worst-case execution time for each basic block of the program under examination.

The microarchitecture analysis consists of a chain of sub-analyses for different parts of the hardware, like value analysis (to find values of registers, in particular addresses for memory access), cache, pipeline and memory bus analyses. In our framework, all these analyses are implemented with the PAG tool (*see* [Martin, 1995b; Martin, 1999b]), that uses Abstract Interpretation (AI) (*see* [Cousot and Cousot, 1977a; Nielson et al., 1999]) for analysis.

The second step of a WCET analysis is the worst-case path analysis. Based on the results of the microarchitecture analysis, it computes an upper bound of the actual WCET. We will call this the *predicted WCET* in the following.

Path analyses can be implemented in several ways. Because of good precision and speed, we use Implicit Path Enumeration (IPE) (*see* [Li et al., 1995a; Li et al., 1996]), which uses Integer Linear Programming (ILP) (*see* [Chvátal, 1983]) to find the WCET. In this approach, the ICFG of the program is represented by a set of linear constraints. Further, the objective function contains the execution time of each block of the program. Then, finding the predicted WCET is the problem of maximising the objective function. Chapter 7 will introduce this technique in detail.

Due to important deviation in whether routines are executed in isolation or in contexts, routine invocations can be distinguished by their execution history, e. g., by their *call stacks* as distinctive features. These distinctions are called execution *contexts*. The precise methods of assigning contexts will be introduced in Chapter 3 and Chapter 8.

To make use of contexts, the original ICFG is transformed into one where nodes are split according to their distinctive contexts. The resulting graph, the *ICFG with contexts*, is then used for analysis instead of the original graph without contexts.

Our work group's PAG tool for writing analyses using Abstract Interpretation comes with interprocedural analysis methods, so ICFGs with contexts are can be used directly by the microarchitecture analysis chain.

Up to now, ILP-based path analysis was not well adapted to interprocedural analysis methods. It was shown in previous work (*see* [Theiling et al., 2000]) that it is possible in principle to combine microarchitecture analysis by Abstract Interpretation with path analysis by IPE. However, ways of using arbitrary methods of context computation were still unexamined. Chapter 8 proposes a general method of combining interprocedural analysis methods with ILP-based path analysis.

The task is non-trivial. ILP-based path analysis generates an *objective function* and some sets of constraints of the following types:

Entry constraints. These state that the program entry is executed once.

Structural constraints. These describe incoming and outgoing control flow at each basic block.[1]

[1] A basic block is a sequence of instructions in which control flow enters only at the beginning and leaves at the end with no possibility of branching except at the end.

Loop bound constraints. Each loop needs a maximal iteration count to make the ILP bounded. For good precision of analysis of loops, context distinction is desirable for different iterations. This is made possible by transforming loops into tail recursive functions, so that interprocedural analysis methods become applicable.

User defined additional constraints. To improve precision by adding facts the user knows to the set of constraints.

Most of these constraints can be generated in a straight-forward way even for graphs with contexts. However, recursion poses a problem, since the presence of contexts restructures the analysis graphs w.r.t. the structure of cycles: entry and back edges of cycles in the original graph are not necessarily entry and back edges of cycles in the graph with context. Hence, a correspondence has to be found.

Chapter 8 will present how interprocedural analysis methods can be used for ILP-based path analysis, dealing with the trade-off between analysis precision and speed. On the one hand, high precision by using many contexts is desired, but one the other hand, a distinction by the whole execution history is usually too expensive. For best results, context computation should be as flexible as possible and should be limitable and adjustable for different programs under examination. Therefore, we will outline an algorithm for generating constraints, especially loop bound constraints, for ILP-based path analyses with arbitrary static context computations.

1.4 Scope of this Thesis

We needed ICFGs in a framework for WCET analysis for real-time systems.[2]

In this thesis, I focus on the problem of constructing ICFGs for that WCET analysis framework. I will identify the requirements for real-time systems and present safe, precise and also fast algorithms.

Further, I introduce a novel approach to interprocedural path analysis. Among other things, this will show that the reconstructed ICFGs are perfectly suited for WCET analysis for real-time systems.

Consequently, this document is split into two major parts:

1. The design and implementation of novel algorithms for ICFG reconstruction will be presented in the first part. The modular and versatile tool exec2crl is the result.

[2]Our work group was partially supported by the research project *Transferbereich 14, Runtime Guarantees for Modern Architectures by Abstract Interpretation*, 1999–2001, of Deutsche Forschungsgemeinschaft.

2. A new approach to interprocedural path analysis will be introduced in the second part. The approach is much more generic than previous work.

The following list is a detailed overview of the structure of this work.

Part 1 contains chapters that introduce basic notations, terms and methods.

- **Chapter 2** introduces basic symbols and terms used in the following chapters.
- **Chapter 3** describes control flow graphs with their special properties and requirements for real-time system analysis. Also, methods of interprocedural analysis are introduced here.

Part 2 contains chapters that describe different stages of ICFG reconstruction implemented in our reconstruction tool exec2crl.

- **Chapter 4** describes the steps that are performed during a safe and precise extraction of control flow from binary executables.
- **Chapter 5** outlines the algorithms that are used to automatically transform a vendor's machine description into a very efficient data structure that can be used for classifying single machine instructions.
- **Chapter 6** presents the core of exec2crl, i. e., the algorithms it uses to safely reconstruct the whole ICFG of a program from instruction classifications.

Part 3 contains chapters that present the interprocedural path analysis developed for our analysis framework.

- **Chapter 7** introduces the well-known technique of implicit path enumeration (IPE) that is widely used today for implementing path analyses.
- **Chapter 8** presents our novel extension to IPE for interprocedural analysis.

Part 4 contains chapters that evaluate my work.

- **Chapter 9** presents the experimental results.
- **Chapter 10** concludes this work and discusses possible future work.
- **Chapter 11** relates this work to that of other researchers.
- **Appendix A** depicts many control flow graphs to show how loop constraints are generated in many different situations.

Chapter 2

Basics

This chapter will introduce basic symbols and notations that will be used in the following chapters.

2.1 Selected Mathematical Notations

This section clarifies in brief words the usage of some mathematical symbols in this work. This section is not exhaustive, but only mentions some symbols that might be unclear. Mathematical notation is assumed to be known to the reader.

Definition 2.1 (Tuples)
For an arbitrary domain D and for elements $d_1, d_2, \dots, d_n \in D$, the according n-tuple is written in two possible notations:

unrolled way: $(d_1, d_2, \dots, d_n)$

indexed way: $(d_i)_{i \in \{1,\dots,n\}}$

The domain of tuples of length n is written $D^{1,n}$:

$$D^{1,n} := \{(d_i)_{i \in \{1,\dots,n\}} \mid d_i \in D\} \tag{2.1}$$

The empty tuple will be written ε.

In contrast to this, the domain of vectors of length n is written D^n:

$$D^n := \left\{ \begin{pmatrix} d_1 \\ \vdots \\ d_n \end{pmatrix} \mid d_i \in D \right\} \tag{2.2}$$

Definition 2.2 (Kleene Closure)
Given an arbitrary domain D, we define:

$$D^+ = \bigcup_{n \in \mathbb{N}} D^{1,n} \tag{2.3}$$

$$D^* = D^+ \cup \{\varepsilon\} \tag{2.4}$$

Definition 2.3 (Powerset)
For an arbitrary domain D, let $\mathfrak{P}(D)$ be its power set, i. e., the set of all subsets of D.

$$\mathfrak{P}(D) := \{D' \mid D' \subseteq D\} \tag{2.5}$$

Definition 2.4 (Image)
Given a function $f : M \to N$ and a set $M' \subseteq M$, the image of M' will be written $f(M')$ and is defined as follows.

$$f(M') := \{f(m) \mid m \in M'\} \tag{2.6}$$

The image of f is the special case $f(M)$.

2.2 Program Structure

This section introduces notations that are used to analyse programs. The structure of programs under examination will be clarified.

Let the program under examination be called $\mathcal{P}$.

2.2.1 Programs and Instructions

Analyses work on programs, which are given as a sequence of instructions. Instructions are either machine instructions, as is often the case for real-time system analysis, or more generally minimal statements in the language the analysis works on.

Depending on control flow, the given sequence of instructions is split into basic blocks, which are the basics of analysis.

2.2.2 Basic Blocks

The control flow of the program under examination is defined by jump instructions, which are intraprocedural branches, and call instructions, which are interprocedural branches. The branches divide the program into basic blocks, which control flow enters at the beginning and leaves at the end, without the possibility of branching except for the end of the basic block.

Let the set of basic blocks be V. This set must be finite: $|V| < \infty$.

The reconstruction of control flow includes finding the division into basic blocks. For raw machine code, this is not trivial. It is one topic of this work and will be described in detail in Chapter 6.

In the scope of this work, we will use the following terms. The following terms will be intuitively introduced now and clarified with

2.2.3 Routines

Structuring a program into smaller pieces of code is done in order to re-use parts of the program (usually parameterised) and to get a nicer structure. These re-usable pieces of code will be called *routines*. The words 'function' and 'procedure' occur in literature as well, but this document keeps using 'routine' for the program substructures in order to avoid confusion with mathematical functions.

Let R be the set of routines of $\mathcal{P}$ and let r_0 be the routine to be invoked upon the start of $\mathcal{P}$, i. e., r_0 is the *main routine* of $\mathcal{P}$.

Every basic block belongs to exactly one routine. Let the function $\mathrm{rout} : V \to R$ associate each basic block with its routine.

Let V_f be the set of basic blocks of each routine: $V_f = \{v \in V \mid \mathrm{rout}(v) = f\}$.

Every routine has exactly one basic block that is the first to be executed upon invocation. Let this basic block be called the routine's *start node*. The set $\mathsf{Starts} \subseteq V$ contains all start nodes of $\mathcal{P}$, one for each routine.

Let there be a function

$$\mathsf{start} : R \to \mathsf{Starts} \tag{2.7}$$

that associates the start node with its routine.

Another set of interesting basic blocks is constituted by those that contain routines invocations. These basic blocks are called *call nodes*. Let the set $\mathsf{Calls} \subseteq V$ contain all call nodes of $\mathcal{P}$.

The following function associates call nodes with their invoked start nodes. Call nodes may be associated with more than one start node, if there is more than one possible routine to be invoked. This happens for computed calls.

The function will be defined for all nodes for convenience and returns $\{\}$ for non-call nodes.

$$\begin{aligned} \mathsf{target} : V &\to \mathfrak{P}(\mathsf{Starts}) \\ v &\mapsto \{v' \in V \mid v \text{ invokes } v'\} \end{aligned} \tag{2.8}$$

2.2.4 Control Flow Graph

Each routine has its own control flow graph, consisting of nodes that are basic blocks, and edges representing the control flow between the blocks.

Let $\mathsf{CFG}_f = (V_f, E_f), f \in R$ be the **control flow graph** of routine f.

As mentioned before, a control flow graph has exactly one start node $\mathsf{start}(f)$ via which all control flow enters routine f.

For a path in a graph G, e. g. in CFG_f, from node v_1 to v_2, we will write $v_1 \to_G^* v_2$.

Definition 2.5 (Branch, Jump, Call)
If control flow has several alternative possibilities to continue at run-time after a given basic block, i. e., if a node in a graph has several out-going edges, this situation will be called *a branch*.

Branches in control flow graphs will be called *jumps*.

Branches in call graphs will be called *calls* or *subroutine calls* or *subroutine invocations*. Call graphs will be defined now.

2.2.5 Call Graph

An important structure is a call graph. It is the graph that connects call nodes and start nodes. It is defined by structures already defined: Calls and Starts constitute the nodes, and target restricted to Calls defines the intraprocedural edges. The linkage between start and call nodes is established by adding edges from start to call nodes for each routine. Formally, we define the following.

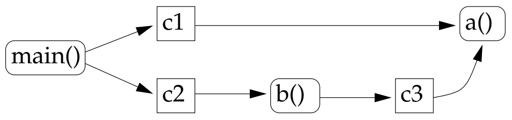

Figure 2.1: CG (without context) of Example 2.2.6. Start nodes are labelled with the name of the routine and a pair of parentheses, call nodes are labelled as shown in the comment in the C source code. Note that our CGs contain no return edges, only call edges.

Definition 2.6 (Call Graph)
Let $\mathsf{CG} = (\hat{V}, \hat{E}), \hat{V} = \mathsf{Calls} \cup \mathsf{Starts}, \hat{E} \subseteq \hat{V} \times \hat{V}$ be the **call graph** of $\mathcal{P}$, where $\hat{E}$ is defined as follows.

$$\begin{array}{rcl} \hat{E} & := & \{(c,s) : c \in \mathsf{Calls}, s \in \mathsf{target}(c)\} \cup \\ & \bigcup_{f \in F} & \{(s,c) : s \in \mathsf{Starts}, c \in \mathsf{Calls} : \\ & & \quad \exists s \to^{*}_{\mathsf{CFG}_f} c\} \end{array}$$

It is required that call nodes have exactly one incoming edge in the CFG. This can be ensured by inserting additional empty nodes for the call nodes that contradict this requirement (the PAG framework does this). This way, together with the above definitions, each call node c also has exactly one outgoing edge in the CFG. In the CG, c also has exactly one incoming edge (from the start node) and possibly several outgoing edges (defined by $\mathsf{target}(c)$).

2.2.6 Example in C

```
void a() {
    ...   // basic block b1
}
void b() {
    a();  // invocation c3
}
int main() {
    a();  // invocation c1
    b();  // invocation c2
}
```

Figure 2.1 shows the call graph of this short program.

Note 1: Definitions of call graphs in other literature often connect routines instead of start and call nodes. However, the call graphs that we are going to use have to distin-

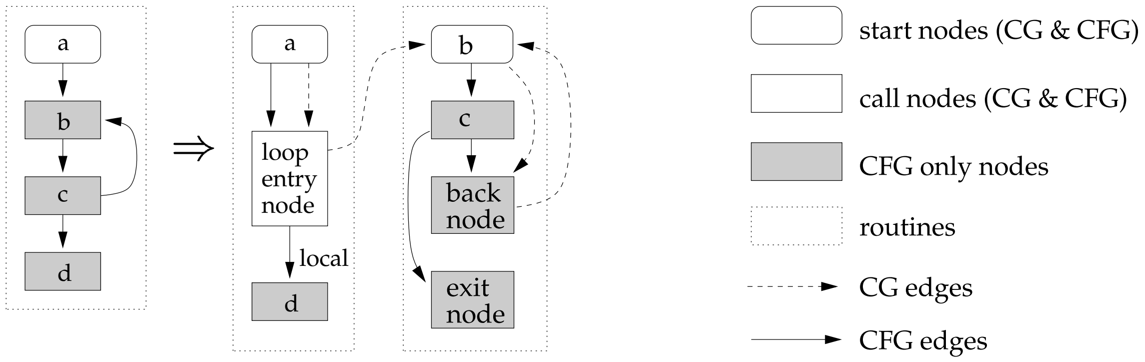

Figure 2.2: CFG modifications by loop transformation. The loop transformation introduces a new routine and new call nodes for each loop and transforms the loop into a recursive routine. Dashed lines represent edges in the call graph, which are introduced by this transformation.

guish call nodes, too. To get the call graphs used in other literature – those that connect routines – simply form super nodes from start and call nodes of the same routine. This way each node corresponds to a routine.

2.2.7 Loops

The term 'loop' will be used for a *natural loop* as defined in [Aho et al., 1986]. A natural loops has two basic properties:

1. A natural loop has exactly one start node which is executed every time the loop iterates. This node is called *header*.
2. A natural loop is repeatable, i. e., there is a path back to the header.

We handle loops and recursion uniformly in our approach. This is done by transforming all loops into recursive routines by making the loop body a routine on its own and inserting interprocedural edges accordingly. The loop transformation that is used to transform loops into routines uses an algorithm from [Lengauer and Tarjan, 1979] to find and extract loops.

Figure 2.2 depicts a loop transformation.

Apart from loops, there must be no other cycles in the control flow graphs. Although this is a restriction, compiled code and well-done hand written assembly code will not use other types of cyclic control flow. The reason for this restriction is the unbounded run-time of control flow cycles. When the path analysis searches the maximal run-time, loops must be bounded with maximal iteration counts in order to make the problem

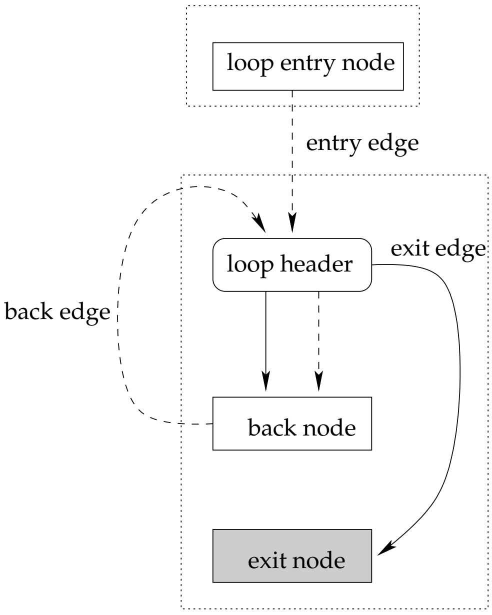

Figure 2.3: A simple loop with all the important edges. Dotted lines and white nodes are in the call graph, the other items are part of the control flow graph

solvable. Because only loop iteration counts are specifiable, only these types of cycles are currently allowed.

After loop transformation, there must be no cycles in the control flow graphs at all. All cycles must have been moved to the call graph and marked as loops.

Let L be the set of loops of program $\mathcal{P}$. Because loops are converted into recursive routines in our framework, it holds that $L \subseteq R$. Therefore, the header of a loop is simply the start node of the loop. Still, we define a function that assigns the header to a loop for clarity.

Definition 2.7 (Loop Header)
The *header of a loop $l \in L$* is defined as follows.

$$\begin{aligned} \text{header} : L &\to \mathsf{Starts} \\ l &\mapsto \mathsf{start}(l) \end{aligned} \tag{2.9}$$

Figure 2.3 shows a simple loop.

Because loops and recursion are the same in our framework, there may be more than one entry for a loop. This case occurs when a recursive routine is invoked from several different call sites. A more complex example of a loop is shown in Figure 2.4 on the next page.

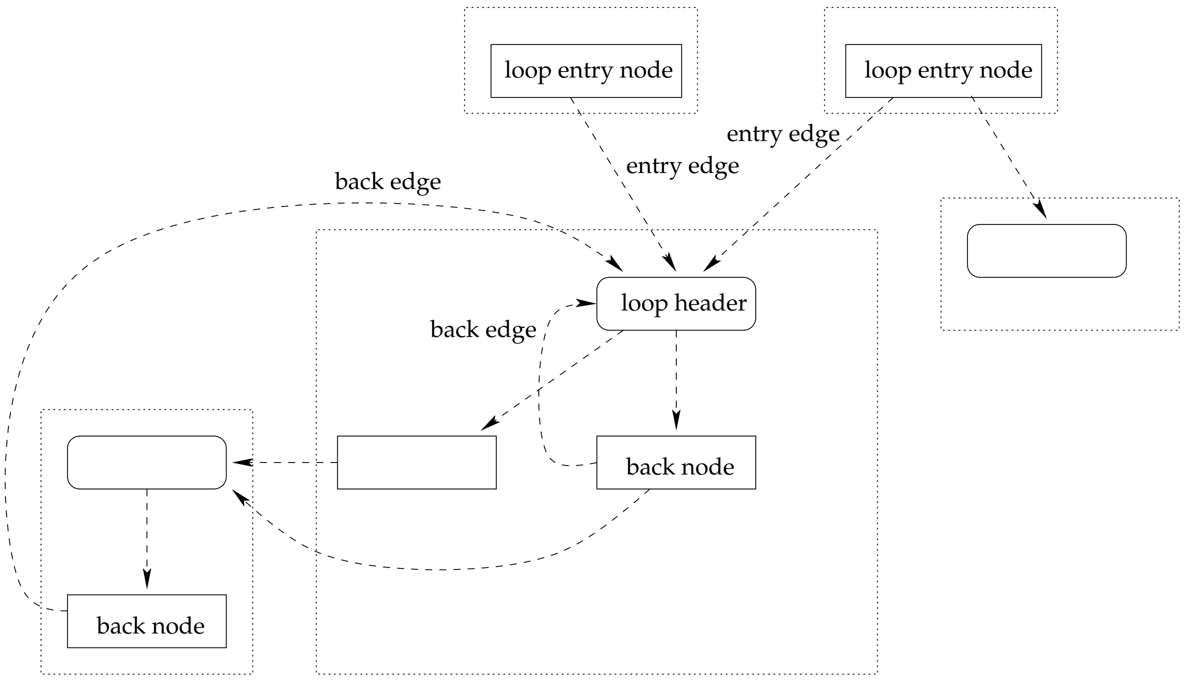

Figure 2.4: Complex recursion, CG only. The loop is entered from two call sites. One of the entry nodes also has an outgoing edge that calls a non-involved routine. There are two back edges, one of which recurses via another function call. Further, one of the back nodes has two outgoing edges, but only one is a back edge. To handle all this, much care has to be taken.

Definition 2.8 (Entry Edges)
Let there be a function

$$\text{entries} : L \to \mathfrak{P}(\hat{E}) \tag{2.10}$$

that assigns to a loop its entry edges.

Let there also be a function that returns the set of back edges of the loop, i. e. those edges that enter the loop from inside the loop. Note that usage of 'inside' here refers to nested re-invocations of the loop as well.

Definition 2.9 (Back Edges)

$$\text{back} : L \to \mathfrak{P}(\hat{E}) \tag{2.11}$$

The number of iterations of loops will be specified using two functions. One for the minimum iteration count and one for the maximum. The iteration bounds will be defined *for each entry* of the loop and, therefore, the two functions take and *loop entry node* as their argument.

Definition 2.10 (Minimum and Maximum Loop Iteration Count)
Let l be a loop and $e \in \text{entries}(l)$ one of its entry edges.

The **minimum loop execution count** per entrance of l via e will be written $n_{\min}(e)$.

The **maximum loop execution count** per entrance of l via e will be written $n_{\max}(e)$.

2.3 Integer Linear Programming

This section introduces the basics of Integer Linear Programming (ILP) briefly. A precise description of the underlying theory can be found in many books (*see* [Chvátal, 1983; Schrijver, 1996; Nemhauser and Wolsey, 1988]).

2.3.1 Linear Programs

This section introduces the structure of Linear Programs. How they can be solved will be shown in the next section.

Definition 2.11 (Comparison of Vectors)
Let $\Delta \in \{\leqq, =, \geqq\}$ be a comparison operator and let $a, b \in \mathbb{R}^n$. Then we define

$$a \Delta b :\Leftrightarrow a_i \Delta b_i,\ \forall i = 1, \ldots, n$$

Definition 2.12 (Linear Combination)
Let $x \in \mathbb{R}^n$ be variable and let $a \in \mathbb{R}^n$ be constant. Then $a^T x$ is called the *linear combination* of x.

Definition 2.13 (Linear Program)
Let $t \in \mathbb{R}^d,\ b \in \mathbb{R}^m,\ A \in \mathbb{R}^{m \times d}$ be known and constant. A *Linear Program* (LP) is the task to maximise $t^T x$ in such a way that $x \in \mathbb{R}^d_{\leqq 0} \wedge Ax \leqq b$. In short, this is written:

$$\max : t^T x \mid Ax \leqq b,\ x \in \mathbb{R}^d_{\leqq 0}.$$

Definition 2.14
In Definition 2.13 the function $C : \mathbb{R}^d \to \mathbb{R}$ where $C(x) = t^T x$ is called *objective function*.

The inequalities given by $Ax \leqq b$ are called *constraints*. x is said to be a *feasible* solution, if it satisfies $Ax \leqq b$. Let $P = \{x \in \mathbb{R}^d_{\leqq 0} \mid Ax \leqq b\}$ be the set of feasible solutions of x. x^* is said to be an *optimal* solution, if $t^T x^* = \max\{t^T x \mid x \in P\}$.

To reduce a problem of minimising to one of maximising, the objective function can be multiplied by -1.

Further, the constraints that are used in the definition of a Linear Program are of the form $a_{k,1}x_1 + a_{k,2}x_2 + \cdots + a_{k,d}x_d \leqq b_k$. Other types of constraints like

$$a_{k,1}x_1 + \cdots + a_{k,d}x_d \ \Delta\ a'_{k,1}x'_1 + \cdots + a'_{k,e}x'_d \tag{2.12}$$

where $\Delta \in \{\leqq, =, \geqq\}$ can be reduced to the basic form by using the following transformations:

1. Instead of $\sum_1 \Delta \sum_2$ write $\sum_1 - \sum_2 \Delta 0$.
2. Instead of $\sum \geqq 0$ write $-\sum \leqq 0$.
3. Instead of $\sum = 0$ write $\sum \leqq 0$ and add the constraint $-\sum \leqq 0$.

There are three cases that can occur when an LP is tried to be solved:

1. $P = \{\,\}$: The LP is *infeasible*.
2. $P \neq \{\,\}$, but $\nexists \sup\{t^T x \mid x \in P\}$. The LP is *unbounded*.
3. $P \neq \{\,\}$, and $\exists \max\{t^T x \mid x \in P\}$. The LP is *feasible* and has a finite solution.

To find the solution of a linear program, upper bounds of the objective function must be computed. The problem of finding the least upper bound is also an LP that is defined as follows.

Definition 2.15 (Primal and Dual Problem)
Let $\max : t^T x \mid Ax \leqq b,\ x \in \mathbb{R}^d_{\geqq 0}$ be a Linear Program. Let this program be called *primal problem*. The *dual problem* is the problem of finding the least upper bound of $t^T x$, which is defined as follows: $\min : y^T b \mid y^T A \geqq t^T,\ y \in \mathbb{R}^d_{\geqq 0}$.

The two following theorems hold (*Duality Theorems of Linear Programming*):

Theorem 2.16 (Weak Duality)
Let $\bar{x}$ be a feasible solution of the primal problem $\max : t^T x \mid Ax \leqq b,\ x \in \mathbb{R}^d_{\geqq 0}$ and let $\bar{y}$ be a feasible solution of its dual problem $\min : y^T b \mid y^T A \geqq t^T,\ y \in \mathbb{R}^d_{\geqq 0}$. Then it holds that:

$$\bar{y}^T b \geqq t^T \bar{x}.$$

Theorem 2.17 (Strong Duality)
Let x^* be a feasible solution of the primal problem $\max : t^T x \mid Ax \leqq b,\ x \in \mathbb{R}^d_{\geqq 0}$ and be y^* be a feasible solution of its dual problem $\min : y^T b \mid y^T A \geqq t^T,\ y \in \mathbb{R}^d_{\geqq 0}$. Then it holds that:

$$y^{*T} b = t^T x^* \iff x^* \text{ and } y^* \text{ are optimal.}$$

Corollaries

- If the primal problem is unbounded, the dual problem is infeasible.
- If there are feasible solutions of the primal and the dual problems, then there is an optimal solution. The values of the objective function of the two problems are equal for the optimal solution.

The following *Simplex* algorithm exploits that for a feasible preliminary solution x of the primal problem, there is a solution y of the dual problem. If that solution is feasible in the dual problem, it is optimal (due to the second corollary). If it is not, the basic solution can be improved.

2.3.2 Simplex Algorithm

This section introduces a non-formal description of the Simplex algorithm. There is a vast amount of literature about LP solving and the Simplex algorithm available for the interested reader, e. g. [Chvátal, 1983; Schrijver, 1996; Nemhauser and Wolsey, 1988].

The constraints of a linear program isolate a convex area in $\mathbb{R}^n_{\geqq 0}$. An optimal solution is found in one of the corners of this area. Starting with an arbitrary corner, a better

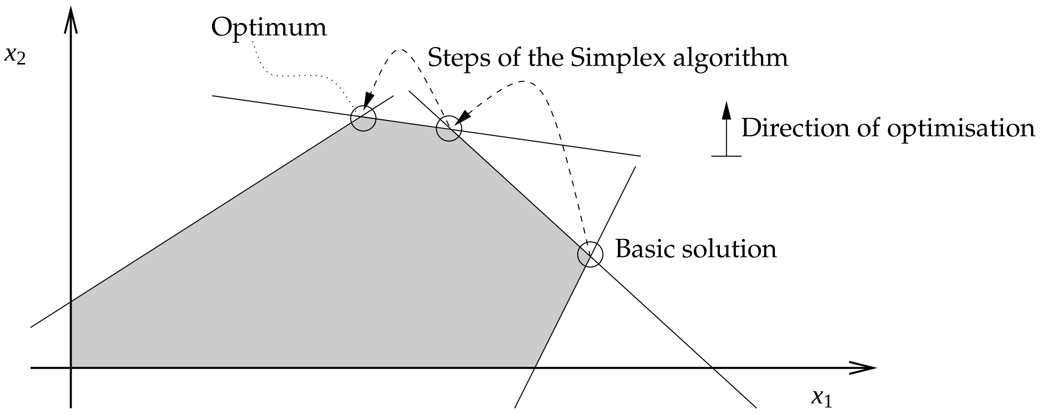

Figure 2.5: The Simplex algorithm in $\mathbb{R}^2_{\geqq 0}$.

solution of the objective function is searched by following one of the outgoing edges of that corner. This is repeated until no adjacent corner has a better value, which means that the optimal solution has been found. Figure 2.5 on the next page illustrates this algorithm.

The simplex algorithm can be used to solve large problems, since for most applications, its runtime is $O(m)$ for m constraints. However, constraints can be constructed so that the algorithm performs in only $O(2^m)$ time (e. g. the Klee Minty cube (*see* [Chvátal, 1983])). There are better algorithms from the complexity point of view, e. g. the Ellipsoid method or the Projective Scaling Algorithm by Karmarker, which have polynomial run-time.

2.3.3 Integer Linear Programs

Many problems only allow integer solutions for the solutions of an LP, i. e., in Definition 2.13 on page 42 it must additionally hold that $x \in \mathbb{Z}^d$. And because we already made the restriction that $x \geqq 0$, it must even hold that $x \in \mathbb{N}_0^d$.

This type of constraint will be needed for the algorithms in Chapter 7, where the variables of the LP are execution counts of basic block, which are naturally integers.

Definition 2.18 (Integer Linear Program)
Let $t \in \mathbb{R}^d,\ b \in \mathbb{R}^m,\ A \in \mathbb{R}^{m\times d}$ be constant and known. An *integer linear program* (ILP) is the task to maximise $t^T x$ in such a way that $x \in \mathbb{N}_0^d \wedge Ax \leqq b$.

$$\max : t^T x \mid Ax \leqq b,\ x \in \mathbb{N}_0^d.$$

To find a solution of an ILP, additional steps have to be taken, because the Simplex algorithm (and others for LP solving) cannot be used directly, since the additional restriction

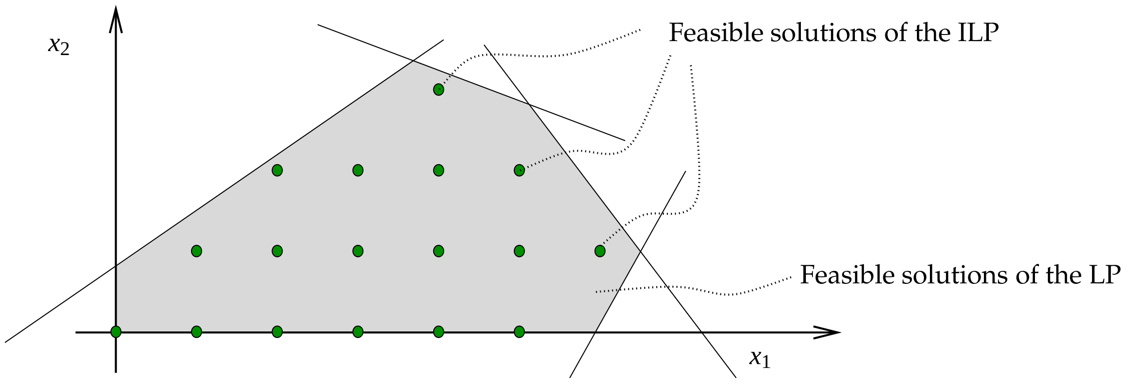

Figure 2.6: Domain of feasibility of an ILPs (grid points) and corresponding domain of feasibility of the LP-relaxed problem (shaded area).

to integer variable cannot be handled by them. Actually, it is $\mathcal{NP}$-complete to solve ILPs. However, in practice, many large ILPs problems are solvable with a moderate amount of effort.

Definition 2.19 (LP-Relaxed Problem)
Let $\max : t^T x \mid Ax \leqq b,\ x \in \mathbb{N}_0^d$ be an Integer Linear Program. Then $\max : t^T x \mid Ax \leqq b,\ x \in \mathbb{R}_{\geqq 0}^d$ is said to be the corresponding *LP-relaxed problem*. In the following, it will also be called *relaxed problem*.

The relaxed problem is used to solve ILPs. It does not contain demands for integer variables and all feasible solutions of the ILP are also feasible for the LP. I. e., starting from the LP the integer property of all variables is tried to be achieved. The following algorithm works like that.

2.3.4 Branch and Bound Algorithm

The basic idea of the Branch and Bound Algorithm is to solve the relaxed LP and then split the domain of feasibility into two sub-problems in order to satisfy the demand for integer variables. Each sub-problem is then solved until all variables are integers.

Let Ψ be an ILP and let Ψ' be the relaxed problem. If it is feasible, solving Ψ' yields a solution $\hat{x} \in \mathbb{R}_{\geqq 0}^d$.

If $\hat{x} \in \mathbb{Z}^d$, so a solution is found for Ψ, too. If not a coordinate $i \in \{1, \ldots, n\}$ is chosen such that $\hat{x}_i \notin \mathbb{Z}$. The two sub-problems $\tilde{\Psi}_1$ and $\tilde{\Psi}_2$ are created from Ψ' by adding one of the following inequalities:

$$x_i \leqq \lfloor \hat{x}_i \rfloor \tag{2.13}$$

$$x_i \geqq \lceil \hat{x}_i \rceil \tag{2.14}$$

These constraints exclude $\hat{x}$ as a solution for $\tilde{\Psi}_1$ and $\tilde{\Psi}_2$. This method is repeated until all variables are integers.

No word was said about major problems and methods used in this algorithm, such as how to choose a coordinate, or which order the sub-problems should be solved in. Again, interested readers should refer to standard literature like [Chvátal, 1983; Schrijver, 1996; Nemhauser and Wolsey, 1988].

There are freely available tools like `lp_solve`[1] that implement very good algorithms for solving ILPs. `lp_solve` was used for this thesis.

[1]`lp_solve` was written by Michel Berkelaar and is freely available at `ftp://ftp.es.ele.tue.nl/pub/lp_solve`.

Chapter 3
Control Flow Graphs

While the previous chapter has already introduced basics about programs, their control flow graphs and call graphs, this chapter will describe in detail the precise structure of the control flow graphs our framework uses. Requirements of CFGs and CGs for real-time system analysis will be discussed.

3.1 Control Flow Graphs for Real-Time System Analysis

To talk about control flow graphs and call graphs simultaneously, the term *interprocedural control flow graph (ICFG)* will be used to refer to all control flow graphs and to the call graph of a program.

Real-time system analysis requires *safe* and *precise* analysis methods. Safety has the highest priority since real-time systems are usually part of a large, safety-critical environment where errors can lead to fatal damage, as mentioned already in the introductory chapter.

3.1.1 Safety

For our WCET analysis framework, this means that all analyses must be based on a safe ICFG in the first place. If the ICFG is unsafe, the whole analysis chain will be unsafe.

To define safety for ICFGs, it must be thought about what unsafety means, since ICFGs seem to be something that either represents a program, or which does not, in which case it must be said to be incorrect. It is not that simple, however, since control flow is sometimes unclear or unpredictable for analyses. Of course, our first requirement is correctness. This is more than obvious:

A safe interprocedural control flow graph must be correct.

Secondly, if any uncertain control flow is encountered, it must be clearly marked for analyses to be able to react to uncertain control flow.

A safe interprocedural control flow graph must mark uncertainties clearly.

Subsequent chapters will reason about how to achieve these goals when reconstructing control flow. This chapter will focus on the precise structure of ICFGs and on how the required information can be made available to analyses.

3.1.2 Precision

For analyses to be precise, the underlying ICFGs must be precise, too. Whenever control flow can be represented precisely or imprecisely, this chapter will discuss that topic.

Precision in control flow is usually an issue for alternative flow, i. e., where the final taken alternative is decided at run-time. Examples are computed jumps (e. g. switch tables) or computed calls (e. g. function pointers or virtual function calls in object-oriented languages). The issue is usually a question of infeasibility: more precision means to be able to predict statically which alternative paths are really infeasible. The more this can be predicted, the more precise the ICFG will be.

3.2 Detailed Structure of CFG and CG

This section describes the precise structure of the ICFGs that are used in this thesis. It is a clarification of the data structures presented in Chapter 2.

The graphs that are used are based on those provided by the PAG framework. However, the graphs used here are computed from the PAG graphs to suite the needs of the presented algorithms best. This section will clarify how these graphs look like.

In order to prevent special cases, like conditional calls, etc., our CFGs and CGs contain additional *empty* basic blocks at specific locations, i. e., when routines are invoked and left. Because of loops being transformed to recursion, these empty blocks also help to avoid special cases here, e. g., there cannot be two loops starting before the same basic block. This can be programmed in Pascal with two nested repeat loops.

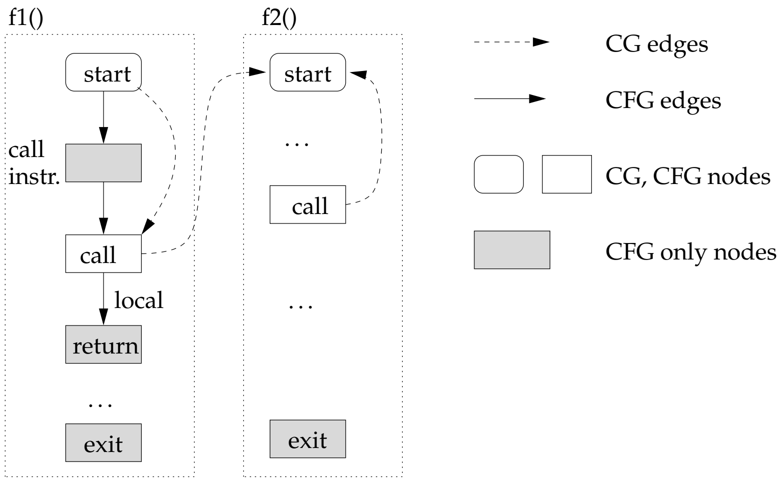

Figure 3.1: CFG and CG of a call of a recursive routine. The two graphs are shown in one figure. This figure clarifies the use of local edges and shows that there are no return edges (e. g. from a node in routine f2 back to the call node in f1).

Four types of empty nodes exist: at each routine invocation, two additional empty nodes are inserted: a *call* node and a *return* node. The actual call instruction is located in the block before the call node. Routines begin with an empty *start* node and returning control flow is gathered in a unique *exit* node.

Our CFGs contain a *local* edge after each call node, because the call graphs will not contain flow information about routine returns. This is the most convenient way of representation for the analyses that will be described later (*see* Section 7.3.3 on page 113).

A routine call with all important nodes is depicted in Figure 3.1.

3.2.1 Alternative Control Flow and Edge Types

Alternative control flow occurs at two levels: in the control flow graph, where if-then-else statements are the most common example, followed by switch-statements, and in the call graph, where function pointers are the most common example. Virtual function calls are usually a special case of function pointers.

To handle alternative control flow in control flow graphs, there are different types of edges. Some analyses need this edge type in order to compute the correct behaviour. E. g. jumps often have different execution times for different types of edges.

We formally define the edge type as a function that assigns a type to each edge.

Definition 3.1 (Edge type)
Let $\text{type} : E \to \{\text{normal}, \text{false}, \text{true}, \text{local}\}$

normal edge: outgoing edge of basic blocks whose control flow exits without alternatives (i. e., without a branch)

false edge: for a conditional jump, this marks the edge that is taken if the branch is not taken. This type of edge is also known as a *fall-through edge*. At each block, there is maximally one of these edges.

true edge: for a jump, this marks possible branch targets of the jump.

local edge: this edge was introduced in the previous section: it is the representation of control flow after a call.

For switch tables, there may be a number of true edges, one for each possible branch target.

Alternative control flow in the call graph is marked in the same way by using multiple outgoing edges from a call node to several start nodes.

3.2.2 Unrevealed Control Flow

If any control flow is unknown, it is *required* that the control flow graph contains information about this. This is vital for analyses, since they might analyse to the wrong thing.

Unrevealed control flow, i. e., edges that are known to exist but with an unknown target, can be marked at the basic block to have additional successors in the control flow graph or the call graph. We introduce two sets to account for this.

Definition 3.2 (Unrevealed edges)
Let $\widetilde{\mathsf{Calls}} \subseteq \mathsf{Calls}$ be the set of call nodes that contain instruction with unknown call targets. Because we cannot have edges with an unknown target, we use this set instead.

For a given routine f, let $\tilde{V}_f \subseteq V_f$ be the set of basic block that contain instructions with unknown jump targets.

3.2.3 Calls

Modern architectures and run-time libraries have several interesting peculiarities that have to be thought about. Many of these peculiarities showed up when the control flow

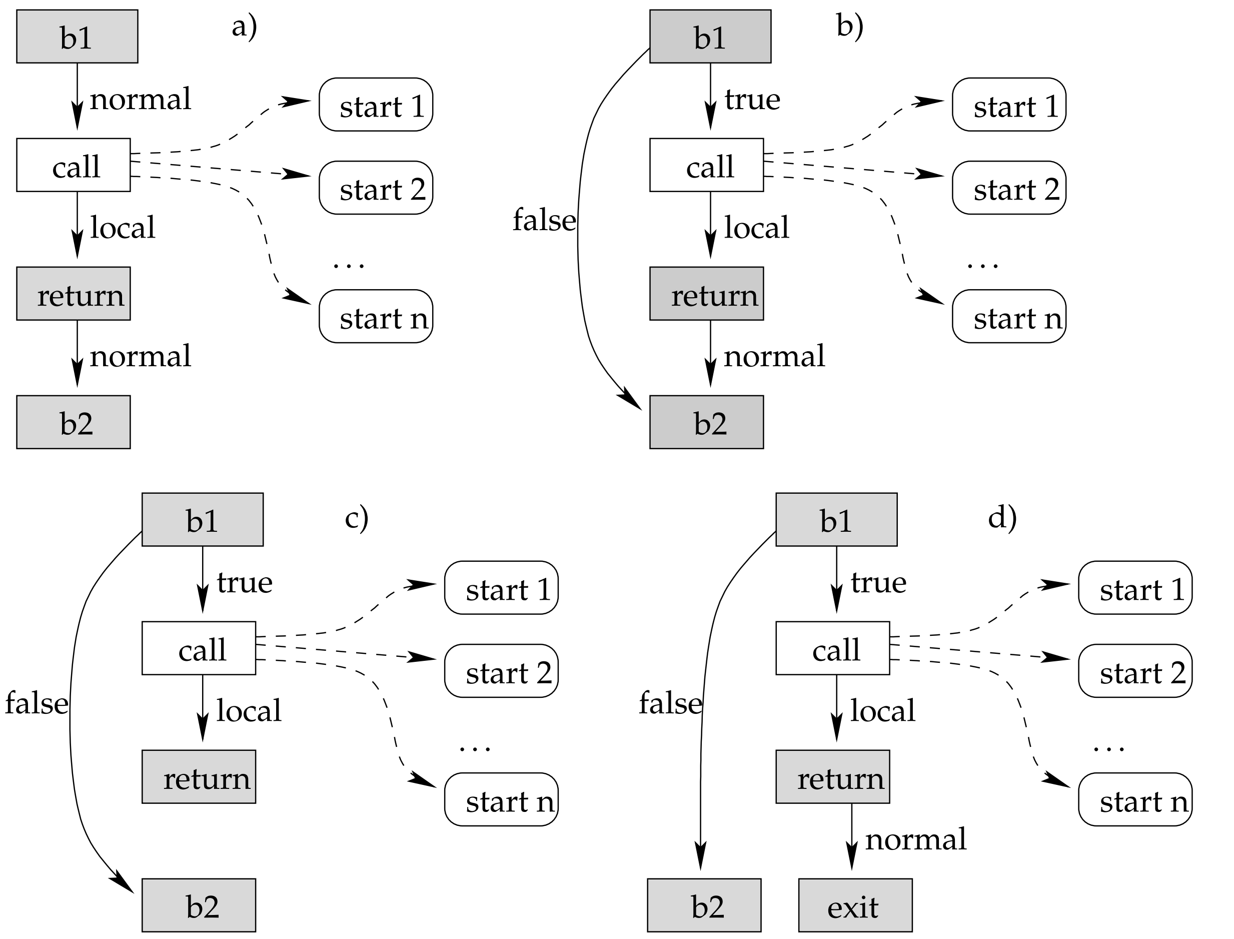

Figure 3.2: Different types of calls and their representation in the ICFG. a) normal call (with several alternative targets), b) conditional call, c) conditional no-return call, e) conditional immediate-return call

reconstruction algorithms (*see* Chapter 6) were implemented for different targets. Calls are more complex than normal jumps, since they involve the mechanism of returning to the caller, so the fall-through edge has a totally different meaning for calls than for jumps. Therefore, the generation of edges needs to be clarified for the interprocedural case as well as for the intraprocedural case.

In the course of the examination of different programs, libraries and architectures, we found the need to distinguish the following types of calls. The categories listed below are not mutually exclusive.

computed calls: calls that use the value of a register as a branch target. These usually result in alternative control flow.

unpredictable calls: calls that have unrevealed call targets.

conditional calls: calls that may possibly not be taken.

not-taken calls: calls that are never taken

no-return calls: calls that never return, e. g., because they invoke a routine that implements an infinite loop, or calls to a system function that exits the program.

immediate-return calls: calls that end the current function immediately when they return.

Handling of computed calls and unpredictable calls has been described already above.

Calls that are not taken are represented by having no call nodes at all.

Whether a call is conditional, not-taken, no-return or immediate-return is represented by edges in the control flow graph. One interesting fact is that calls might *not* return to the caller, but branch to somewhere else when they return. This is the case for no-return and immediate-return calls.

Figure 3.2 on the previous page shows the ICFGs associated with different types of calls.

3.2.4 External Routines

External routine calls are frequent and should be handled by any WCET analysis framework. Our approach is to introduce a basic block of the type *external*, which represents the execution of the external routine. It is like a black box.

Analyses can decide how to handle these external basic block nodes. The WCET analysis will have to assume that the run-time of such blocks is known, so either a library of pre-analysed run-times is needed, or the user has to be queried.

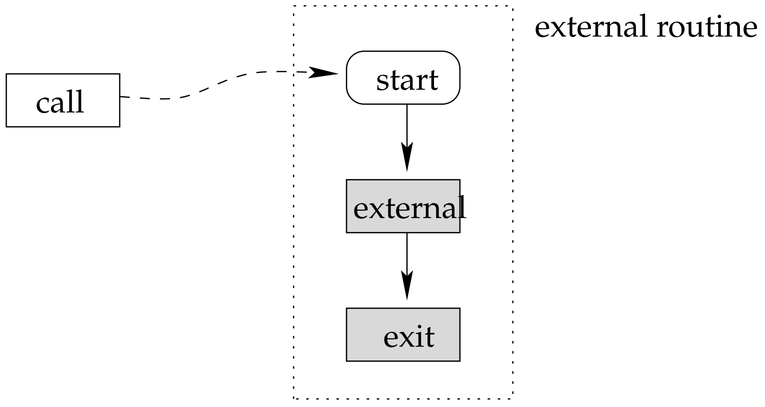

Figure 3.3: External routine call: an *external* node is introduced that represents the external routine as a black box.

3.2.5 Difficult Control Flow

Programmers may use strange concepts of structure and produce something that is executable, but with weird control flow. This chapter deals with these cases.

Examples of weird, or better *difficult* control flow are the following.

- Jumps into loops past the loop header.
- Entering routines at different basic blocks.

Unfortunately, even so-called high-level programming languages sometimes support the generation of structures that are difficult. E. g. most imperative programming languages support a `goto` command that allows for jumping to any point in the current procedure. This way entering loops past the header is possible.

Some old imperative languages that are still in wide use, like C, even do not enforce a clear block-structure for their own structuring mechanisms. E. g., while and case statements need not be nested correctly, triggering the same problem of entering loops past the header. An infamous example is Duff's device, used to unroll a typical memory copy loop and interlace it with the initial aligning case. This is shown in Figure 3.4 on the next page.

Many cycles that are not natural loops could be transformed into a natural loop by unrolling them once. Duff's device is one example for this. Usually, it is not clear which block should be the loop header then, because with different entries it is unclear which block inside the loop is executed as many times as the loop is executed.

The second example, entering routines at several basic blocks can usually only be programmed when using the assembly or machine language directly. Although this is assumed to be very bad coding style, it can often be reconstructed to nice control flow by

```
unsigned int n = (count + 7) / 8;
switch (count % 8) {
    do {
        case 0:  *to++ = *from++;
        case 7:  *to++ = *from++;
        case 6:  *to++ = *from++;
        case 5:  *to++ = *from++;
        case 4:  *to++ = *from++;
        case 3:  *to++ = *from++;
        case 2:  *to++ = *from++;
        case 1:  *to++ = *from++;
    } while (--n > 0);
}
```

Figure 3.4: Duff's device. The loop is entered at several points by interlacing switch statement and while loop in C.

introducing additional routines (e. g., when the same routine tail is used by two routines, this tail can be made a routine on its own if no jumps leave that new routine).

However, such a structure cannot *always* be reduced to nice control flow, so a full automation cannot be expected. Therefore, it seems unwise to start implementing without observing the important special cases that should be handled automatically. Our framework is very flexible to easily allow such extensions as soon as they are encountered.

3.3 Contexts

Contexts were introduced in previous work already. They were used for analysis with the PAG framework and described in most detail in [Martin et al., 1998] and [Martin, 1999b]. This section gives a brief introduction needed to understand the subsequent chapters. Further, the newest development of our analysis framework is outlined by presenting the VIVU(n, k) context mapping with customised unrolling.

Our analysis framework provides the possibility of categorising different executions of basic blocks by the control flow that led to its execution. These classes are called *contexts*. Each basic block must only be assigned a finite number of contexts to ensure the termination of the analysis.

There are different approaches for assigning contexts.

By the value of parameters. The idea is that routine invocations that use the same parameters are identical for the analysis. This approach is called *functional approach*.

This technique may be used for analyses using Abstract Interpretation. The distinction criterion of routines is rather the abstract value of the analysis than the parameters of the routine. For this analysis method to yield only a finite number of contexts, the abstract domain must be finite, which is a limitation.

However, one problem with the functional approach is the potentially large number of contexts that is unknown before the analysis. Further, the contexts are computed *dynamically* during the course of the analysis and cannot be re-used in subsequent analyses since different abstract domains are usually used.

By the routine invocation history. These routine invocations used for context computation are specified in the call graph. Therefore, this approach is called *call graph approach*.

Since the routine invocations are known before the analysis starts, the contexts can be computed *statically* with this approach. So this approach is easily applicable to multi-stage analyses where several sub-analyses can use the same set of contexts.

Throughout our framework for WCET analysis, the *call graph approach* is used for analyses. Any other static approaches of context computation could be used as well.

Contexts are computed in different ways, depending on the desired level of precision and the acceptable computation effort for the specific analysis problem. The computation depends on the execution history by which the basic block is reached. The computation of contexts will be called a *mapping* and will be defined formally below.

Mappings that follow the call graph approach are *finite abstractions* of all possible call histories of a routine. The call history of a routine can be represented by a string of call edges that represent the path of the invocation of that routine. This string is called *call string*.

Definition 3.3
Let $S \subseteq \hat{E}^*$ be the set of call strings.

Of course, with the presence of recursion, $|S|$ may be infinite. An operator $\oplus$ is used to compute a finite set of contexts for a set of call strings. Like call strings, contexts are also represented by strings, where the links of the strings are from a domain $\hat{\Theta}$, which depends on the mapping. Elements from $\hat{\Theta}$ are called **context links**, in analogy with chain links.

Definition 3.4 (Mapping, Connector)
A *mapping* is a pair $(\hat{\Theta}, \oplus)$, where the *context connector* is a function

$$\oplus : \hat{\Theta}^* \times \hat{E} \to \hat{\Theta}^*.$$

To compute a context from a call string, let $\oplus$ be applied recursively to each call string link.

$$\begin{aligned} f_\oplus : S &\to \hat{\Theta}^* \\ s_1 \circ s_2 \circ \cdots \circ s_n &\mapsto (((\varepsilon \oplus s_1) \oplus s_2) \oplus \ldots \oplus s_n) \end{aligned} \tag{3.1}$$

Let the set of contexts $\Theta_\oplus \subseteq \hat{\Theta}^*$ be the image of $f_\oplus$.

$$\Theta_\oplus = \{ f_\oplus(s) | s \in S \}$$

$\oplus$ is called a *finite context connector*, if $|\Theta_\oplus| < \infty$.

All connectors will be demanded to be finite in the following. Therefore, the term *connector* will be used for a finite context connector as an abbreviation.

If it is clear from context, Θ will be written instead of $\Theta_\oplus$.

3.3.1 CallString(k)

A very simple mapping is the CallString(k) mapping, which simply limits the length of the call strings to k elements. Only the most recent call edges are considered for context distinction.

First, we need the operation that limits strings to length k.

Definition 3.5 (Strings of limited length)
For an arbitrary domain D, let $|d|_k, d \in D^*$ be defined as follows.

$$|(d_n, d_{n-1}, \ldots, d_1)|_k = \begin{cases} (d_n, d_{n-1}, \ldots, d_1) & \text{if } n \leq k \\ (d_k, d_{k-1}, \ldots, d_1) & \text{otherwise.} \end{cases}$$

Definition 3.6 (CallString(k))
Let CallString$(k) = (\hat{E}, \oplus_k)$, where $k \in \mathbb{N}_0$, and

$$(e_1, e_2, \ldots, e_n) \oplus_k e_{n+1} = |(e_1, e_2, \ldots, e_n, e_{n+1})|_k$$

Since most calls only have a single target, instead of writing the edges in the call string, it is common to only write the call nodes for simplicity.

$\mathsf{CallString}(0)$ corresponds to non-interprocedural analysis, since all contexts have length 0 and, therefore, yield no context distinction at all.

Of course, k is a tuning factor to limit the complexity of the mapping to make the analyses perform well.

In Example 2.2.6, basic block `b1` in routine `a()` is executed with two different call stacks: `c1` and `c2` $\circ$ `c3` depending on the control flow that led to the invocation of routine `a`. Starting from $\mathsf{CallString}(2)$, we thus get two contexts for basic block `b1`.

3.3.2 Graphs with Context

Connectors can be used to define new graphs, namely, control flow graphs and call graphs *with context*. These graphs are the basis of all of our interprocedural analyses.

The call graph with context, $\mathsf{CG}^\star$, is defined as follows:

Definition 3.7 (Call graph with context)
Let Θ be the set of contexts and $\oplus$ a finite context connector and let $\mathsf{CG} = (\hat{V}, \hat{E})$ be a call graph and let f_0 be its main routine. Recall from Definition 2.6 on page 37 that $\hat{V} = \mathsf{Calls} \cup \mathsf{Starts}$.

Then a *call graph with context* is a graph $\mathsf{CG}^\star := (\hat{V}^\star, \hat{E}^\star)$, where $\hat{V}^\star \subseteq \hat{V} \times \Theta$ and $\hat{E}^\star \subseteq \hat{V}^\star \times \hat{V}^\star$ are defined recursively from $\hat{V}$ and $\hat{E}$, respectively, using the connector $\oplus$.

- The main routine with the empty context is part of $\hat{V}^\star$:
  $(f_0, \varepsilon) \in \hat{V}^\star$.
- Edges from start nodes to call nodes do not change context:
  $\forall (v, \vartheta) \in \hat{V}^\star, v \in \mathsf{Starts}, \forall (v, v') \in \hat{E} \quad \Rightarrow$

  $$(v', \vartheta) \in \hat{V}^\star \text{ and}$$
  $$((v, \vartheta), (v', \vartheta)) \in \hat{E}^\star.$$
- Edges from call nodes to start nodes change context according to $\oplus$:
  $\forall (v, \vartheta) \in \hat{V}^\star, v \in \mathsf{Calls}, \forall (v, v') \in \hat{E} \quad \Rightarrow$

  $$(v', \vartheta \oplus (v, v')) \in \hat{V}^\star \text{ and}$$
  $$((v, \vartheta), (v', \vartheta \oplus (v, v'))) \in \hat{E}^\star.$$

The set of routines with context is a set of pairs of routines and all their corresponding contexts.

Definition 3.8 (Routine with context)
The set of contexts of a routine r is written $\Theta(r)$. It is defined as follows:

$$\Theta(r) := \{\vartheta \mid \vartheta \in \Theta, (\mathsf{start}(r), \vartheta) \in \hat{V}^\star\}$$

The set $R^\star$ of *routines with context* (r, ϑ) is defined as follows.

$$R^\star := \{(r, \vartheta) \mid r \in R, \vartheta \in \Theta(r)\}$$

A control flow graph with context, $\mathsf{CFG}^\star$, is defined as follows:

Definition 3.9 (Control flow graph with context)
Let $(r, \vartheta) \in R^\star$ be a routine with context and let $\mathsf{CFG}_f = (V_f, E_f)$ be the control flow graph of routine r.

A *control flow graph with context* is the graph $\mathsf{CFG}^\star{}_{r,\vartheta} = (V^\star_{r,\vartheta}, E^\star_{r,\vartheta})$, where

$$V^\star_{r,\vartheta} := \{(v, \vartheta) \mid v \in V_f\}$$

and

$$E^\star_{r,\vartheta} := \{(e, \vartheta) \mid e \in E_f\}.$$

Thus, control flow graphs with context are isomorphic to their corresponding, original control flow graph without context. Their nodes are simply extended by a context.

For convenience, we combine all nodes of all graphs with context in one set.

Definition 3.10 (Set of all nodes)
Let $V^\star := \bigcup\limits_{r \in R^\star} V^\star_r$

Accordingly, the set of all edges is defined as follows.

Definition 3.11 (Set of all edges)
Let $E^\star := \bigcup\limits_{r \in R^\star} E^\star_r$

Definition 3.12 (Other structures with contexts)
The sets $\mathsf{Calls}^\star$ and $\mathsf{Starts}^\star$ are defined by distinguishing nodes from CG by a context:

$$\begin{aligned}\mathsf{Calls}^\star &:= \hat{V}^\star \cap (\mathsf{Calls} \times \Theta)\\ \mathsf{Starts}^\star &:= \hat{V}^\star \cap (\mathsf{Starts} \times \Theta)\end{aligned}$$

Similar definitions apply to sets of unrevealed control flow.

$$\begin{aligned}\widetilde{\mathsf{Calls}}^\star &:= \hat{V}^\star \cap (\widetilde{\mathsf{Calls}} \times \Theta)\\ \tilde{V}^\star_{r,\vartheta} &:= V^\star_{r,\vartheta} \cap (\tilde{V}_r \times \Theta) \quad \forall (r,\vartheta) \in R^\star\end{aligned}$$

Further, edge types do not change with the presence of contexts.

$$\mathrm{type}(e,\vartheta) \;:=\; \mathrm{type}(e) \quad \forall (e,\vartheta) \in E^\star$$

Finally, in order to talk about the possible contexts of a node, we define the following.

Definition 3.13 (Set of Contexts of a Node)
The set of contexts that are distinguished for a given node v in a control flow graph with context $\mathsf{CFG}^\star$ will be written $\Theta(v)$. It is defined as follows.

$$\Theta(v) = \Theta(\mathrm{rout}(v))$$

3.3.3 Iteration Counts for Contexts

With the introduction of contexts, we allow the minimum and maximum iteration count (*see* Definition 2.10 on page 41) to be defined per entry edge and per context. So we extend $n_{\min}$ and $n_{\max}$ as follows.

The **minimum loop execution count** per entrance of that loop via an entry edge $e \in \hat{E}^\star$ will be written $n_{\min}(e)$. The **maximum loop execution count** per entrance will be written $n_{\max}(e)$.

Figure 3.5 on the next page depicts the $\mathsf{CG}^\star$of Example 2.2.6. It can be seen from the figure that the $\mathsf{CallString}(2)$ $\mathsf{CG}^\star$ is maximally precise w.r.t. control flow, i. e., no control flow from two different calls ever joins in deeper calls. In contrast to this, in the $\mathsf{CallString}(0)$ $\mathsf{CG}^\star$ on the right, control flow from the calls `c1` and `c2` joins when `a()` is invoked from `c3`.

3.3.4 Recursive Example

This section will clarify how different mappings make different $\mathsf{CGs}^\star$. Consider the following program:

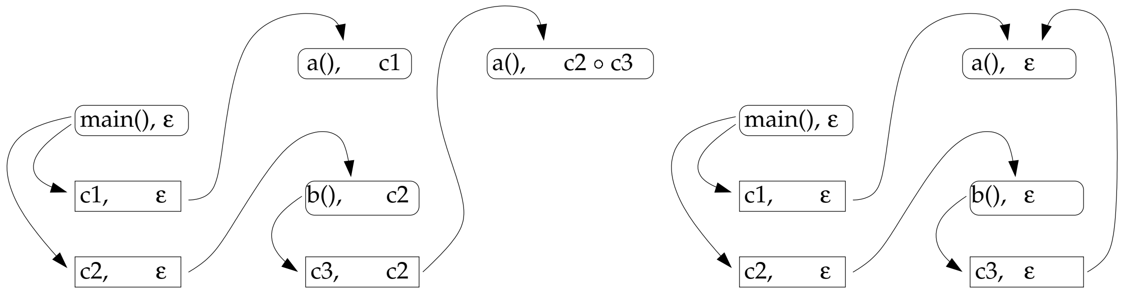

Figure 3.5: CG*: each node is a pair of basic block and context. a) on the left: CallString(2), b) on the right: CallString(0). b) is isomorphic to the CG of this program.

Example

```
void a (int x)
{  ...
   a(x-1);   // c2
   ...
}

int main (int, char**)
{
    ...
    a(5);    // c1
    ...
}
```

The contexts for CallString(2) and CallString(1) are as follows:

	CallString(2)	CallString(1)
for main()	ε	ε
for a()	c1	c1
	c1 ∘ c2	c2
	c2 ∘ c2	

As can be seen, the 'older' parts of the execution history are chopped off.

3.3.5 VIVU(n, k)

For better precision of loop analysis, we have developed a mapping technique that distinguishes the first few iterations from all other iterations, which are joined in one context. By this, loops are *virtually unrolled*.

To do this, the CallString(k) approach is modified to add a *saturated counter* to each context link in order to count how often a routine is recursively invoked.

Saturation of the counter is indicated by the symbol $\top$. Loop back nodes do not occur in contexts anymore, but instead, the corresponding counter is incremented. VIVU(n,k) is the mapping where n distinctions are the maximum, i. e., the counter may have the values $1,\ldots,n-1,\top$, and where the contexts may not be longer than k elements.

Several VIVU mappings have been introduced before (*see* [Martin, 1999b]). The VIVU mapping that will be introduced here is the most recent development involving different loop unroll counts per loop.

The idea is that in the best case, a loop should be unrolled as often as it is maximally iterated for maximal precision. Because there might be problems with complexity, an unroll limit n is added to the mapping. [1]

Definition 3.14 (Saturated Set of Positive Integers)
For $n \in \mathbb{N} \cup \{\infty\}$, let

$$\overline{\mathbb{N}}_n := \begin{cases} \{1,\ldots,n-1,\top\} & \text{if } n \in \mathbb{N}, \\ \mathbb{N} \cup \{\top\} & \text{otherwise.} \end{cases}$$

Definition 3.15 (Saturated sum)
For $n \in \mathbb{N}$, let $i +_n j, i \in \overline{\mathbb{N}}_n, j \in \mathbb{N}_0$ be defined as follows.

$$i +_n j = \begin{cases} \top & \text{if } i = \top \vee i + j \geq n \\ i + j & \text{otherwise.} \end{cases}$$

With this definition, we can now define VIVU(n,k). Also recall that $n_{\max}(e)$ is the maximum loop iteration count.

Definition 3.16 (VIVU(n,k) –"VIVU-4")
Let $\hat{E}^{\text{call}} := \hat{E} \cup \text{Calls} \times \text{Starts}$, i. e., those CG edges that enter a routine.

[1] In the PAG framework, the style of mapping introduced here is known as VIVU-*4*. (And the version where k is the constant unroll count for all loops is known as VIVU-*ht*).

Let $\mathsf{VIVU}(n,k) = (\hat{E}^{\text{call}} \times \overline{\mathbb{N}}_n, \oplus_n^k)$, where $k \in \mathbb{N}_0 \cup \{\infty\}, n \in \mathbb{N} \cup \{\infty\}$, and

$$\begin{aligned} &((c_\nu, s_\nu), i_\nu)_{\nu \in \{1,\dots,l\}} \oplus_n^k (c_{l+1}, s_{l+1}) \\ &= \begin{cases} ((c_\nu, s_\nu), i_\nu)_{\nu \in \{1,\dots,\lambda-1\}} \circ ((c_\lambda, s_\lambda), i_\lambda +_{\min\{n, n_{\max}(c_\lambda, s_\lambda)\}} 1) & \text{if } \exists \lambda \text{ such that } s_\lambda = s_{l+1} \\ & \text{(use the minimal } \lambda \text{ here)} \\ \left| ((c_\nu, s_\nu), i_\nu)_{\nu \in \{1,\dots,l+1\}} \right|_k \text{ where } i_{l+1} := 1 +_n 0 & \text{otherwise.} \end{cases} \end{aligned}$$

Note: the minimal λ in the first clause of the definition is used for formally getting a complete definition: when successively generating contexts from ε, there is maximally one such λ.

Claim 3.17
$\oplus_n^k$ is well-defined.

Proof
The only thing that might be unclear is why the saturated addition may be used without problems, since n is allowed to be $= \infty$.

To see this, see that $\min\{n, n_{\max}(c_\lambda, s_\lambda)\} < \infty$ for any n, even if $n = \infty$, since it is required that a maximal loop bound is given for each loop. So $n_{\max}(c_\lambda, s_\lambda) < \infty$ for every c_λ. ▭

Since most calls only have a single possible target, it is common to only write the call nodes for simplicity instead of the complete call edge in the VIVU context links.

Because recursion is folded in the VIVU-approach by the introduction of a saturated counter, VIVU generates finite context sets even if $k = \infty$, since nothing but call graph cycles, i. e. recursion, leads to infinite call strings. However, this has to be proven.

Claim 3.18
$\oplus_n^k$ is a finite context connector.

Proof
It must be shown that $\oplus_n^k$ produces finitely many contexts only.

Unfortunately, the underlying domain of context links $\hat{E}^{\text{call}} \times \overline{\mathbb{N}}_n$ is infinite for $n = \infty$. However, for any given loop entry edge $e \in \mathsf{entries}(l), l \in L$, it holds that $\min\{n, n_{\max}(e)\} < \infty$.

So there is a maximum saturated index for each program, namely $n_0 := \max\{\min\{n, n_{\max}(e)\} \mid e \in \mathsf{entries}(l), l \in L\} < \infty$, since $|\mathsf{Calls}| < \infty$. Therefore, for a given program, context links are rather in $\hat{E}^{\text{call}} \times \overline{\mathbb{N}}_{n_0} \subseteq \hat{E}^{\text{call}} \times \overline{\mathbb{N}}_n$. Because $\left|\hat{E}^{\text{call}}\right| < \infty$ and $n_0 < \infty$, it follows that $\left|\hat{E}^{\text{call}} \times \overline{\mathbb{N}}_{n_0}\right| = \left|\hat{E}^{\text{call}}\right| \cdot n_0 < \infty$.

What is left to be shown is that each context that can be produced has finite length. For $k < \infty$, this is clear. The maximum length is k in that case.

If $k = \infty$, there are still only finitely many contexts, since by Definition 3.16 on the previous page, no edge with the same start node can occur twice in one context (because these edges are collapsed by the use of a counter). So the maximal length of a context is $|\mathsf{Starts}| < \infty$. ▭

Figure 3.6 on the next page also shows a $\mathsf{VIVU}(n,k)$ mapping for the example recursion to show how the mapping works.

Most significantly, the counter element of $\mathsf{VIVU}(n,k)$ prevents that the $\mathsf{CG}^\star$ contains joins for every recursion, because the contexts are not shifted, but simply a counter is incremented. This yields better precision w.r.t. execution history.

3.3.6 Example

```
void a(int i) {
   ...
       a(...); // c3
   ...
}
int main() {
   a (10);     // c1
   a (20);     // c2
}
```

Figure 3.6 on the next page shows the CG and some $\mathsf{CGs}^\star$ for different context mappings.

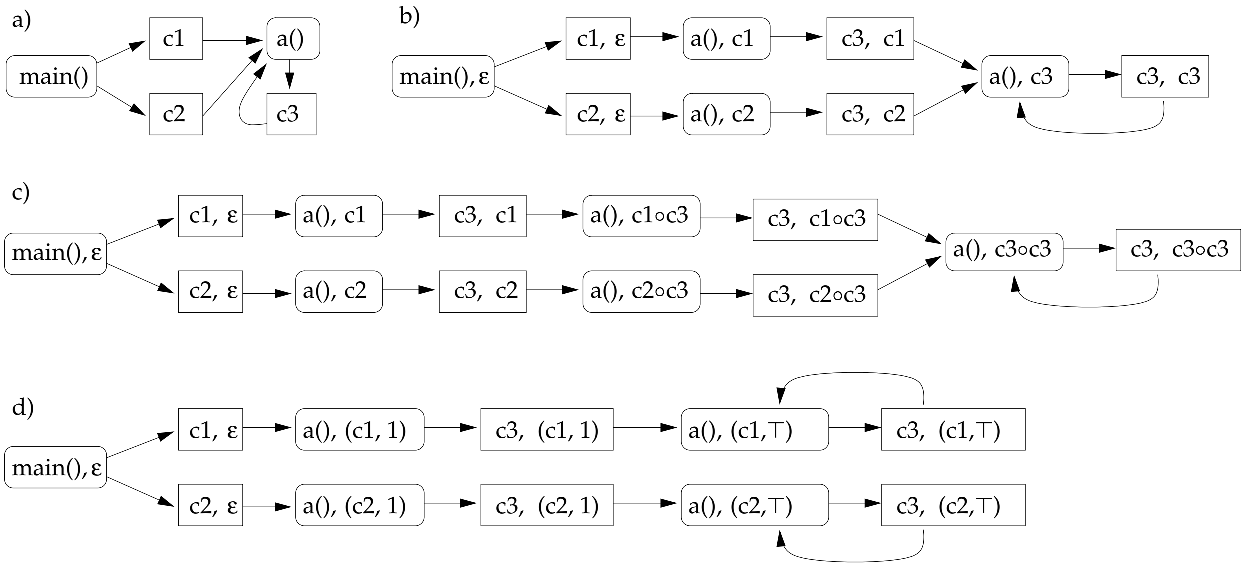

Figure 3.6: a) CG of Example 3.3.4. b) CG* with CallString(1) mapping: the distinction by the two calls from `main()` is always lost in `a()`, because of the recursion. c) CG* with CallString(2): regardless of the maximum length, `a()` is never distinguished by the call from `main()`. d) CG* with VIVU$(2, 1)$ mapping: the two calls in main remain distinguished in spite of the recursion.

Part II

Control Flow Graphs and Binary Executables

Chapter 4
Introduction

Analyses for WCET prediction for real-time systems usually work on executable programs. The reason is that modern hardware involves techniques that are only predictable at a level close to hardware. Examples for these techniques are caches and pipelines.

Caches improve execution time by storing recently used data. Reading and writing to a cache is much faster than writing to main memory, therefore, assuming that recently used data is likely to be used again, accesses can be sped up.

This additional store between the main memory and the processor (sometimes organised in several layers with different sizes and access times) makes program execution time depend on the execution history. For an analysis to be able to take cache behaviour into account, it must know about accessed memory addresses.

Pipelines improve execution speed by overlapping the processing of subsequently executed instructions. Due to dependencies between instructions, this overlap is usually not perfect, but instead, instructions sometimes stall until dependencies are resolved. An example is an instruction that has to wait for a result of a previously executed instruction before it can use that result for its own computations.

Due to this, instructions' execution times depend on the instructions that have been executed before. Also, pipeline behaviour usually depends on cache behaviour, since if an instruction waits for data from main memory, dependencies in the pipelines may be resolved in parallel.

To summarise, for modern architectures it is usually necessary for a precise analysis to know *memory access addresses*. I. e., it is not sufficient to know the names of data and code labels, but the precise addresses on the hardware should be known for making precise predictions.

Therefore, *statically linked executables* where all the low-level information are typically needed for a precise WCET analysis. The contrast to assembly or source code is as follows:

Machine instructions. In assembly programs, one assembly instruction might correspond to several machine instructions, e. g., some processors contain specialised versions of instructions where a register operand is fixed, which can be stored in less space.

On source code level, there is no information at all about what instructions are executed on the processor, since code generation is the task of the compiler. Particularly in the presence of sophisticated code optimisations, predictions about generated machine instructions are usually not possible.

For WCET analysis, it is important to precisely know which machine instruction is used, because the execution behaviour is different.

Addresses. On assembly level (also on higher levels), branches are specified by names, i. e., labels. For most modern processors, WCET analysis needs the addresses that the processor uses to predict its behaviour, since accesses to different addresses may result in different execution times.

Program analyses, including WCET analysis, usually work on an interprocedural control flow graph (ICFG), which must be available for all parts of the analysis chain. Chapter 3 has introduced ICFGs in detail.

When we started our research project, we needed such an ICFG from the very beginning in order to perform analyses. Work about WCET prediction usually starts with the assumption that the ICFG of the program is available.

To our best knowledge, there was no work in literature prior to our research that described a method of retrieving a CFG from binaries. This might have been the case, because modern architectures become more and more complicated making the retrieval of an ICFG more and more complex, or because other work groups were always supplied with and, therefore, could rely on debug information from the compiler.

However, there are cases where only the executable program is available, without debug information, from which the ICFG has to be reconstructed. Furthermore, hand-written assembly code that is compiled into the binary does not contain ICFG information from the compiler. Further, trusting the compiler about its debug information is usually not safe.

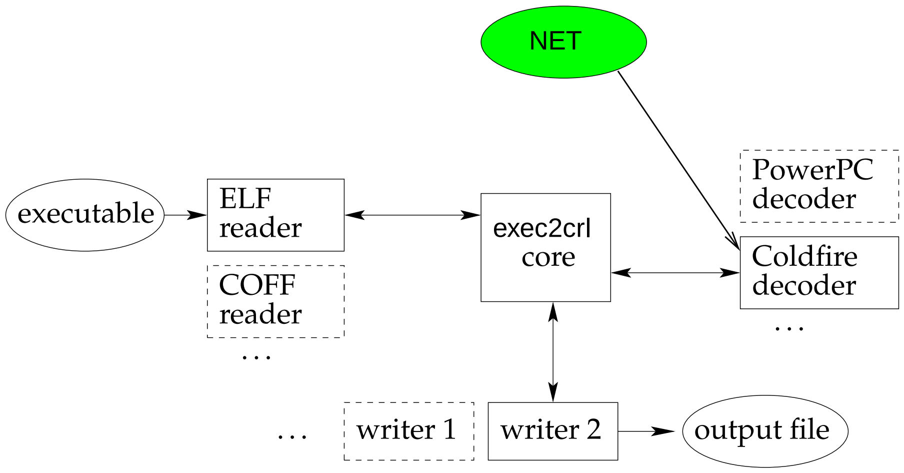

Figure 4.1: exec2crl: reader modules load executables; decoder modules, with the help of NET specifications, classify machine instructions for the core, which reconstructs the control flow graph; writer modules write the CFG into output files.

The following chapters will describe in detail our method of reconstructing control flow from binaries.

When analysing real-time systems, this control flow has to be safe and precise for analyses to be, too. Therefore, a generic tool named exec2crl was developed that reads binary executables, analyses machine instructions and reconstructs the ICFG for analyses of real-time systems.

The exec2crl tool is now used in all of our major projects on real-time system analysis developed at Universität des Saarlandes and it is also used in commercial tools developed by AbsInt Angewandte Informatik GmbH. Although first developed for WCET analysis, it is now also used for stack analyses, visualisation tools and will most likely be used for optimisation frameworks, too.

Figure 4.1 shows the design of exec2crl. It consists of modules for readers, decoders and writers, making it modular and generic.

4.1 Problems

The exact reconstruction of an ICFG from the binary for modern architectures is very difficult. Architectures use most different features and every new microprocessor seems to introduce new features and, thereby, new problems for reconstruction. For this reason, the ICFG reconstruction tool, exec2crl, is designed to consist of modules that can easily be adapted to new architectures and, along with that, to new problems.

Typical problems of CFG reconstruction on modern hardware include the following:

- memory indirections that are used to influence control flow (jump or call tables, routine variables, etc.),
- ambiguous usage of machine instructions,
- support for multiple instruction sets that are switched while the program is executed. Even worse, sometimes a sequence of bytes at a fixed address might be executed in different instruction sets.

In the following chapters, examples for these problems will be shown.

For some problems, a constant propagation would be helpful to get precise control flow. However, for such an analysis, an ICFG is needed, so there is a chicken and egg problem.

Our solution to this chicken and egg problem is similar to that of [De Sutter et al., 2000], namely to compute an approximation of a conservative ICFG first, which is annotated with the aspects of uncertainty. This ICFG is then suitable for a subsequent analysis (e. g. a constant propagation) to resolve the uncertainties left.

4.2 Steps of Control Flow Reconstruction

The process of ICFG reconstruction can be split into two parts:

- classification of bytes in the input byte stream from the executable,
- recursive reconstruction of control flow based on these classifications.

Figure 4.2 shows these two parts.

The classifier reads a stream of bytes from the executable.

The reconstruction part uses the classifier to get a classification for the bytes at a given address. This classification contains precise information about the machine instruction at this address, which is required to reconstruct the control flow. The result of the recursive reconstruction is the desired control flow graph.

The classification of single instructions from a stream of bytes will be described in detail in Chapter 5. The recursive reconstruction of the CFG from the decoded instructions will be dealt with in Chapter 6.

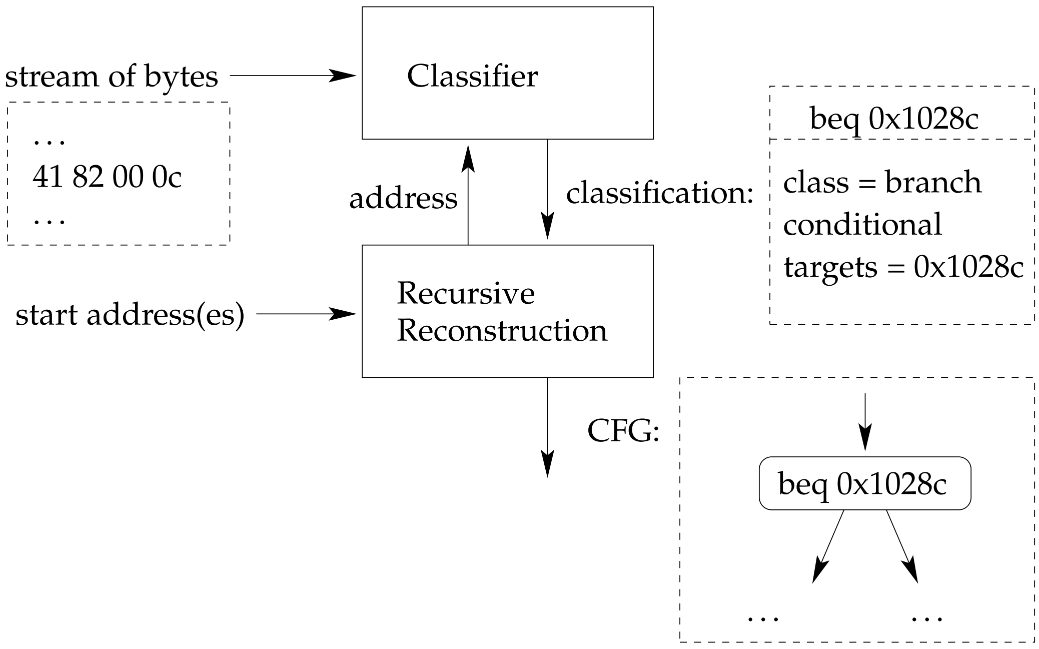

Figure 4.2: Reconstruction of control flow is divided into two parts.

4.3 Versatility

Although our WCET framework for real-time systems only works with statically linked executables, the ICFG reconstruction algorithm should also be able to handle object files and partially linked executables with external routines, since our tool should be versatile. It should be usable for other purposes, too, e. g. for optimisation or other static analyses (e. g. stack usage analysis).

Therefore, the following chapters also focus on handling external routines.

Chapter 5
Machine Code Decoding

5.1 Introduction

In the first step of control flow reconstruction, it is necessary to efficiently extract machine instructions from a byte stream. The reconstruction algorithm will demand a classification of a machine instruction for a byte stream and an offset position. So we face the problem of matching the list of patterns for machine instructions given in the user manual against a sequence of bytes. Debuggers and analysers all face this task. Usually this step is implemented manually (e. g. in the BinUtils package (*see* [Binutils])).

Because we analyse real-time systems, our task is to decode byte streams into instructions, which must be classified precisely for *safe* analysis.

Manual implementation for every target architecture, however, is an error-prone task. Instead, it is desirable to use the vendor's machine code documentation directly to write a specification and have the decoder generated automatically. This way, for every target, only the specification has to be written, thereby increasing the degree of safety.

5.1.1 Bit Patterns

This chapter presents an algorithm whose input is a set of bit patterns, one for each machine instruction to be recognised. This set of bit patterns can be taken directly from the architecture's manual. These bit patterns are characterised as follows: for each bit, Input bit stream: **10**010100101...

000?	$\mapsto$ Instruction 'A *op1*'	Step 1: Mismatch
01??0	$\mapsto$ Instruction 'B *op1*'	Step 2: Mismatch
01??1	$\mapsto$ Instruction 'C *op1*'	Step 3: Mismatch
10	$\mapsto$ Instruction 'D'	Step 4: Match
11??	$\mapsto$ Instruction 'E *op1, op2*'	(not tried to be matched for this input stream)

Figure 5.1: Linear Way of Decoding with search complexity of O(#patterns) for each instruction to be decoded. The left side shows an example set of bit patterns consisting of five instructions. The right side shows how a simple algorithm would check each pattern in the set until a matching one is found.

Instr.	Bit Pattern b_0	b_1	b_2	b_3
A	0	$*$	$*$	0
B	1	$*$	$*$	1
C	0	$*$	0	1
D	0	$*$	1	1
E	0	0	0	0

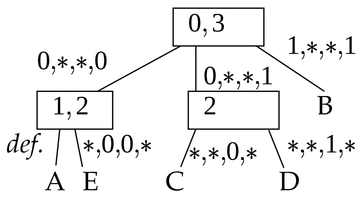

Figure 5.2: Example input for four bit commands and the computed decision tree. The nodes are labelled with the set of bit indices tested in that node. Specialised bit patterns are handled by a default edge labelled *def.* (E is a specialisation of A).

it is specified whether its value is *zero*, *one* or *insignificant*.

Such a set of bit patterns can be used to decode a bit stream almost directly, but very inefficiently, by matching each bit pattern against a given bit stream. This method has linear runtime (in the size of the set of bit patterns). Figure 5.1 shows this method of decoding. This solution is not acceptable and, therefore, a decoding method was developed that is based on decision trees.

5.1.2 Selected Design Goals

Our algorithm uses the set of bit patterns to recursively compute a decision tree for decoding. The decoding algorithm only accesses those bits that the user specified to be significant, and only tests each bit maximally once. Figure 5.2 shows a simple example.

A major advantage is that our algorithm needs no user defined order in which bits shall be tested and no specification of bit fields (e. g. primary, secondary opcode) in the machine code, whereas programmers of decoders that are implemented manually have to cope with deciding about the order of bit tests manually, too.

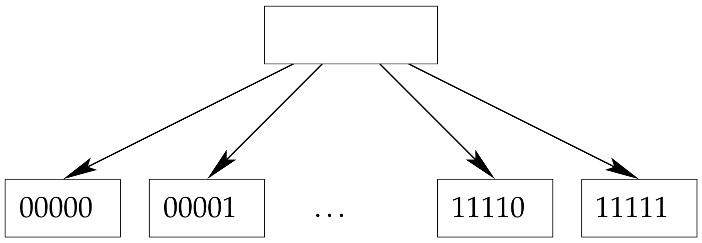

Figure 5.3: A minimally deep decision tree for 5 bits: the root has 32 children. This kind of tree is infeasible for 32 bit processors, of course.

Our algorithm facilitates writing a specification from vendor manuals that are organised as a long list of machine instructions as well as from bit field based manuals that are divided into instruction groups by e. g. a primary opcode. The framework has interfaces for both specification methods. Other styles are easily supported by simply listing all possible instructions. We even succeeded in converting an architecture manual in PDF format into a specification skeleton automatically.

The generated decision tree consists of inner nodes that describe how to make a decision and of leaves that contain results. In the framework, the leaves contain machine instruction classifications suitable for reconstruction of a control flow graph (*see* [Theiling, 2000]). They will be used in the following chapter to reconstruct the control flow. Each decision node describes which bits have to be tested in the input bit string to select a child at this node.

The decision tree should be as shallow as possible in order to require the smallest number of tests. Our algorithm computes a partition at each inner node of the decision tree that tests the maximally possible number of bits at that node. This involves testing non-adjacent bits in one step. This is an advantage compared to other approaches.

In addition to being shallow, the data structure should also be cheap w.r.t. memory consumption. E. g., an ideally shallow tree for decoding could consist of 2^n children directly at its root to be able to decode n bit machine instructions, resulting in a tree depth of only 1. Obviously, the number of nodes is infeasibly huge e. g. for 32 bit processors. Figure 5.3 shows such a trivial tree.

Furthermore, our tree is required to always test all significant bits for all inputs even if the final selection decision can be drawn from fewer bits. This is because the algorithm operates in the safety critical environment of real-time system analysis, where every part is required to be *safe*. In this safety critical environment, the putatively superfluous test serves to detect malformed input bit strings.

In general, sets of bit patterns need not be decidable, i. e., there may be more than one pattern that matches the input bit string. Undecidable sets of bit patterns do occur in spite of expecting existing CPUs to know what to do next from the bits they execute.

Of course, the CPU deterministically decides what to do next (if a valid instruction is executed). However, there may be an instruction with a general pattern and a special instruction that is exceptional, where the special instruction is handled first. This might be reflected in the manual by a general bit pattern and a more specific one, specifying something different. Because this method of specification is quite frequent, our algorithm can handle these specialisations.

So our algorithm is able to handle specialisations of machine instructions, i. e., patterns that are subsumed by others. This is done by a default child that is used if no special child was found during a decision. This child must always be a leaf node.

We have implemented a decoder for the Coldfire architecture, the PowerPC and the ARM/Thumb architecture using this technique. Sets of bit patterns have already been tested for the Infineon C166 processor.

5.1.3 Chapter Overview

This chapter is structured as follows. Section 5.2 introduces decision trees for decoding machine instructions formally. Then, Section 5.3 introduces our algorithm in detail. After that, Section 5.4 presents an efficient way of implementing the algorithm and shows its run-time.

5.2 Data Structure

Given a mapping of bit patterns to machine instruction classifications, the goal is to construct a decision tree for implementing that mapping. Formally, this can be described as follows:

Definition 5.1
Let $\mathbb{B} = \{0, 1\}$ be the set of bits. Let $n \in \mathbb{N}$. A *bit pattern b* is a string of bits together with a set of significant bit indices: $b \in \mathbb{B}^n \times \mathfrak{P}(\mathbb{N})$. Thus, n is the width of the bit patterns.

Let D be a set of machine instruction classifications (whose precise structure is irrelevant for the algorithm). Then $f_0 : \mathbb{B}^n \times \mathfrak{P}(\mathbb{N}) \to D$ is a mapping from bit patterns to classifications.

A pattern could have been defined as a tuple over $\{0, 1, *\}$, but this would have complicated the definition of the algorithms in the following.

Also note that defining that all bit patterns have the same length n does not mean that machine commands have the same length. Shorter patterns can simply be padded with insignificant bits. But for the sake of easy presentation, the length was fixed to n.

In the following, we will regard the input for the algorithm as the set that represents f_0, so we will treat $f_0 \subseteq \mathbb{B}^n \times \mathfrak{P}(\mathbb{N}) \times D$. Let $F := \mathbb{B}^n \times \mathfrak{P}(\mathbb{N}) \times D$ to improve readability.

For a triple $(b,m,d) \in F$, we define

$$\begin{array}{rcll} bits(b,m,d) & = & b & \textit{the bit values} \\ mask(b,m,d) & = & m & \textit{the indices of significant bits} \\ data(b,m,d) & = & d & \textit{the classification} \end{array}$$

We will often show insignificant bits as $*$.

In the following definition, the instruction classifications are used as terminal nodes of decision trees for binary decoding.

Definition 5.2
A *decision tree* is a labelled tree (V,E) where $V = D \cup N$, D the set of terminal nodes, N the set of inner nodes and $E \subseteq N \times (N \cup D)$ the edges of the tree.

Node labels are assigned by a function $node\_label(v) \subseteq \mathbb{N}, v \in N$ which are the bit numbers of the bits to be tested at node v.

For $e \in E$ let $edge\_label(e) \in \mathbb{B}^n \cup \{\text{default}\}$ be the function that labels an edge e.

Edge labels are required to unambiguously mark outgoing edges, i. e., $\forall (n,n_1),(n,n_2) \in E, n_1 \neq n_2 \Rightarrow edge\_label(n,n_1) \neq edge\_label(n,n_2)$.

5.2.1 Selection Algorithm

A decision tree can be used to select a machine code classification from a bit string as follows. Let $(b_0,\ldots,b_{k-1}) \in \mathbb{B}^*$ be the input bit string of length k. In the decoder application, this is a block of bytes from the executable of which the first instruction is to be classified by a $d \in D$. d stores the bit width of the command, so that this many bits can be skipped and the decoding can advance to the next instruction in the bit string.

The following selection algorithm selects the first instruction from the bit string by using the decision tree.

During the algorithm, v is the current node in the decision tree and v_d will be the most recently encountered default node, i. e., the most specific one.

Step 1 Start the selection by letting v be the root node of the tree and $v_d = \text{undef}$.

Step 2 If at the current node $v \in N$, there is an edge $e = (v,v')$ such that $edge\_label(e) = \text{default}$, then let $v_d = v'$.

	bit 1	bit 2	bit 2
A	1	1	1
B	1	0	$*$
C	1	$*$	$*$
D	$*$	$*$	$*$

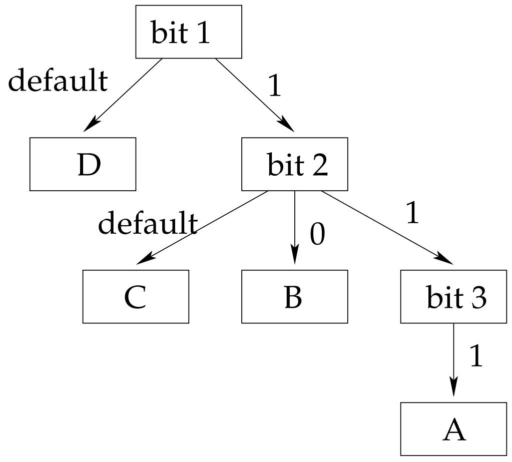

Figure 5.4: Matching of (1,1,0) requires default node backtracking to find the match C. Without it, selection would fail because the decision node for bit 3 has no default node, so we must backtrack to the default node at the node for bit 2.

Step 3 If v is a leaf, that node is the algorithm's result.

Step 4 At the current node $v \in N$, try to select an outgoing edge $e = (v, v')$ such that $\forall i \in \mathit{node\_label}(v)$:

$$\begin{aligned} & i < k \\ \wedge\ & \mathit{edge\_label}(e) \neq \text{default} \\ \wedge\ & \mathit{edge\_label}(e)_i = b_i \end{aligned}$$

If such an edge e exists, go to Step 2 with $v := v'$. (Since edge labels uniquely mark outgoing edges, maximally one such node exists.)

If e does not exist, and if $v_d \neq$ undef, go to Step 3 with $v := v_d$ and let $v_d =$ undef.

Otherwise, let the selection fail, since no classification exists for the input bit pattern.

This selection algorithm keeps track of the most recent default node in order to be able to backtrack if the selection algorithm fails on subsequent nodes. The backtracking is important for the algorithm only to fail if there is no matching pattern:

Without keeping track of old default nodes, no node would be found for the input $(1,1,0)$, although C matches (*see* Figure 5.4). Note that we do not need a *stack* of default nodes for backtracking, since the default nodes are required to be leaves, so no failure can occur in subtrees of default nodes.

Efficient Implementation

The selection algorithm can be implemented very efficiently if $(b_0, \dots, b_{k-1})$, $\mathit{edge\_label}(e)$ and $\mathit{node\_label}(v)$ are implemented as machine words (insignificant bits set to zero). We will write the conversion to bit tuples (thus, machine words) using parentheses, e. g.:

$$(\mathit{node\_label}(v)) = (m_i)_{i=0,\dots,n-1} \text{ where} \tag{5.1}$$

$$m_i = \begin{cases} 1 & \text{if } i \in \mathit{node\_label}(v) \\ 0 & \text{otherwise} \end{cases} \tag{5.2}$$

Children of $v \in N$ are stored in a hash table at node v that is indexed with the labels $\mathit{edge\_label}(e)$. Then, a child can be selected by indexing the hash table with $(b_0, \dots, b_{k-1})$ `bit_and` $(\mathit{node\_label}(v))$. (This operation possibly needs padding to equal bit lengths. Typically, padding is done to the width of machine words). If the hash table lookup fails, a default child can be selected if one exists.

5.2.2 Restrictions on Pattern Sets

The goal of the algorithm presented in the following section is to compute N, E, $\mathit{node\_label}$ and $\mathit{edge\_label}$ in such a way that the number of edges and nodes is kept small. Insignificant bits shall never be tested by the above selection algorithm. Significant bits shall only be tested once.

We do not expect that a decision tree can be built for all input bit pattern sets. Consider the following patterns:

$$\begin{array}{ll} \text{A} & 0 * * * \\ \text{B} & * * * 0 \end{array} \tag{5.3}$$

It is unclear which pattern should be selected for e. g. $(0, 0, 0, 0)$.

One way of resolving this problem is by assigning priorities to ambiguous bit patterns. However, our bit patterns are descriptions of micro processors, so we expect them to be unambiguous since the processor can identify them uniquely as well. Therefore, we decided that prioritisation need not be included in our algorithm.

Furthermore, our algorithm will not handle pattern sets like the following, which provide a unique match for all inputs, but require that insignificant bits be tested.

$$\begin{array}{ll} \text{A} & 1\,0 * \\ \text{B} & 0 * 1 \\ \text{C} & * 1\,0 \end{array} \tag{5.4}$$

Again, we assume that microprocessors will not have machine code bit patterns organised like that. Techniques to handle these patterns by testing some of the insignificant bits are described in [Laville, 1991] for functional languages with argument pattern matching.

5.3 Automatic Tree Generation

We consider a decision tree where all possible bit combinations are checked in the root node to be infeasible due to the typically huge number of $O(2^n)$ edges.

The goal will be to have few nodes and few edges. We decided that the we will not check any insignificant bits, which will naturally bound the number of nodes and edges, because bit patterns not in the input will not be checked in the tree. With this prerequisite, the depth of the tree will be the measure of quality.

The principle of the construction will be to make inner nodes in such a way that they test maximally many significant bits at once, since they have to be tested anyway. On the other hand, the algorithm will prevent testing any insignificant bits in order to keep the out-degree of the nodes small.

5.3.1 Idea

The idea of our algorithm is *recursive partitioning* of the input set of bit patterns. First, a set of bits is computed that are significant for all patterns. Then, the input set is partitioned into subsets that have different values for these significant bits. For each set, the algorithm recurses. The recursive function of the algorithm returns a new node with the sub-tree underneath. Together with the subset of the input bit patterns, a mask of already tested bits will be passed down the recursion to prevent double testing of bits (this will be called *gmask* in the algorithm).

Figure 5.5 depicts the idea of recursive partitioning the bit patterns.

At the beginning of the algorithm, we assume all bits to be potentially significant, so the initial bit mask is $\{0,\ldots,n-1\}$. So in order to compute the decision tree, make_tree is invoked in the following way, where f_0 is the set of machine code bit patterns from the user.

```
make_tree ($f_0$, $\{0,\ldots,n-1\}$)
```

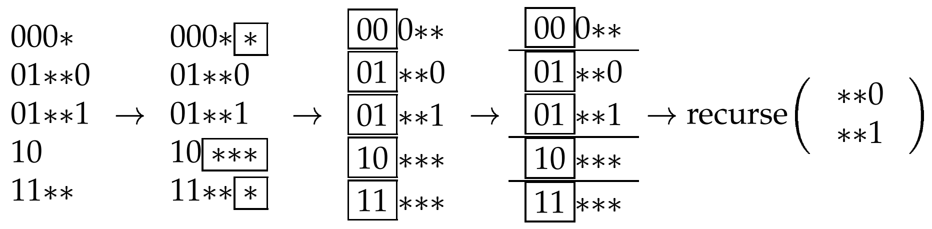

Figure 5.5: Recursive partitioning for a small example. Step 1: pad bit patterns to equal length. Step 2: Identify columns of significant bits. Step 3: Make a partition according to significant pattern bits. Step 4: Recurse for non-singleton partitions.

5.3.2 Algorithm

The algorithm is depicted in Figure 5.6 on page 82 and will be described in detail now.

Throughout the algorithm, we require $f \neq \{\,\}$. This is needed for well-definedness at some points.

Step 1 of the algorithm computes a bit pattern of bits that are significant in all patterns in f. The bit pattern is maximal, i. e., a bit is only found to be insignificant if there is a pattern where it is insignificant, due to the definition of the set intersection.

Deciding about termination in Step 2 works by checking that no significant bits remain and that f is a singleton. It is necessary to ensure that no significant bits are left in *mask*, since the selection algorithm must test all significant bits in the input bit string even if there is only one candidate left for selection. This must be done in order to detect malformed input bit strings.

In Step 3, we know that no leaf, but an inner node will be generated.

For the sake of simplicity, explaining Step 4 will be postponed. For now, we assume that if a default node was selected, it is the correct one, that its pattern has been excluded from f and that $mask \neq \{\,\}$ after Step 4.

In Step 5, the selection mask for the new node is known and assigned as a node label.

Partitioning in Step 6 groups bit patterns that have the same bit values for the significant bits defined by *mask*. The function returns the set of equivalence classes for each element of f. An efficient implementation will be given later.

```
fun partition ($f \subseteq F$, $mask \subseteq \mathbb{N}$)
  return $\{$ equ_class($p$) : $p \in f \}$
  where equ_class ($p$) =
    $\{p' : p' \in f$ such that $\forall i \in mask : bits(p')_i = bits(p)_i\}$
```

Note that each equivalence class equ_class(p) contains at least one element, namely p,

```
fun make_tree ($f \subseteq F$, $gmask \subseteq \mathbb{N}$)
returns $\in N \cup D$
  – Step 1: compute a bit mask of bits that are significant for all patterns
  $mask := gmask \cap \bigcap_{p \in f} mask(p)$

  – Step 2: possibly terminate: f must be singleton
  if $mask = \{\}$ and $|f| = 1$
    return $data(p)$ where $f = \{p\}$

  – Step 3: construct a new node
  $v$= new InnerNode

  – Step 4: decide about default node and edge
  if $mask = \{\}$
    ($v^{\mathrm{def}}$, $f$, $mask$):= get_default ($f$, $gmask$)
    $e^{\mathrm{def}}$ := new Edge ($v, v^{\mathrm{def}}$)
      with $edge\_label(e^{\mathrm{def}})$ := default

  – Step 5: label the current node
  $node\_label(v) := mask$

  – Step 6: make partition of f using mask
  $\{f_1, \ldots, f_k\}$ := partition ($f$, $mask$)

  – Step 7: recurse on subsets and add edges
  for $i$ in $\{1, \ldots, k\}$
    $v'$:= make_tree ($f_i$, $gmask \setminus mask$)
    $e'$:= new Edge ($v, v'$)
      with $edge\_label(e')$ := get_label($f_i, mask$)

  – Step 8: return the new node
  return $v$
```

Figure 5.6: Decision tree generation algorithm

so no empty sets will be used during the recursive calls in Step 7, thus the new sets all fulfil the requirement made in Step 1.

Finally in Step 7, the function make_tree invokes itself recursively for all subsets found in Step 6. The bits that have been tested at node v are excluded from the new *gmask* to prevent repeated testing of the same bits. Computation of an appropriate edge label remains to be defined.

```
fun get_label ($f_i \subseteq F$, $mask \subseteq \mathbb{N}$) returns $\in \mathbb{B}^n$
– Extract significant bits from some element of $f_i$
  return value_bits($p$) for some $p \in f_i$
  where value_bits $(p)_j = \begin{cases} bits(p)_j & \text{if } j \in mask \\ 0 & \text{otherwise} \end{cases}$
```

This function is well-defined since for every pair of elements of f_i, the bit values selected by *mask* are equal due to the construction of the equivalence classes in the partitioning step.

5.3.3 Default Nodes

In the previous section, the handling of default nodes was postponed. To understand when these are needed, assume the following input to the algorithm:

$$\begin{aligned} f &= \{\,((0,0),\{\,\},A), \\ &\quad\ ((0,0),\{1\},B)\} \end{aligned}$$

Here, A subsumes B and the computation of *mask* in Step 1 will yield $mask = \{\,\}$ with f not being a singleton.

At this point, the default node should select A and the decision node should use the second bit to check whether B should rather be selected. If we made A the default node and repeated the computation of *mask* in this example, the effect would be as desired.

When the algorithm arrives at a node requiring a default node, significant bits common to all masks will always have been processed already, because otherwise the intersection of the masks is non-empty, therefore, the algorithm would not have arrived in get_default. So finding the default node is very easy: its set of remaining significant bits must be empty. This this node subsumes all others, therefore it classifies as a fall-back node, if no pattern that is more special matches.

There must be at most one node with this property, otherwise, the input set is undecidable as A and B in the following example:

```
fun get_default ($f \subseteq F$, $gmask \subseteq \mathbb{N}$)
    – Compute the set of bit patterns that have empty remaining bit masks
    $M := \{p : p \in f$ and $mask(p) \cap gmask = \{\,\}\}$
    if $|M| \neq 1$
        fail

    – Similar to Step 1, get a mask. Fail if empty.
    $mask := gmask \cap \bigcap_{p \in f \setminus M} mask(p)$
    if $mask = \{\,\}$
        fail

    – Return the result, M is a singleton
    return $(data(p), f \setminus M, mask)$ where $M = \{p\}$
```

Figure 5.7: The function that computes the default node and the new bit mask

	b_0	b_1	b_2	b_3
A	1	0	$*$	$*$
B	1	0	$*$	$*$
C	1	0	0	$*$
D	1	0	0	0

(5.5)

So we have seen that a) finding the default node is trivial by searching for an empty remaining bit mask and b) the algorithm need not recurse in the default node, because it must be a single input bit pattern: $|M| = 1$. We can simply use the data of that pattern as a leaf node.

Figure 5.7 shows the function get_default.

The algorithm fails if the set of bits is still irresolvable after exclusion of the default node. An example input for this situation would be the following:

	b_0	b_1	b_2	b_3
A	1	0	$*$	$*$
B	1	0	0	$*$
C	1	0	$*$	0

(5.6)

This function fulfils the constraint that after Step 4: $mask \neq \{\,\}$.

5.3.4 Unresolved Bit Patterns

get_default can be extended to handle bit patterns like (5.4) on page 79 but care must be taken: obviously, a bit has to be tested that is insignificant in some pattern. In (5.4), any bit could be chosen for disambiguation purposes. However, because machine instructions may have different lengths, decoding might fail although a valid instruction is in the input. As an example, consider (5.4) and an input bit string of $(1, 0)$. Clearly, pattern A should be selected. But if the algorithm had selected bit index 2 to resolve the pattern set, a node checking for a bit outside the input bit string is encountered before the correct decision can be drawn. Decoding would fail because the input bit string has fewer bits.

This is a similar problem as that of pattern sets in some lazy functional languages, where accessing insignificant arguments of a function in order to select a pattern might lead to non-termination if that operand does not terminate (*see* [Laville, 1991]).

Furthermore, in practice, we may have byte-swapped input, so in an implementation, the problem of test bits being outside the input bit string occurs at both sides of the bit patterns if the bit string is not known to be byte-swapped or not at pattern compilation time. In (5.4), the second bit should be selected, because this bit is either significant, or there are significant bits to both sides (and holes are impossible). So it can be concluded that the input bit string will contain the middle bit, if it contains a valid instruction.

To optimise the disambiguation w.r.t. the number of nodes and edges that are required, the number of patterns for which insignificant bits must be tested should be minimised.

This problem is non-trivial, but we do not expect it to occur with machine specifications anyway, so we did not try to implement a way of disambiguation.

5.3.5 Termination

Termination happens by either failing, in get_default, or succeeding, in which case the recursion comes to an end normally.

It can be seen immediately that in each new incarnation of a recursion, *gmask* contains fewer bit indices, as some are deleted in Step 7 by the non-empty *mask*, so eventually, *gmask* becomes empty and the algorithm terminates.

5.3.6 Proof of Correctness

Correctness of the selection and make_tree algorithms is defined in the following way. Assume that a decision tree can be computed. This implies that the input set is resolvable. Using that tree, the selection algorithm

1. always selects an input pattern that is matching if the set is resolvable,
2. selects the most specific pattern if more than one pattern matches,
3. never fails if a pattern matches unambiguously,
4. always tests all significant bits to have the desired value.

We will prove this claim by induction on the maximal number n of remaining significant bits in the input pattern set, taking into account the value of *gmask*.

$\mathbf{n = 0}$: Step 1 finds $mask = \{\,\}$. There are two possibilities:

Case 1: $|f| = 1$. This means that a node with the data of that pattern can be constructed. The recursion terminates.

During the selection, all of the above correctness prerequisites are fulfilled: the pattern matches (no more bits are significant), the most specific one is selected (there is only one), the algorithm does not fail (so it does not fail even of matching patterns exist), and all remaining significant bits have been tested (there is none left to be tested).

Case 2: $|f| \gneqq 1$: The pattern set is irresolvable and the algorithm fails. (3) holds, too, since the set is ambiguous.

$\mathbf{n+1}$: Assume the claim to be true for all numbers of remaining significant bits $\leqq n$. We now prove this is is true for $n+1$. After Step 1, there are two major cases:

Case 1: $mask \neq \{\,\}$: This means that no default node is needed.

The claim holds for all recursion steps, because some bits are removed from *gmask*, so $|gmask| \leqq n$ in all the recursive steps.

1. Partitioning makes clusters of patterns that are equal at the bits in *mask*. So when testing these bits, the selection algorithm makes the only correct choice and selects a pattern that is matched by the bits in *mask*. Because the claim holds for the recursion, subsequent selection steps also select the correct patterns for the remaining bits. So in total, the correct pattern is selected.
2. Because the default node is selected after all other patterns have been tested, the most specific subset of patterns is selected, since all patterns that failed a match have strictly more bits set. This holds in the recursion steps, too, so the most specific pattern is selected.
3. If no pattern matches, the selection algorithm either chooses the most specific default node (which matches) or fails, which means that no default node was available, so no pattern matches.
4. The bits in *mask*, which are significant in all patterns, will all be tested. The recursive steps make sure that all other significant bits will also be tested, so the claim is fulfilled for $n+1$, too.

Case 2: $\mathit{mask} = \{\,\}$. If there is only one pattern left, the argument is the same as for $n = 0$.

Assume that $|f| > 1$. A default node will be selected. If this succeeds, we have shown in Section 5.3.3 above that the default node is the least specific node and that all its significant bits have been processed. Furthermore, the number of significant bits of the default node is $\trianglelefteq n$ since the other patterns all have strictly more significant bits.

1. If it is selected, it is the correct choice as the number of bits is $\trianglelefteq n$.
2. Because the default node is selected after all other patterns do not match, the most specific one is selected (the other patterns have strictly more significant bits).
3. Analogously to the previous case, the selection algorithm only fails if no default node is available.
4. All significant bits of the default node have been tested.

For the other patterns, a new mask is computed in the same way as before, but excluding the default node. So the argument is the same as for $\mathit{mask} \neq \{\,\}$ (note that it has been shown that the default node is the least specific one, so the argument about specificity is valid, too).

Because we start the recursion with *gmask* containing all potentially significant bits, and the claim was proven for all remaining significant bits, the claim holds for all significant bits at the beginning.

5.4 Efficient Implementation

The algorithm can be implemented very efficiently by using bit masks if we require that a machine word has at least n bits, thus enough to store all values $\in \mathbb{B}^n$ directly. It can be assumed that operations on machine words, like bitwise 'or', 'and' or 'not' work in $O(1)$.

Bit masks can be stored in machine words by setting bits to 1 if the bit number of that bit is in the masking set or to 0 otherwise.

The input set f_0 can be stored efficiently in an array. The current subset can be marked using two integers as parameters of make_tree marking the first and last index of the subset in this array. In the recursive step, this works as follows: When partitioning, the sub-array is sorted locally considering only the bits in the bit mask. This way, the new partitions are adjacent in the sub-array and can be passed down in the same way.

Further, in the algorithms in the next chapter, the selection algorithm is used very frequently in order to classify instructions. To further improve performance, decision trees can be compiled together with the selection algorithm into ANSI C source code that can be compiled to get a very fast classification tool. We implemented this for exec2crl.

5.4.1 Complexity

With the help of the previous section a run-time for the algorithm can be computed. Let $m = |f_0|$ be the size of the input set and n the maximal width of the input patterns.

In each step of the algorithm, almost all steps work in $O(|f|)$ but partitioning takes $O(|f| \log |f|)$ due to the sorting that is done.

In each step, at least one bit is removed from $gmask$, so recursion depth is maximally n. In the worst case, only two partitions are made in each step, one consisting of 1 element, the other of all but this element. Then the run-time is $T(n,m) = O(n + \sum_{i=m,\dots,m-n+1} i \log i) = O(n + n \cdot m \log m)$. So if $n = m$, it becomes $O(m^2 \log m)$.

This worst case run-time looks slow. However, we expect m much larger than n, because the input is machine code patterns, where there are much more commands than bits in a machine word. We also expect that the recursion is much more shallow than n, since usually only few groups of bits have to be looked at to select a command. In total, we expect the recursion depths to be around $\log(m)$, since with $\log(m)$ bits, maximally m commands can be coded. Run-time then becomes quasi-linear in m.

The experiments have shown that the trees are even more shallow than $\log(m)$, so practice has justified the assumption.

5.4.2 Generalisation

The bit patterns that were used above can be viewed as sets of boolean attributes. This means that the algorithm is directly usable in applications where property tables with boolean attributes are the input. The benefit is parallel testing of attributes in each decision step and the possibility to have insignificant attributes.

Of course, the alphabet could also be extended to be non-boolean (only an equality operator is required). However, the algorithm's major efficiency results from working with machine words, so that parallel testing of several attributes works in $O(1)$. But if the attribute values can be distributed to several bits (e. g. a four-value attribute uses two bits instead of one), the algorithm can still be applied.

5.5 Summary

This chapter has shown how a decision tree can be built from a bit pattern set to be used in order to quickly select a bit pattern matching an input bit stream. For using this selection for decoding, the bit patterns will be associated with a precise classification of the machine instruction. This is used in the next chapter for reconstructing a safe ICFG.

Chapter 6

Reconstruction of Control Flow

6.1 Introduction

This chapter focuses on the second step of the CFG approximation, namely the approximation of a conservative CFG by using knowledge about the compiler and the target architecture. We construct the approximative CFG with the real-time system analysis in mind, i. e., it must be *safe* and must be *as precise as possible*. The next steps, refining the CFG by constant propagation, loop reconstruction, and then performing analyses has been discussed in literature (e. g. in [Ferdinand et al., 1999b; Kim et al., 1996; Li et al., 1996; Martin, 1999b; Ramalingam, 2000; Sreedhar et al., 1996; De Sutter et al., 2000; Theiling and Ferdinand, 1998]).

A bottom-up algorithm will be presented that overcomes some deficiencies of top-down algorithms. This chapter will also describe how top-down algorithms for ICFG reconstruction work and work out their flaws in detail. Very briefly, top-down algorithms rely on information about routine boundaries from executables. These are usually given as start and end addresses. It is a common compiler technique, however, to store certain data in code sections, e. g. target addresses of switch tables. When searching for target addresses by looking at each instruction of a routine separated by the above method, the data portions might be misinterpreted as instructions and incorrect target addresses might be used for control flow reconstruction.

Another aspect is that routines might be interlocked if a cache-aware compiler is used. This can also not be described by using start and end addresses.

A bottom-up approach does not suffer from these deficiencies. Each instruction *must* be classified completely and correctly before it is used in analyses. Based on these safe classifications, jump and call targets are used to compute routines and their extents. This means that data portions will be skipped and interlocked routines can be handled correctly. Finally, a bottom-up algorithm does not rely on additional information from the executable. Instead, if available, it can be used for consistency checks.

Our approach aims at retargetability, so it was designed to be generic w.r.t. the underlying architecture, the used compiler and the input format of the executable. This was achieved by a module concept allowing extensions.

For two selected architectures, it will be shown that the CFG approximation algorithm is able to reconstruct the total CFG without the need of a constant propagation.

6.1.1 Overview

This chapter is structured as follows. Section 6.2 will identify the problems CFG reconstruction faces and will present the principal top-down algorithm to show its deficiencies. In Section 6.2.3, the algorithm will be introduced informally in order to make clear the idea. Section 6.2.4 will formalise the bottom-up approach to CFG reconstruction. Section 6.3 will present the module interface, Section 6.4 will show how our generic algorithms work and how they solve the problems. Section 6.5 will give an overview of the modules and describe examples for given architectures.

6.2 Approaches to Control Flow Reconstruction

Recall that a program's inter-procedural control flow graph (ICFG) is split into two parts.

1. A *call graph* (CG) describes the relationship between *routines*. Its nodes are call nodes and start nodes.
2. Each routine has a *control flow graph* (CFG), describing the control flow inside the routine. The edges in the CFG describe jumps and fall-through edges.

The CG-edges and CFG-edges are called *branches*.

The input of a CFG approximation is a binary executable, object code, or an assembly file. These contain a series of instructions, coded as bytes or text. Additional information may (but need not) be available: entry points, label and routine addresses, label and routine names, relocation tables, etc.

6.2.1 Top-Down Approach

A top-down approach to ICFG reconstruction works by relying on compiler generated information that has to be present in the input file. We consider binary input here. In the first step, the input byte stream is split into routines:

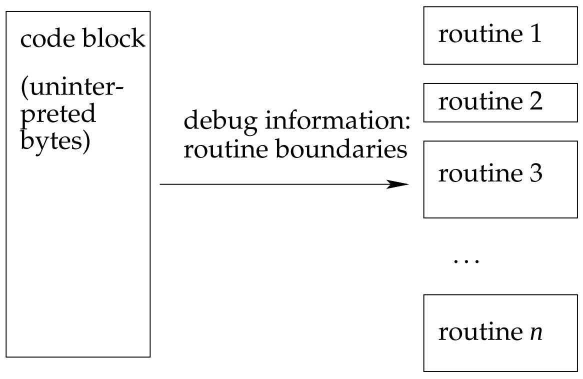

The second step is to sequentially decode each instruction in each routine in order to get a stream of instructions for each routine.

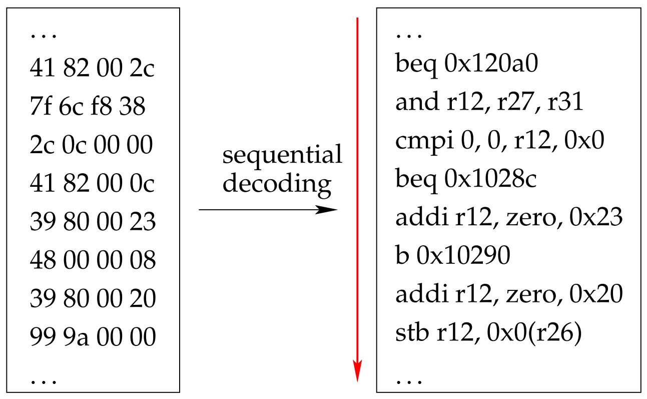

```
...
41 82 00 2c
7f 6c f8 38
2c 0c 00 00
41 82 00 0c
39 80 00 23
48 00 00 08
39 80 00 20
99 9a 00 00
...
```

```
...
beq 0x120a0
and r12, r27, r31
cmpi 0, 0, r12, 0x0
beq 0x1028c
addi r12, zero, 0x23
b 0x10290
addi r12, zero, 0x20
stb r12, 0x0(r26)
...
```

These instructions can then be interpreted step by step in order to find basic blocks. Basic block boundaries are reconstructed at targets of branches and directly after branches.

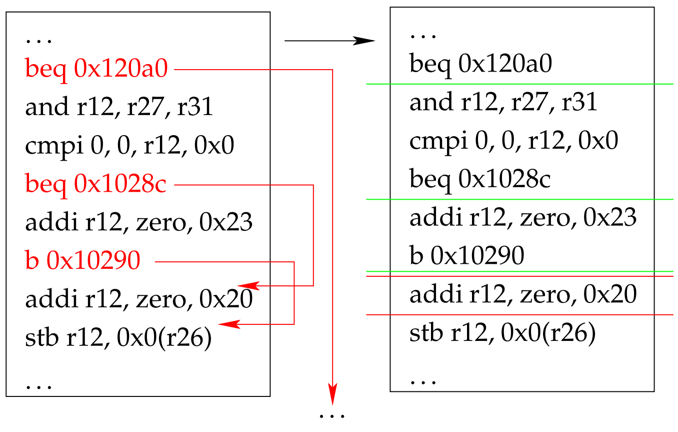

```
...
beq 0x120a0
and r12, r27, r31
cmpi 0, 0, r12, 0x0
beq 0x1028c
addi r12, zero, 0x23
b 0x10290
addi r12, zero, 0x20
stb r12, 0x0(r26)
...
```

```
...
beq 0x120a0
---------------------
and r12, r27, r31
cmpi 0, 0, r12, 0x0
beq 0x1028c
---------------------
addi r12, zero, 0x23
b 0x10290
---------------------
addi r12, zero, 0x20
---------------------
stb r12, 0x0(r26)
...
```

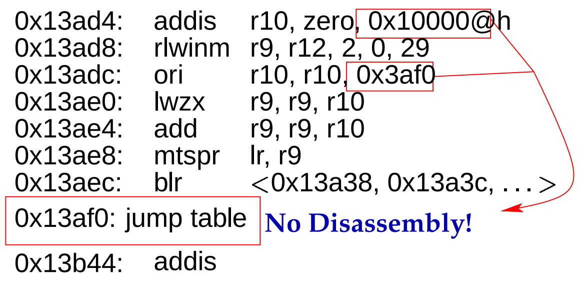

```
0x13ad4:  addis   r10, zero, 0x10000@h
0x13ad8:  rlwinm  r9, r12, 2, 0, 29
0x13adc:  ori     r10, r10, 0x3af0
0x13ae0:  lwzx    r9, r9, r10
0x13ae4:  add     r9, r9, r10
0x13ae8:  mtspr   lr, r9
0x13aec:  blr     <0x13a38, 0x13a3c, ...>
0x13af0: jump table
0x13b44:  addis
```

Figure 6.1: A jump table in code sections as inserted by many compilers makes sequential decoding infeasible.

In the final step, edges are inserted between basic blocks according to branch targets and simple continuing control flow.

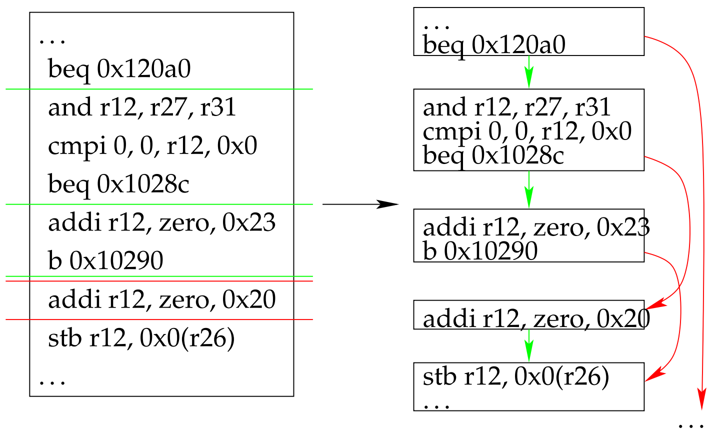

In the best case, this very simple method yields the correct control flow. However, programs are far away from this nice structure as mentioned before. The most obvious problem is that compilers often store data in code sections, making sequential decoding infeasible. This immediately breaks the applicability of a top-down approach. Figure 6.1 shows this problem.

The next section will discuss more problems and will further elucidate why we used a bottom-up algorithm in our approach instead.

6.2.2 Problems Unsolved by Top-Down Approach

1. Branch targets have to be determined. This might not always be possible for computed branches (Figure 6.2).

   Examples are switch tables, exception handling code, etc. The tool for CFG approximation should resolve as many of them as possible.
2. Delay slots complicate the computation of the basic block boundaries.

```
movh     d11, 45057
addi     d11, d11, -14584
ld.a     a15, [a12]0x0
ld.bu    d9, [a15]0x0
add      d15, d9, -43
mov      d1, 58
jlt.u    d1, d15, L2
mov.a    a3, d11
addsc.a  a15, a3, d15, 2
ld.a     a15, [a15]0x0
ji       a15
```

```
jge.u    d9, 5, L1
movh.a   a15, 45057
lea      a15, [a15]-0x3a44
addsc.a  a15, a15, d9, 2
ld.a     a15, [a15]0x0
ji       a15
```

Figure 6.2: Examples for switch table code generated by the HighTec GNU C compiler for TriCore. The aspects that have to be extracted (the switch table base address and its size) are in bold. Instructions that need not be considered are in italic. They were inserted by the optimising compiler's instruction scheduler.

```
cmpli    0, 0, r12, 0x14
bgt      L4
lis      r10, 0x10000@h
slwi     r9, r12, 2
ori      r10, r10, 0xd44
lwzx     r9, r9, r10
add      r9, r9, r10
mtlr     r9
blr
```

```
mflr     r0
stw      r0, 0x4(r1)
stwu     r1, -0x10(r1)
addi     r11, r1, 0x10
...
lwz      r0, 0x14(r1)
mtlr     r0
ori      r1, r11, 0x0
blr
```

Figure 6.3: On the PowerPC (*see* [PowerPC, 1997]), `blr` is used for switch tables (on the left) as well as for routine exits (typical routine prologue and epilogue on the right). Routine exits are not necessarily at the end of the routine.

3. Instruction sets may have instructions that are ambiguous w.r.t. how program flow is controlled.

   E. g. it might be complicated to find the end of a routine, because the given target does not have a dedicated 'return' instruction (Figure 6.3).
4. Guarded code makes analysis complicated.
5. On architectures with very long instruction words (VLIW), instructions consist of several operations, of which more than one may be branches. The semantics of this situation differs from target to target.
6. Object code and linked binaries are analysed, so multiple entry points and external routines must be handled.
7. Procedures might be interlocked or overlapping due to optimising compilers or handwritten assembly.
8. Data portions might be contained inside code blocks.

If a branch target is unknown, that branch is marked so subsequent analyses can decide whether to transform the CFG to contain *chaos nodes* (*see* [De Sutter et al., 2000]).

The ICFG is approximated in two steps. First, a conservative ICFG is produced, then a static analysis is performed to refine it, like constant propagation by abstract interpretation. The precise CFGs must be known, since if any CFG-edge is missing, it might jump *anywhere* and influence analysed properties at *any* point of the program. Assuming well-formed compiler output assembler, it may be possible to restrict the scope of interference to one routine.

If a table of all labels is available, these are the only possible targets of unpredictable jumps.

Fortunately, uncertain or missing inter-procedural edges are easier to handle (they cannot split basic blocks). Subsequent analysis steps can assume worst case without invalidating the results at other points of the program. Knowing calling conventions (e. g. *callee save registers*), it may then be possible to perform intra-procedural analyses without interference.

6.2.3 Intuition of Bottom-Up Approach

This section will introduce the ideas behind the CFG reconstruction algorithm intuitively.

The algorithm for bottom-up CFG reconstruction uses two agendas. The algorithm uses these as the basis for two nested loops. The outer loop gathers routines, so its agenda contains routine entry addresses. The inner loop finds the extents of each routine: it uses an agenda of instruction addresses for each routine.

The algorithm starts by putting the executable's entry address onto the outer agenda. The outer loop of the algorithm simply puts routine start addresses on a fresh agenda for the inner loop. Figure 6.4 shows these steps.

The inner loop successively decodes at addresses from its agenda to classify instructions that belong to that routine. After the precise classification, new addresses can be found that also belong to that routine. Figure 6.5 shows two successive steps of that loop. Figure 6.6 on page 96 shows the situation for jumps, which may have several possible successors, and for calls, which reveal new routine entries that are then put onto the outer loops' agenda of routine start addresses.

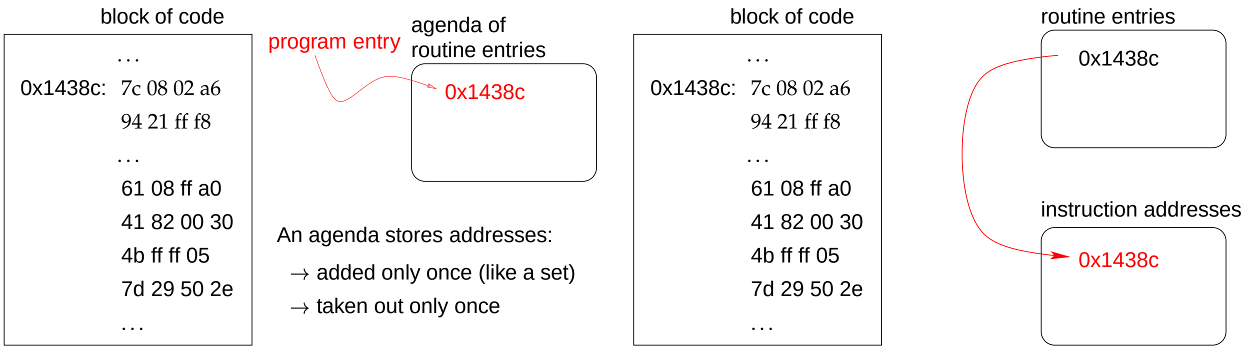

Figure 6.4: Left: program entries are put onto the agenda of routine start addresses, right: the agenda for finding routine instructions is initialised with routine start address.

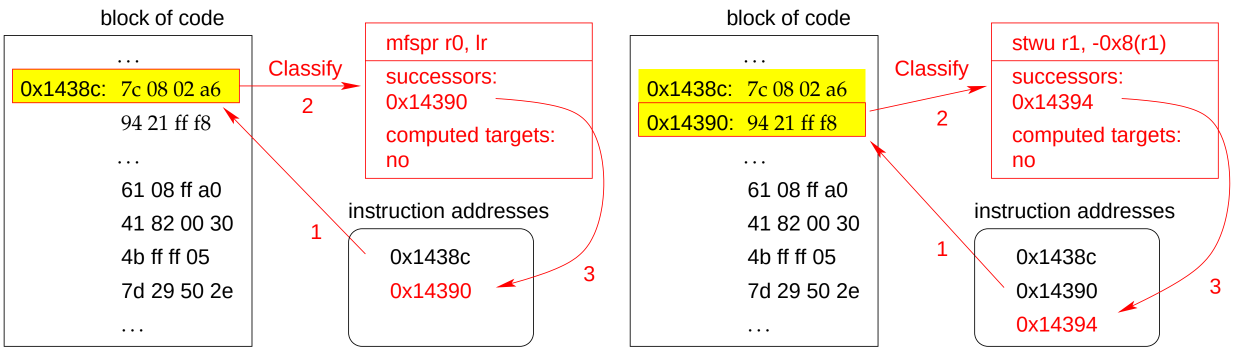

Figure 6.5: Two steps of the decoding algorithm: successively, the extents of a routine are reconstructed by classifying instructions form the agenda.

6.2.4 Theory

In the following, the bottom-up approach of ICFG computation will be formalised. Technical details are suspended until subsequent sections.

Let f, g be functions. $f \circ g$ denotes functional composition: $(f \circ g)(x) = f(g(x))$. Let M be a set. $|M|$ is the cardinality of M, $\mathfrak{P}(M)$ the power set of M.

Let $M = (I, c, j)$ be a machine description with I the instruction set containing all concrete instructions possible on that machine. Let $c : I \rightarrow \mathfrak{P}(\mathbb{N})$ be the mapping of instructions to their call target addresses, $j : I \rightarrow \mathfrak{P}(\mathbb{N})$ the mapping of instructions to their jump target addresses and to the address of the immediately following instruction if that is reachable. We assume that

It is assumed that c and j can be computed from $i \in I$ alone, i. e. an instruction contains all information about target addresses without further memory lookup. This is

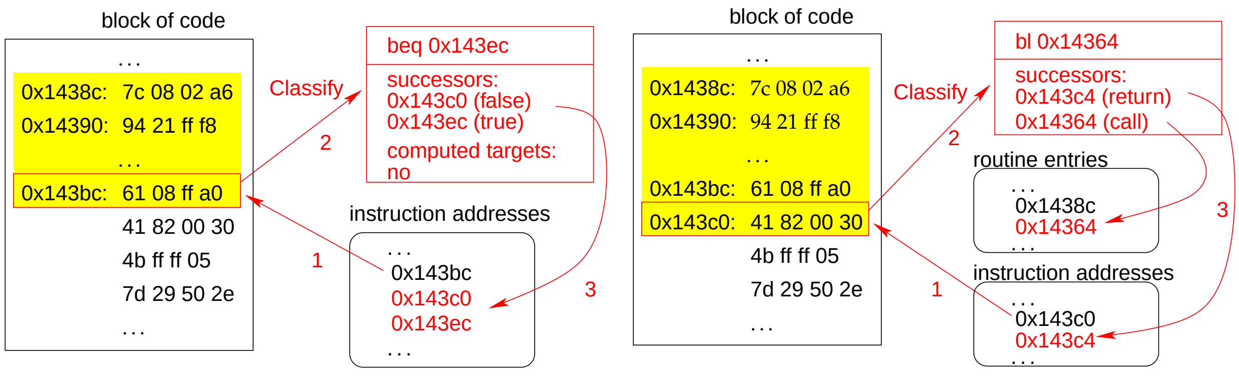

Figure 6.6: Left: a jump with two successors in the CFG, right: a call with a return address in the CFG and a routine start address.

no restriction, it only avoids the extra arguments of an address and a memory lookup function to c and j.

Let $P(M) = (A, e, s)$ be a binary of M, with $A \subseteq \mathbb{N}$, $|A| < \infty$ the finite set of addresses that contain instructions, $e \in A$ the program entry address, $s : A \to I$ the mapping from addresses to instructions, i. e. the memory contents.

We assume that no jumps or calls leave the executable, so we restrict j and c to $I \to \mathfrak{P}(A)$. Further, j and c shall be omniscient w.r.t. computed branch targets. The next sections will be more general. It is no problem to extend the construction to sets of entry points to analyse object files.

To describe the ICFG, the following must be known:

- the set $R \subseteq A$ of routine entry addresses,
- for each $r \in R$, the set $b(r) \subseteq A$ of all addresses of instructions belonging to the routine starting at r.

By $j \circ s$ and $b(r)$, each routine's CFG is fully described.

The CG is described by c and R, as $c \circ s$ describes all CG edges when applied to each $b \in b(r), r \in R$.

The series (R_n, b_n) will be used to define R and b.

The first routine starts at the entry point: $R_0 := \{e\}$. Let

$$\begin{aligned} b_0 : R_0 &\to A \\ r &\mapsto \{r\} \end{aligned} \tag{6.1}$$

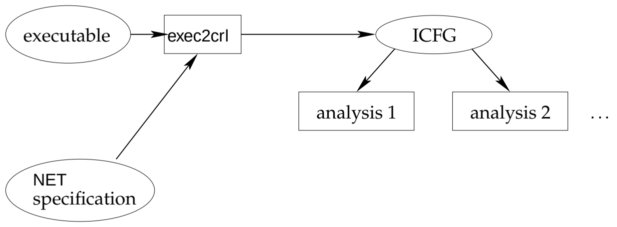

Figure 6.7: The structure of our analysis framework. The part discussed here is exec2crl. exec2crl provides the analyses with a control flow graph, NET provides many architectural dependent information.

For R_{k+1}, $c \circ s$ finds routine entries from $b_k(R_k)$:

$$R_{k+1} := R_k \cup \bigcup_{r \in R_k} \bigcup_{b \in b_k(r)} c(s(b)) \tag{6.2}$$

For the routines already known, edges are found by $j \circ s$, and for new ones, the routine entry address is used:

$$\begin{aligned} b_{k+1} : R_{k+1} &\to \mathfrak{P}(A) \\ r &\mapsto \begin{cases} b_k(r) \cup \bigcup_{b \in b_k(r)} j(s(b)) & \text{if } r \in R_k \\ \{r\} & \text{else} \end{cases} \end{aligned} \tag{6.3}$$

For some k, $(R_{k+1}, b_{k+1}) = (R_k, b_k)$, as $|A| < \infty$ and addresses are never removed. So $R := R_k$ and $b := b_k$.

6.3 Modular Implementation

Figure 6.7 shows the our framework's structure. exec2crl approximates the ICFG. Figure 6.8 depicts its modules.

CRL files (Control flow Representation Language, [Ferdinand et al., 1999a; Langenbach, 1998]) store the resulting ICFGs. It is a generic format not depending on the target architectures. CRL consists of routines, containing basic blocks, containing instructions, containing operations. Each structure can store additional information in *attributes*, e. g. to mark unpredictability. We use CRL in our framework to store ICFGs; other output formats can be supported by adding another writer modules to exec2crl.

NET files describe how operands and instructions are represented in the analysis. There is one NET file for each target architecture. This file defines the view of all analyses on the machine by assigning names to the bare numbers that occur in machine instructions.

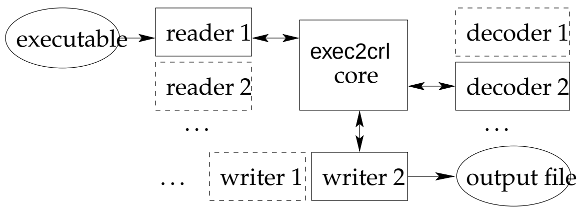

Figure 6.8: Module concept and communication of exec2crl. The currently selected modules are framed with a solid line, the unselected ones with a dashed line. The core implements the CFG approximation algorithms, generic code slicing and generic machine code pattern matching functionality.

E. g. registers and operations types are usually simply numbers, which are translated to register names and mnemonics with the help of NET files. NET files are used in exec2crl's decoder modules in order to build decision trees and then to generate CRL files.

ICFG reconstruction is generic to work for many targets. Modules wrap target and file format dependent parts.

Reader Modules: *Readers* split streams into code and data, extract entry points and routine and label names, useful for human users. Henceforth, we assume to have binary input, though assembly can be handled, too.

Writer Modules: *Writers* store ICFGs as CRL or generate visualisation files, e. g. Graph Description Language files (*see* [Sander, 1994]).

Decoder Modules: A *decoder* exists for every architecture family, possibly parameterised for the processor and the compiler. Its main task is to classify instructions.

The following aspects exist. * means the information can be marked preliminary so post-processing is needed.

- the instruction width in bytes,
- the operations contained in the instruction (for non-VLIW architectures, there is exactly one operation),
- the number of delay slots of an instruction,
- the impact of the operations on control flow: whether they are normal operations, jumps, calls, or returns,*
- fall-through edges (if the next instruction is reachable),*

```
procedure find_cfg(program_entry)
    a= new Agenda
    g= new CallGraph
    a.insert(program_entry)
    while not a.empty
        Routine r= find_routine(a.get_next)
        g.add_routine(r)
        a.insert(r.call_targets)
    return g
```

Figure 6.9: The outer decoding loop in pseudo code.

- jump targets, call targets,*
- implied call targets. E. g. from calls to well-known routines like atexit in C, routine entries are extracted.*

Decoders also classify operations to make available the operands to subsequent analyses. The classifications can be used for generic code slicing and pattern matching provided by the exec2crl framework.

6.4 The Core Algorithms

CFG approximation works with an outer loop that collects routines and CG edges, and an inner one finding CFGs.

6.4.1 Gathering Routines

The analysis starts at the entry address. To traverse the executable it uses an *agenda* that consists of a stack of routine start addresses (and possibly additional information about each address) and a hash table marking addresses already processed to prevent multiple processing.

The outer loop (Figure 6.9) puts addresses of routines onto the agenda, which are determined by find_routine.

6.4.2 Decoding a Routine

In the following, the term *safe set of targets* is used for a set of branch targets that is:

```
procedure find_routine($routine\_entry$)
  $r$= new Routine
  $a$= new Agenda
  $c$= new Set of Address        – routine's call targets
  $a$.insert($routine\_entry$)
  forever
    while not $a$.empty
      Instruction $i$= $D$.decode_instr($a$.get_next)
      $r$.add_instruction($i$)
      $c$.insert($i$.safe_call_targets)
      $a$.insert($i$.safe_successors, $i$.delay_slots)
    if $D$.finalise_routine($r$) = FINAL
      $r$.call_targets= $c$
      return $r$
    $c$.insert($r$.revealed_call_targets)
    $a$.insert($r$.revealed_jump_targets)
```

Figure 6.10: Pseudo code for find_routine. ***R*** is the reader module, ***D*** is the decoder module currently in use.

either a super-set of the real set of feasible branch targets,

or otherwise a possibly non-exhaustive set of branch targets that is clearly marked to be non-exhaustive.

This definition guarantees that either all possibilities of control flow have been found, or that the analysis is provided with the information that something is missing. The latter information can be used to assume the worst case for that analysis in that situation.

This is important for real-time system analysis because we must not allow an arbitrary approximation to the possible control flow, but we must compute a *safe* one. This means that the reconstruction algorithms and its implementation must be designed in such a way that they are always aware of missed branch targets.

Figure 6.10 shows the algorithm for the routine decoder.

- safe_successors returns all addresses that are possibly reached from the given instruction. These are all jump targets and fall-through edges. It is important to mark unpredictable aspects to be preliminary for later examination by finalise_routine.

  This function cannot return computed branch targets due to the limited scope of one instruction.

- delay_slots returns the addresses of delay slots. Some analyses will account for annulled delay slot instructions (e. g. on the SPARC architecture).
- safe_call_targets returns addresses of safe callees.
- finalise_routine checks and resolves uncertainties. The whole routine is analysed to decide from the context what uncertain operations really do.
- revealed_jump_targets returns computed jump targets. The compiler must be known, e. g. to find switch tables.
- revealed_call_targets does the same for call targets.

External Routines

By knowing the program's address space, calls that leave it can be marked to be external.

Additional Information

Information about routine boundaries, sections types (code vs. data), labels, etc., is used to check consistency of the approximated ICFG. Routine and label names are attached to the output.

6.4.3 Properties of the Algorithm

The problems listed in Section 6.2.2 are solved either directly or by providing an extensible plug-in mechanism. This section refers to the problem items.

The algorithm finds overlapping routines (6.2.2.7), i. e. those that share code portions, like merged routine tails produced by some optimising compilers. This would not be possible by splitting byte blocks according to routine boundaries and branches given in the input program, as top-down approaches try. Overlapping routines are analysed as separate ones that use the same addresses.

The algorithm finds interlocked routines (6.2.2.7), which may be produced by cache-aware compilers. No consecutive block structure is assumed by the algorithm. This cannot be done by only using boundary information. Accordingly, *holes* in the code (pieces of data) can be handled (6.2.2.8).

The algorithm is prepared for switch tables and other dynamic program flow (6.2.2.1). The decoders may use pattern matching and code slicing to detect them.

Delay slots are handled during the ICFG approximation and made available to subsequent analyses (6.2.2.2).

Uncertainties are marked clearly in the ICFG. So subsequent constant propagation can disambiguate computed branches (6.2.2.1) and conditions of guarded code (6.2.2.4). If something keeps yet unresolved, analyses are provided with that fact to take it into account.

The module system solves problems by allowing architecture and compiler dependent plug-ins when needed. This holds for all problems from Section 6.2.2, but is especially useful for computed branches(6.2.2.1), ambiguous instructions (6.2.2.3) and VLIW instructions (6.2.2.5).

For code with multiple entries, the algorithm can simply add them to the initial agenda (6.2.2.6).

By starting from several entry points and then doing a recursive decoding, a reachability analysis is performed. The run time for decoding is, therefore, usually very good compared to a total decoding of all routines. This will be especially useful for analysing unlinked object code when no smart linker has yet performed this analysis.

If information about routine entries is available from the reader module, all the routine entries can optionally be inserted into the main agenda when the algorithm starts. Then, even unreachable parts of the executable are analysed.

Worst-Case Runtime

Let n be the number of routines, m the number of instructions in the program, $T_o(n,m)$ the runtime of the outer loop (Figure 6.9), $T_i(m)$ the runtime of the inner loop (Figure 6.10) and $T_r(m)$ the runtime of $\boldsymbol{D}$.finalise_routine.

The outer loop iterates over routines, so the worst case runtime is $T_o(n,m) = n \cdot T_i(m)$. The inner loop will execute the body only for new branch targets, as a hash table marks processed addresses. At most m iterations will be performed. By using universal hashing the expected runtime per operation is $O(1)$, so $T_i(m) = O(1) \cdot m \cdot T_r(m)$.

If $\boldsymbol{D}$.finalise_routine resolves everything by iterating all instructions and looking at only a constant number of other instructions for each of them, it follows $T_r(m) = O(m)$. This is the case for all implemented decoders.

So the total worst-case runtime is $T_o(n,m) = O(n \cdot m^2)$.

Expected Runtime

Expected runtimes will be called $\hat{T}$. The previous paragraph makes pessimistic assumptions. The inner loop only re-iterates if uncertainties occur. Usually the number of repetitions is small compared to the number of instructions per routine. (E. g. the PowerPC decoder has one re-iteration due to ambiguous routine prologue and epilogue code, but only re-iterates if switch tables are found). So $\hat{T}_i(m) = O(1) \cdot m + c(m) \cdot T_r(m)$ where $c(m)$ is the expected number of re-iterations for m instructions. We expect $c(m) \ll m$.

The top-level loop's runtime should rather be $T_o(n,m) = O(1) \cdot n + \sum_{i=1}^{n} T_i(m_i)$, where m_i is the number of instructions per routine and $\sum_{i=1}^{n} m_i = m$. So in total, almost linear runtime is expected:

$$\hat{T}_o(n,m) = O(n) + O\big((1+c(m)) \cdot m\big), \quad c(m) \ll m$$

Comparison to Top-Down Approach

The worst case runtime of a top-down approach typically is $T(n,m) = O(n+m)$. It splits the program into routines and analyses each instruction. Our approach is slightly more complex, but it solves the problems we encountered. In practice, even large executables are processed in only a few seconds, so the difference is only theoretical.

6.5 Implementation

To be able to analyse large executables, data structures for storing decoded routines are not kept but freed as soon as a routine is analysed. This keeps the analysis small as these structures tend to be large (for each operation, a fine-grained classification is generated).

Reader modules are straightforward to implement. Plug-ins to read ELF, Coff, Intel Hex, IEEE695, and Motorola S-Record files have been implemented.

Decoder modules are more interesting. The routines for disambiguating operations are usually complex. Focusing on processors for embedded systems, we completed the implementation of decoder plug-ins for the Infineon TriCore (Rider B) architecture, the IBM PowerPC (we validated the models 403GCX, 555 and 755 to be decodable), the Motorola Coldfire 5307 and the ARM 5 architecture including both ARM and Thumb mode and automatic detection of instruction set switching.

In the following, some selected architectures will be presented.

6.5.1 PowerPC

The PowerPC has no dedicated 'return' instruction (*see* Figure 6.3 on page 93). Instead, a jump to the address contained in the *link register* (`LR`) is performed. Subroutine calls fill `LR` with the return address. If the callee is a leaf routine not calling other subroutines, this address is not necessarily stored on the system stack but may be kept in `LR` until the routine returns.

The problem is that the compiler also uses `LR` for other computed branches, making the instruction `blr` ambiguous. E. g. switch tables are implemented this way, too.

The finalise_routine function for PowerPC is implemented to analyse the `blr` instruction's context to find switch tables and disambiguate return instructions. If any additional jump targets are found, the analysis of the routine has to do another iteration.

Because the compiler we used has an instruction scheduler, the instructions performing a return or a switch are in general not adjacent. Code slicing was used to trace register usage and certain machine instruction patterns. Because the decoder provides generic information about instruction operands, the slicing algorithms are implemented in a machine independent way.

For recognising typical slices, a highly customisable pattern match generator was used to match them against known machine code patterns. It generates C code that matches C or C++ data structures. Most parts of the patterns are machine independent (e. g. the access to the operands), but of course, the machine instructions themselves are not. However, the pattern language is very concise so that the PowerPC decoder needed less than 200 lines to match several sorts of switch tables, routine prologues and epilogues, etc. The patterns can contain variables in order to extract interesting constants or registers from the machine code.

To show what happens when a routine is finalised and how pattern matching is used, we assume that a switch table is to be revealed for a PowerPC processor. Figure 6.11 shows what must happen in order to extract addresses from a switch table that was implemented by a computed branch: first, the start address and the number of entries of the branch address table must be found. Then, these entries must be extracted and put onto the decoding agenda.

Figure 6.12 shows how the switch table is recognised. First, exec2crl tries to cut a slice out of the code that might be relevant. To do this, registers leading to the computation of the register containing the branch target are traced. On the slice that was found, pattern matching is performed in order to recognise typical switch table code.

The pattern matching also instantiates some important values from the machine code: the start address (in two parts here) of the branch target table and its size. With the help of these values, exec2crl can extract the branch targets from the binary data and reconstruct the branch targets accordingly.

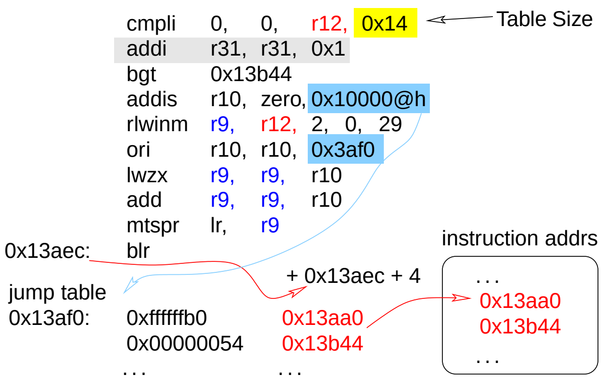

Figure 6.11: Example switch table on the PowerPC architecture: principle steps for extraction of possible branch targets at the computed branch `blr`.

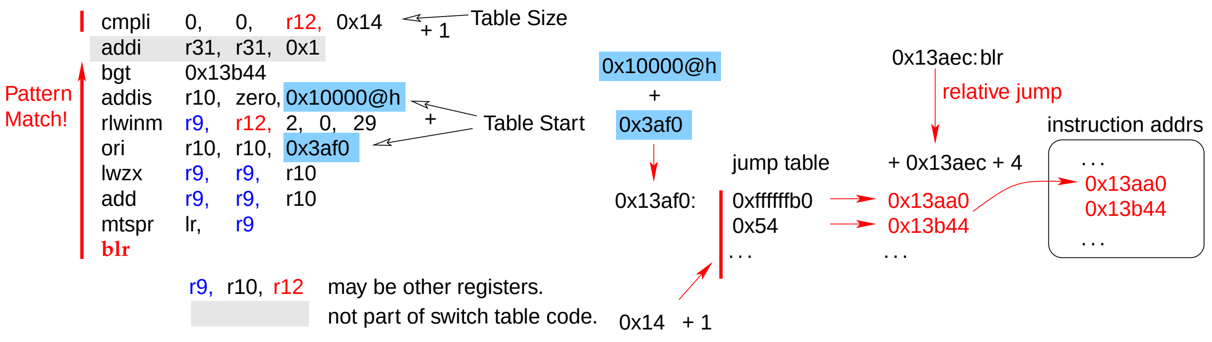

Figure 6.12: Left: code slicing and pattern matching recognise a switch table and extract address and size, right: a branch target table is read and converted to branch target addresses. In the example, an offset has to be added to the values in the table since the branch is relative to the current value of the program counter.

6.5.2 Infineon TriCore

Because the TriCore architecture has dedicated instructions for subroutine calls and returns, no complex disambiguation was necessary for them.

Switch tables also occurred in TriCore code. We have implemented a similar mechanism to recognise them as for the PowerPC and found that because of generic slicing code and pattern matching techniques, the implementation was very concise.

6.5.3 ARM

The ARM decoder has to deal with similar peculiarities as the PowerPC decoder, particularly a link register instead of a push/pop call mechanism. Computed branches are simple MOVE commands in the ARM architecture. The same mechanisms as for the

PowerPC solve the recognition problems.

Additionally, the ARM architecture is available with two instruction sets that can be switched by special branch instructions. The additional instruction set mode introduced for embedded systems, the Thumb mode, features shorter machine instructions in order to make the code more compact.

The problem of dealing with mode switches during reconstruction is solved in exec2crl by having an instruction set tag at each address on the decoding agendas. By this, the algorithms handle mode switches elegantly without any need for modifications.

Part III

Path Analysis

Chapter 7
Implicit Path Enumeration (IPE)

After the previous chapters have shown how to reconstruct CFGs from binaries for real-time system analysis, the following chapter will show how the CFGs are used in a central analysis for WCET prediction, namely the *path analysis*.

This chapter will introduce the path analysis methods by Implicit Path Enumeration (IPE) for graphs without context. IPE generates an ILP to perform path analysis.

Most types of generated constraints of that ILP can be directly used in the next chapter, where the new algorithm for loop bound constraints for graphs with context will be presented.

7.1 Times and Execution Counts

The following symbols will be used.

Definition 7.1
As introduced in the previous section, the **execution time** per execution of a node in a graph $G = (V, E)$ will be written $\mathrm{t}(v), v \in V$. In the ILP, these symbols are *constants* provided by previous analyses.

```
if $v_1$ then
    $v_2$
else
    $v_3$
fi
$v_4$
```

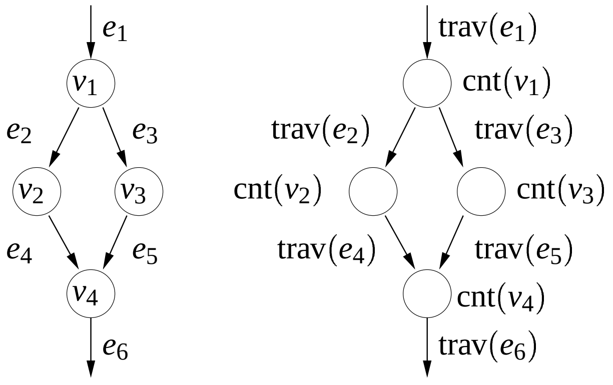

Figure 7.1: Nodes with execution counts and edges with traversal counts.

Also according to the previous section, the **execution count** of a node in G will be written $\text{cnt}(v), v \in V$. The traversal count of an edge in G will be written $\text{trav}(e), e \in E$. In the ILP, these symbols are *variables* and will be derived from a solution of the ILP. Figure 7.1 shows the correspondence of nodes and edges to node execution counts and edge traversal counts.

As introduced in Section 2.2.7 on page 38 already, the minimum loop execution count per entrance of that loop via an entry edge $e \in E$ will be written $n_{\text{min}}(e)$. The maximum loop execution count per entrance will be written $n_{\text{max}}(e)$. In the ILP, these symbols are *constants* provided either by previous analyses or by the user.

All these symbols can be used for all kinds of graphs, i. e. with or without context information.

7.2 Handling Special Control Flow

For ILP generation, we have to handle unknown control flow in the control flow graphs and call graphs. The uncertainties in question are clearly marked, but we have to decide what to do with them now.

7.2.1 External Routine Invocations

External routines are represented in the control flow graphs as normal routines that contain a special *external* node that represents the routine as a black box. It is required that the execution time is known for this black box and that it is annotated correctly. This way, the algorithms in the following sections handle external nodes and normal basic block nodes uniformly.

7.2.2 Unresolved Computed Branches

It will be assumed that there are *no* unresolved computed branches in the control flow. There is no easy way to weaken this assumption, since unresolved computed branches represent unknown paths that have unknown run-time. E. g., with the presence of unknown branches, there may be unknown loops, so the run-time might be unbounded. Because the analyser cannot know this, it has no means of conservatively approximating the run-time. The only conservative way of handling unknown branches is to state that the run-time is unpredictable.

7.2.3 Unresolved Computed Calls

It will be assumed that there are *no* unresolved computed calls in the control flow graph. If this is not the case after the automatic control flow reconstruction, the user is required to add additional information, e. g., the precise set of possible call targets for a given call node. Also, external nodes with additional timing information may have to be added manually for unresolved call targets that are outside the scope of the executable.

Clearly, this restriction cannot be weakened, since the runtime of every node must be statically known to compute a static WCET approximation.

Further, this restriction on the control flow graph means that whenever a call node is encountered that has no call targets, this call node is infeasible, since no alternative is given. The absence of call targets cannot be caused by unknown call targets, since these are prohibited here.

7.2.4 No-return calls

No-return calls also pose a problem. For a call to not return may either mean that the invoked routine ends the program immediately, or that it contains an infinite loop. Infinite loops, of course, have unlimited run-time, so we have to exclude them from our analysis anyway. So we assume that all no-return calls immediately stop the program.

For this reason, no-return calls are handled a bit like immediate-return calls, since the current path ends at the call under examination. Depending on whether this happens unconditionally or whether the no-return call is conditional, the property of not returning propagates to outer routine calls.

Currently, the framework needs the help of the user to determine no-return calls, but if the need arises in the future, an additional, special reachability analysis could be applied to the CFGs to find this property automatically in many cases.

Note that if there really are reachable infinite loops, these are detected as loops by the analyser, and if the user (and a value analysis) cannot give an upper bound, the analyser rejects the program.

7.3 ILP

This section describes how an ILP is generated for worst case path analysis. The techniques are described in detail in previous work, e. g. in [Li et al., 1996; Theiling and Ferdinand, 1998].

7.3.1 Objective Function

The WCET $t_{\max}$ of a program can be computed if a path through the program is known that leads to the maximal execution time. Let $v_0, \ldots, v_n, v_i \in V$ be such a path. The runtime is the sum of the execution times of each node:

$$t_{\max} = \sum_i \mathrm{t}(v_i)$$

The idea about Implicit Path Enumeration (IPE) is a re-formulation of this sum. The problem with the above formulation is that a path must be known that executes in worst-case time. However, programs usually have exponentially many paths, so checking each path for its specific execution behaviour is infeasible for interesting programs.

To overcome this problem, IPE *counts* executions of basic blocks, instead of analysing paths explicitly. In the above sum, we count the occurrences of each node $v \in V$. Formally, let $\mathrm{cnt}(v)$ be defined as follows.

$$\mathrm{cnt}(v) = \{i \mid i \in \{1, \ldots, n\}, v = v_i\}$$

Then the above sum can be reformulated as:

$$t_{\max} = \sum_{v \in V} \mathrm{t}(v) \cdot \mathrm{cnt}(v)$$

This sum is a linear combination, since the execution times are constant in the ILP as they have been computed in a previous step of the analysis.

$$\sum_{v \in V} \underbrace{\mathrm{t}(v)}_{\text{const}} \cdot \underbrace{\mathrm{cnt}(v)}_{\text{var}}$$

So the sum can be used in the objective function of the ILP and be maximised. The constraints of the ILP will restrict the possibilities of control flow so that the approximated

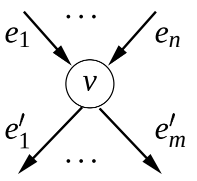

$$\sum_{i=1}^{n} \mathrm{trav}(e_i) = \mathrm{cnt}(v) = \sum_{i=1}^{m} \mathrm{trav}(e'_i)$$

Figure 7.2: Incoming and outgoing control flow can be formulated by equations between node execution counts and sums of edge traversal counts.

maximum of the objective function will be the predicted WCET of the program under examination.

Therefore, the objective function of the generated ILP is as follows.

$$\max : \sum_{v \in V} \mathrm{t}(v) \cdot \mathrm{cnt}(v)$$

7.3.2 Program Start Constraint

Let $v_0 := \mathsf{start}(r_0)$ be the start node of the program. Since the WCET for *one* execution of the program is to be derived, its execution count is 1 (we do not permit recursion back to the program entry).

$$\mathrm{cnt}(v_0) = 1$$

7.3.3 Structural Constraints

For all nodes, we sum up the outgoing and incoming control flow. Figure 7.2 shows the idea of these constraints.

The following constraints are generated from the CFGs.

$$\forall f \in R, v \in V_f, \{(v,v') \in E_f\} \neq \{\,\} : \quad \mathrm{cnt}(v) = \sum_{(v,v') \in E_f} \mathrm{trav}(v,v') \tag{7.1}$$

$$\forall f \in R, v \in V_f, \{(v',v) \in E_f\} \neq \{\,\} : \quad \mathrm{cnt}(v) = \sum_{(v',v) \in E_f} \mathrm{trav}(v',v) \tag{7.2}$$

Because of the local edges, call nodes are handled correctly by these constraints (recall Figure 3.1 on page 49).

Care has to be taken at nodes with no incoming edges (e. g. start nodes of functions) or no outgoing edges (e. g. exit nodes of functions), since it is usually wrong to generate constraints of the form $\mathrm{cnt}(v) = 0$, as these nodes are really potentially executed. Therefore, these constraints are excluded in the description above, to prevent empty sums to be generated that way.

From the CG we have to generate the following equations that state that start nodes are executed as often as their entry edges are traversed in total. Further, we state by a constraint that a call node is executed as many times as its call edges are traversed.

$$\forall v \in \mathsf{Starts}: \quad \mathrm{cnt}(v) = \sum_{(v',v)\in\hat{E}} \mathrm{trav}(v',v) \tag{7.3}$$

$$\forall v \in \mathsf{Calls}: \quad \mathrm{cnt}(v) = \sum_{(v,v')\in\hat{E}} \mathrm{trav}(v,v') \tag{7.4}$$

Note that empty sums are correct here in contrast to the CFG case, as start nodes that are not called are not executed, thus have an execution count of 0. Further, call nodes that do not call any routine are also infeasible and, therefore, also have an execution count of 0.

Infeasible Nodes and Edges

Our microarchitecture analysis is able to find infeasible paths in many cases. To account for these by preventing that infeasible paths are considered in the path analysis, additional constraints are generated for each $v \in V$ that is infeasible:

$$\mathrm{cnt}(v) = 0.$$

According constraints are generated for infeasible edges $e \in E$:

$$\mathrm{trav}(e) = 0.$$

Edge Weights

Our framework also allows the user to weight edges of the program for more flexibility and higher precision. This feature is used by our pipeline analysis since it is very frequent that fall-through edges of branches have a different execution time as the edge corresponding to the branch.

To support this, edge weights are introduced and added to the objective function.

It is very easy to extend the ILP formulation to handle weighted edges. The ILP has variables for edge traversal counts already, which can be used in a straight-forward manner in the objective function, too.

To do this, let $\mathrm{t}(e)$ be the time the edge e contributes to the runtime of the program. These numbers can be computed by a previous microarchitecture analysis just like the node execution times. Edge traversal times are more general than node execution times, because node execution times can be distributed onto edge traversal times for the same effect.

To have the maximum degree of freedom of formulation, we will allow both node execution times and edge traversal times to be defined.

This adds more precision and more flexibility to the framework.

precision: instead of only talking about execution times of nodes, one can exactly clarify the time that is consumed to leave one node and enter another, i. e. pairs of nodes can be weighted.

flexibility: The user who wants to use edge weights can decide whether they want to use edge weights only, or have a basic node weight and assign differences to edges only where necessary. Note that weights may be negative, so *speed up* can be represented by edge weights.

The full objective function with node and edge weights is as follows:

$$\max : \sum_{v \in V} \mathrm{t}(v) \cdot \mathrm{cnt}(v) + \sum_{e \in E} \mathrm{t}(e) \cdot \mathrm{trav}(e) \tag{7.5}$$

7.3.4 Loop Constraints

Loop constraints bound the number of iterations of a loop. They are specified as the minimum and maximum number of iterations for each invocation of the loop. Because the ILP-based approach adds up the execution counts on the loop entry nodes, the most precise measure is the *ratio between the number of executions of the loop entry node and the number of executions of the start node of the loop*. Recall that for an entry edge e_0, the minimum and maximum ratios are $n_{\min}(e_0)$ and $n_{\max}(e_0)$, resp. (*see* Definition 7.1).

Note that there may be more than one loop entry node for recursive loops (but not for transformed iterative loops). In order to distinguish each of them, the minimum and maximum loop counts are given for each loop entry node, not for each loop.

A loop is executed as many times as its *header* is executed. To limit the number of iterations of the loop per entry, the execution count of the header must be compared to the traversal counts of the loop's entry edges (*see* Figure 7.3 on the next page).

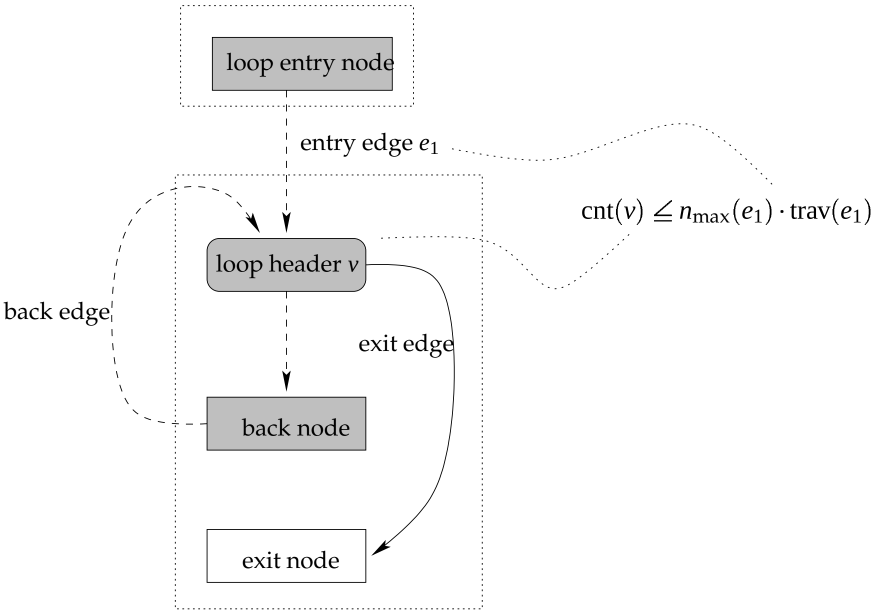

Figure 7.3: Loop bound constraint for maximum loop iteration for a simple loop l

Loop bound constraints are generated as follows for each loop l:

$$\begin{aligned}\mathrm{cnt}(\mathrm{header}(l)) &\geqq \sum_{e\in\mathrm{entries}(l)} n_{\min}(e)\cdot\mathrm{trav}(e)\\ \mathrm{cnt}(\mathrm{header}(l)) &\leqq \sum_{e\in\mathrm{entries}(l)} n_{\max}(e)\cdot\mathrm{trav}(e)\end{aligned}$$

7.3.5 Time Bounded Execution

It is frequent that a real-time system makes use of an external timer, e. g., to synchronise execution with hardware events. For a loop waiting for a hardware timer it would be nice if the user could specify the maximum execution *time* for such a loop, instead of the maximum iteration *count*.

Let l be a loop. The total execution time of l is the time consumed by executing and traversing each block and edge belonging to l. The nodes and edges belonging to l form a subset of V and E, resp.

Let $V(l) \subseteq V$ be the set of basic blocks that belong to l and let $E(l) \subseteq E$ be the set of edges belonging to l. Similar to the formula of the objective function (*see* Equation 7.5 on the previous page), the total execution time t_l of l is:

$$t_l = \sum_{v\in V(l)} \mathrm{t}(v)\cdot\mathrm{cnt}(v) + \sum_{e\in E(l)} \mathrm{t}(e)\cdot\mathrm{trav}(e)$$

We want to specify the maximum and minimum execution time for l *per execution*. So for each entry edge e of l, let the maximum execution time of l be $t_{\max}(e)$ and let the minimum execution time of l be $t_{\min}(e)$.

Because these execution times are given per execution, we compare the total execution time of l to its minimum and maximum execution times multiplied by the traversal counts of all its entry edges.

$$t_l \leqq \sum_{e \in \text{entries}(l)} t_{\max}(e) \cdot \text{trav}(e) \tag{7.6}$$

$$t_l \geqq \sum_{e \in \text{entries}(l)} t_{\min}(e) \cdot \text{trav}(e) \tag{7.7}$$

As can be seen, these constraints are fine-grained enough to have the maximum and minimum execution times specified differently for each invocation of the loop l.

7.3.6 User Added Constraints

Users may add constraints to the ILP. Theoretically, users may add arbitrary constraints (there is no restriction in our framework for this), but practically, the problem is that this would require knowledge of the ILP, which most users do not have.

Instead, users will most probably want to reason about the relation between execution counts of basic blocks. Therefore, our framework allows the user to add constraints that relate two blocks' execution counts. E. g. 'v_1 is executed (at least, at most) n times as often as v_2'.

These statements can most easily be translated into constraints:

$$\text{cnt}(v_1) = n \cdot \text{cnt}(v_2)$$

Instead of $=$, the operators $\leqq$ and $\geqq$ may be appropriate.

These constraints are then simply added to the generated ILP.

Chapter 8
Interprocedural Path Analysis

This chapter will introduce path analysis for graphs with context. It is the result of my research in this area (*see* [Theiling, 2002]), improving the precision and flexibility of the existing framework. The algorithms are implemented in a tool called pathan, which is part of the WCET analysis framework.

8.1 Basic Constraints

In this section, the ideas from the previous chapter will be the basis for generating an ILP for graphs with contexts.

It is important to note that the graphs with context information still represent control flow in the same way as the normal graph: edges mark control flow and nodes represent basic blocks. The fact that context information has split one block or edge into many ones does not influence this fact, because the edges are inserted at context changes exactly according to the possibilities of context change. I. e. usually a call node has an outgoing edge in the call graph that changes the context and enters the start node of another routine.

Of course, this is no surprise, because the PAG framework introduces these graphs for analysis, so they are constructed to work in the same way as graphs without contexts.

So in short, the basic idea of ILP generation still works on graphs with contexts in the same way it does on graphs without.

8.1.1 Objective Function

The objective function for graphs with contexts follows the same idea as the one for graphs without contexts: it adds up the execution time each basic block in any of its contexts contributes to the total execution time. So the objective function is:

$$\max : \sum_{v \in V^\star} \mathrm{cnt}(v) \cdot \mathrm{t}(v) + \sum_{e \in E^\star} \mathrm{trav}(e) \cdot \mathrm{t}(e)$$

8.1.2 Program Start Constraint

Let v_0 be the start node of the program in the start context. As for graphs without context, it is executed once:

$$\mathrm{cnt}(v_0) = 1$$

8.1.3 Structural Constraints

Structural constraints only consider control flow locally at one node. As stated before, control flow is represented in the same way in graphs with and without contexts. So the structural constraints from Section 7.3.3 on page 113 can be applied directly to graphs with contexts.

The following constraints are generated from the CFGs*.

$$\forall f \in R, v \in V_f^\star, \{(v,v') \in E_f^\star\} \neq \{\,\} : \quad \mathrm{cnt}(v) = \sum_{(v,v') \in E_f^\star} \mathrm{trav}(v,v') \tag{8.1}$$

$$\forall f \in R, v \in V_f^\star, \{(v',v) \in E_f^\star\} \neq \{\,\} : \quad \mathrm{cnt}(v) = \sum_{(v',v) \in E_f^\star} \mathrm{trav}(v',v) \tag{8.2}$$

And for start and call nodes:

$$\forall v \in \mathsf{Starts}^\star : \quad \mathrm{cnt}(v) = \sum_{(v',v) \in \hat{E}^\star} \mathrm{trav}(v',v) \tag{8.3}$$

$$\forall v \in \mathsf{Calls}^\star : \quad \mathrm{cnt}(v) = \sum_{(v,v') \in \hat{E}^\star} \mathrm{trav}(v,v') \tag{8.4}$$

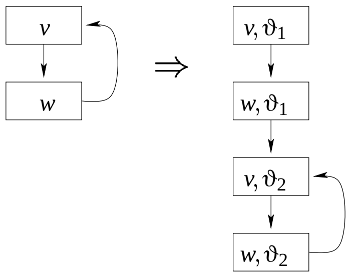

Figure 8.1: A loop in the CG and the same loop in the CG* (e. g. VIVU$(2,1)$). The cycle in the CG does not correspond to a cycle in the CG*: $v \to w \to v$ is split into two parts: its first iteration (context ϑ_1) and all other iterations (context ϑ_2), so the iteration count of the cycle in the CG* is different from the loop iteration count. Note that in this section, all figures will show call graphs if not stated differently.

8.2 Loop Bound Constraints

In contrast to most other kinds of constraints, precise loop bound constraints cannot easily be generating for graphs with contexts. One problem is that the contexts of different basic blocks of a loop differ in non-trivial ways, because the involved edges and nodes are in different routines in the graph and the context mapping may have assigned them in most different ways.

Figure 8.1 shows another problem of loop bound constraints for call graphs with contexts: the original entry and back edges of a loop in the CG correspond to edges in the CG* that are not necessarily part of a cycle there (due to unrolling for instance). However, talking about iterations of a loop, we talk about that loop in the CG. So we have to generate constraints on items in the CG* that correspond to the loop in the CG.

The loop bound constraints will be introduced in several steps for easier understanding. First, a very simple solution will be introduced that reduces to the method presented for graphs without contexts in the previous chapter. It will be shown that these constraints have bad precision and that better ones are desirable.

Second, the special case of VIVU(x,∞), i. e. VIVU without context length restriction is presented, for which loop bound constraints with maximal precision can be easily generated.

Finally, an efficient algorithm will be presented that generates loop bound constraints for arbitrary mappings.

8.2.1 Simple Loop Bound Constraints

Let $\mathsf{CFG}_r = (V_r, E_r)$ be a control flow graph for a routine r. For all the contexts $\vartheta \in \Theta(r)$ by which r is distinguished, let the control flow graph with contexts be $\mathsf{CFG}^\star{}_{r,\vartheta} = (V^\star_{r,\vartheta}, E^\star_{r,\vartheta})$.

The control flow passing through a block $v \in V$ is distributed to all of its contexts in the control flow graph with context. Therefore, the total amount of times v is executed is a sum over all of its contexts.

$$\mathrm{cnt}(v) = \sum_{\vartheta \in \Theta(v)} \mathrm{cnt}(v, \vartheta).$$

An analogous equation holds for edges.

For this reason, for any constraint that was generated for graphs without contexts, a corresponding constraint can be generated for graphs with contexts by simply replacing $\mathrm{cnt}(v)$ by the above sum. Of course, this is true for loop bound constraints, too, which leads to the simple approach to generating loop bound constraints.

Recall the loop constraint for maximum iterations for a loop l in the call graph without context:

$$\mathrm{cnt}(\mathrm{header}(l)) \leqq \sum_{e \in \mathrm{entries}(l)} n_{\max}(e) \cdot \mathrm{trav}(e)$$

Replacing the execution count of the header and the traversal counts of each entry edge by their sum over all contexts, we get

$$\sum_{\vartheta \in \Theta(\mathrm{header}(l))} \mathrm{cnt}(\mathrm{header}(l), \vartheta) \leqq \sum_{e \in \mathrm{entries}(l)} n_{\max}(e) \cdot \left(\sum_{\vartheta \in \Theta(e)} \mathrm{trav}(e, \vartheta) \right).$$

Distributing the coefficients of the last sum, we get a linear combination again. Figure 8.2 depicts this constraint.

$$\sum_{\vartheta \in \Theta(\mathrm{header}(l))} \mathrm{cnt}(\mathrm{header}(l), \vartheta) \leqq \sum_{e \in \mathrm{entries}(l)} \sum_{\vartheta \in \Theta(e)} n_{\max}(e) \cdot \mathrm{trav}(e, \vartheta)$$

A trivial improvement is to use the iteration counts per context.

$$\sum_{\vartheta \in \Theta(\mathrm{header}(l))} \mathrm{cnt}(\mathrm{header}(l), \vartheta) \leqq \sum_{e \in \mathrm{entries}(l)} \sum_{\vartheta \in \Theta(e)} n_{\max}(e, \vartheta) \cdot \mathrm{trav}(e, \vartheta) \tag{8.5}$$

Of course, for the iteration minimum, we get an according constraint using the same steps:

$$\sum_{\vartheta \in \Theta(\mathrm{header}(l))} \mathrm{cnt}(\mathrm{header}(l), \vartheta) \geqq \sum_{e \in \mathrm{entries}(l)} \sum_{\vartheta \in \Theta(e)} n_{\min}(e, \vartheta) \cdot \mathrm{trav}(e, \vartheta) \tag{8.6}$$

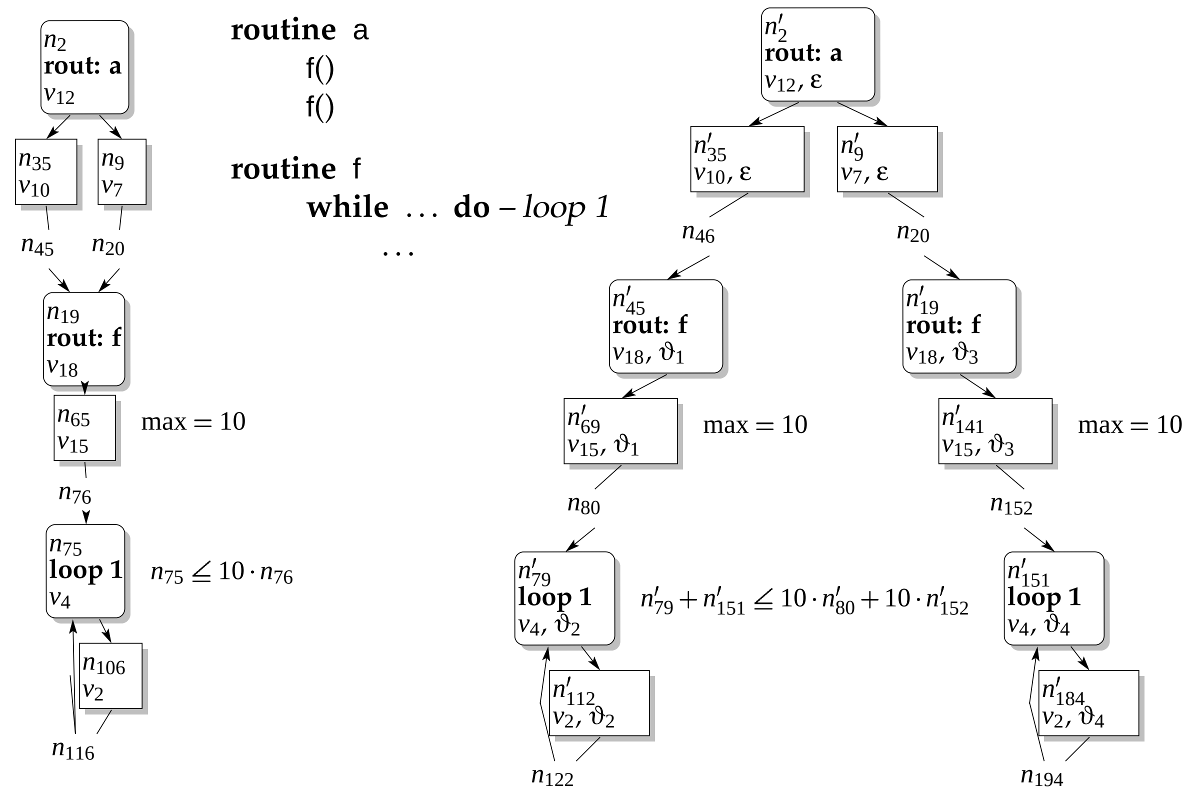
n_2 **rout: a** v_{12}
n_{35} v_{10}
n_9 v_7
n_{45}
n_{20}
n_{19} **rout: f** v_{18}
n_{65} v_{15}
max = 10
n_{76}
n_{75} **loop 1** v_4
$n_{75} \leqq 10 \cdot n_{76}$
n_{106} v_2
n_{116}
routine a
f()
f()
routine f
while … **do** – *loop 1*
…
n'_2 **rout: a** v_{12}, ε
n'_{35} v_{10}, ε
n'_9 v_7, ε
n_{46}
n_{20}
n'_{45} **rout: f** v_{18}, ϑ_1
n'_{19} **rout: f** v_{18}, ϑ_3
n'_{69} v_{15}, ϑ_1
max = 10
n'_{141} v_{15}, ϑ_3
max = 10
n_{80}
n_{152}
n'_{79} **loop 1** v_4, ϑ_2
$n'_{79} + n'_{151} \leqq 10 \cdot n'_{80} + 10 \cdot n'_{152}$
n'_{151} **loop 1** v_4, ϑ_4
n'_{112} v_2, ϑ_2
n'_{184} v_2, ϑ_4
n_{122}
n_{194}

Figure 8.2: Simple loop bound constraints for graphs with contexts. Left: CG, right: CG⋆ (VIVU$(1, \infty)$). The n_i are abbreviations for cnt(…) or trav(…). Basically, contexts are simply neglected by summing up the counts of all contexts. The loop constraints on the right are generated from those on the left by the substitutions $n_{75} = n'_{79} + n'_{151}$ and $n_{76} = n'_{80} + n'_{152}$.

These loop bound constraints are more imprecise than necessary. Consider Figure 8.3 on page 124. There are two different programs, the first analysed without context distinction, which has two routines each containing a loop, and the other one analysed with VIVU$(1, \infty)$, which only contains one routine with a loop. By use of VIVU, the routine in the latter case is analysed inline, so the two CGs⋆ are isomorphic.

However, loop constraints are different in that figure. In the case of two proper routines, two loop constraints are generated for the loops in each routine. For the VIVU case, only one loop constraint is generated because contexts are neglected.

To see why the loop constraints are quite imprecise, imagine that one of the loops in the CGs⋆ is slower. In the figure, n_{112} is marked to be slower in the left part of the right graph. By the loop bounds on the right, the constraints permit that n_{151} is assumed to be 19 while n_{79} is 1 (provided that $n_{80} = n_{152} = 1$), since the sum is only constrained to be $\leqq 20$. This leads to overestimation of the run time, since the slower loop can in reality not really be executed 19 times, since we know that its maximal iteration count is 10 in

```
routine a
    f()
    g()

routine f
    while ... do – loop 2
        ...

routine g
    while ... do – loop 1
        ...
```

```
routine a
    f()
    f()

routine f
    while ... do – loop 1
        ...
```

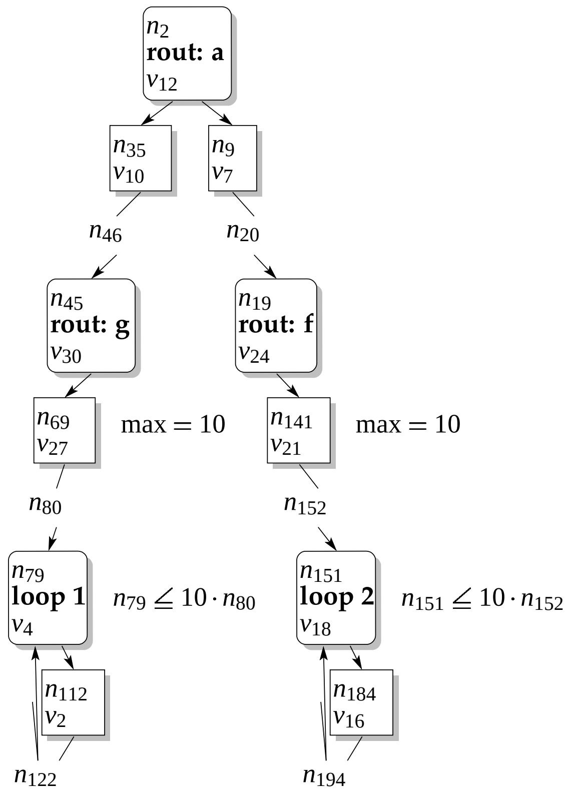

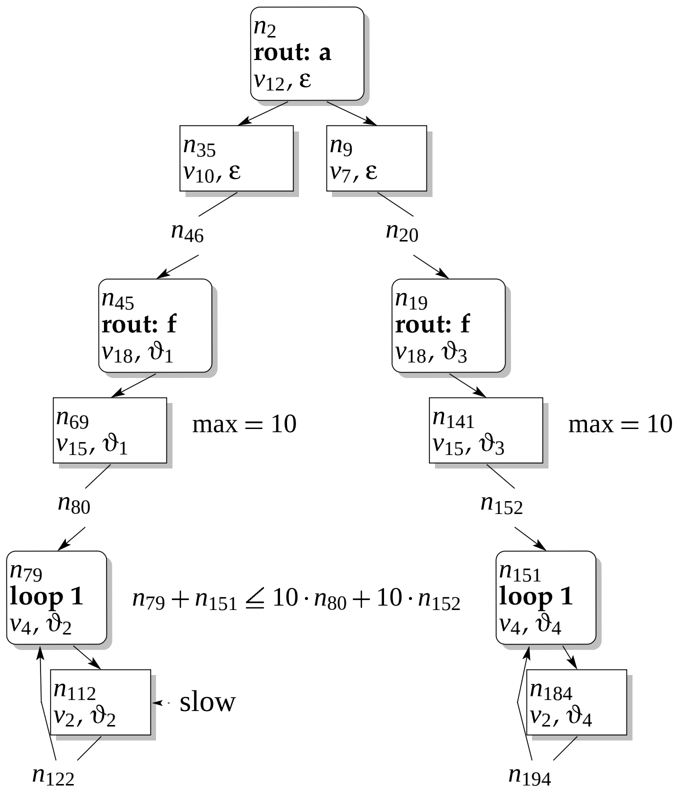

n_2 rout: a v_{12}, ε
n_{35} v_{10}, ε
n_9 v_7, ε
n_{46}
n_{20}
n_{45} rout: f v_{18}, ϑ_1
n_{19} rout: f v_{18}, ϑ_3
n_{69} v_{15}, ϑ_1
max = 10
n_{141} v_{15}, ϑ_3
max = 10
n_{80}
n_{152}
n_{79} loop 1 v_4, ϑ_2
$n_{79} + n_{151} \leqq 10 \cdot n_{80} + 10 \cdot n_{152}$
n_{151} loop 1 v_4, ϑ_4
n_{112} v_2, ϑ_2
slow
n_{184} v_2, ϑ_4
n_{122}
n_{194}

Figure 8.3: Left: two function f and g containing a loop each, are invoked from a. The program is is analysed without contexts. Right: the same function f containing a loop, is called twice from a. The program is analysed with VIVU$(1, \infty)$, thus f has two different contexts. The CGs* are isomorphic, but simple loop bounds differ due to neglecting contexts on the right. This leads to imprecision (*see* text).

each context.

In the left graph, in the case of properly distinguished routines, this consequence is impossible, since each loop is handled separately.

So our goal will be to get loop bound constraints that are most precise. This means that we want to distinguish loop invocations to a maximal degree that is possible for a given mapping.

Before we handle the case of arbitrary mappings, it will help to have a close look at loop bound constraints for VIVU without context length restriction, since these mappings do full inlining of loops, providing the same degree of precision as a program with separate routines for each loop.

8.2.2 Loop Bound Constraints for VIVU(x, ∞)

Figure 8.3 shows intuitively by isomorphic CGs* that it should be possible to generate the same loop bound constraints for the CG* on the right, which has one loop, distinguished in two contexts, as for the one on the left, which has two loops each in a different routine: good constraints are obviously possible for the left graph, so they should be adapted to the right graph.

This section will introduce maximally precise loop bound constraints for VIVU(x, ∞), for some x. Further, we will assume that loops have exactly one entry edge here. The arbitrary case will be handled in the next section.

An important term of the following sections will be a *dominator*.

Definition 8.1 (Dominator)
In a graph G, a *dominator* v_0 of a node v has the property that all paths from the start node to v contain v_0.

In the context of loops, loop headers are dominators of the nodes in the loop, because all control flow that enters the loop must pass through the loop header.

In the graphs with contexts, the original nodes are usually split into several nodes distinguished by contexts. These will be called *instances* of the corresponding original node in the graph without context. Most importantly here, the original loop header, which is the dominator of all nodes inside that loop, is split into several nodes by context distinction. Because we consider arbitrary static mappings, the distinction may be done in such a way that the original dominator is not a dominator in the graph with context anymore, since it may be possible that control flow enters the loop in the CG* via *several different* instances of the original dominator.

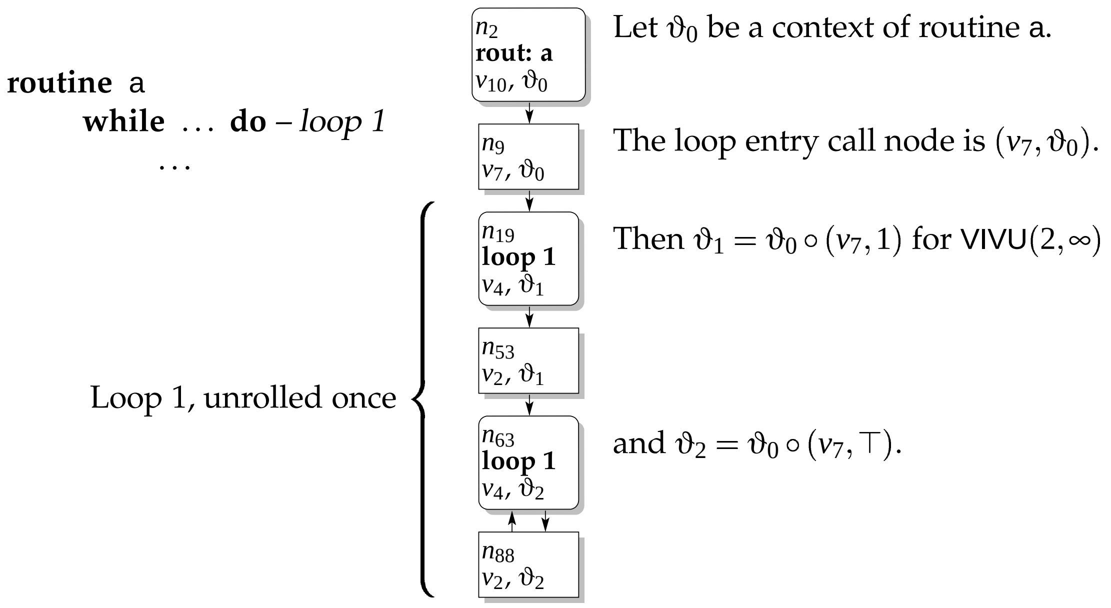
routine a
while … **do** – *loop 1*
…
Loop 1, unrolled once
n_2 **rout: a** v_{10}, ϑ_0
n_9 v_7, ϑ_0
n_{19} **loop 1** v_4, ϑ_1
n_{53} v_2, ϑ_1
n_{63} **loop 1** v_4, ϑ_2
n_{88} v_2, ϑ_2
Let ϑ_0 be a context of routine a.
The loop entry call node is (v_7, ϑ_0).
Then $\vartheta_1 = \vartheta_0 \circ (v_7, 1)$ for VIVU$(2, \infty)$
and $\vartheta_2 = \vartheta_0 \circ (v_7, \top)$.

Figure 8.4: For VIVU without context length restriction, e. g. VIVU$(2, \infty)$, nodes contained in a loop have a context prefix equal to the prefix of the entering edge (i. e., the context of the entering call node).

However, VIVU without context length restriction has the property that instances of dominators are still dominators in the CG*. (The loops in the CG* may be unrolled, though.) This property is the result of the particular context computation that never loses track of a distinction ever made by a loop entry edge, because the context length is not restricted. We will use this property to generate precise loop bound constraints for VIVU without context length restriction.

Consider Figure 8.4. The call node of the entry edge of loop 1 has context ϑ_0. All the nodes that are inside loop 1 have a context with prefix ϑ_0. This is due to the fact that contexts have no length restriction, so additional calls never remove distinctions ever made in the context up to that call.

This fact leads to a possibility of generating more precise loop bound constraints for VIVU mappings by partitioning the instances of nodes by the context of the entry edge. Obviously, this is also the most precise method of distinction, since loop bounds are given per entry and every entry is distinguished by a different VIVU context on the entry edge, and, therefore, it is handled in a separate loop bound constraint.

For each instance of an entry edge $(e, \vartheta_0) \in \text{entries}(l)$ of loop l, and for VIVU(x, ∞), loop bound constraints can be generated as follows.

$$\sum_{\vartheta_0 \circ \vartheta \in \Theta(\text{header}(l))} \text{cnt}(\text{header}(l), \vartheta_0 \circ \vartheta) \leq n_{\max}(e, \vartheta_0) \cdot \text{trav}(e, \vartheta_0) \tag{8.7}$$

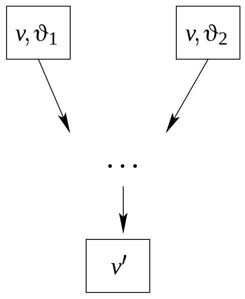
$$\begin{tikzcd}
\boxed{v,\vartheta_1} \arrow[dr] & & \boxed{v,\vartheta_2} \arrow[dl] \\
& \cdots \arrow[d] & \\
& \boxed{v'} &
\end{tikzcd}$$

Figure 8.5: Node v' is reachable from two instances of dominators: v, ϑ_1 and v, ϑ_2. So v' must be handled in the same loop bound constraint, since control flow may reach v' from either v, ϑ_1 or v, ϑ_2.

As can be seen, contexts of the header are considered in contexts that have the prefix ϑ_0.

8.2.3 Loop Bound Constraints for Arbitrary Mappings

As mentioned in the previous section, with arbitrary mappings, computation of loop bound constraints is more difficult since dominators in the CG are no dominators in the CG* anymore.

The basic idea for generating most precise loop bounds is to partition the instances of dominators of the loop. We will then generate a loop bound constraint for each set in the partition.

Consider Figure 8.5. To see how to make the partition, see that when v is reachable from several instances of its original dominator, these instances must be handled in the same loop bound constraint, since together, they act like one dominator for v: all control flow must pass through one of these nodes to reach v. So these instances of dominators should be in the same partition.

Moreover, for maximum precision, the partition should be maximal, i. e., the number of sets in the partition should be maximal to get the maximum number of distinct loop bound constraints.

So the main idea for an algorithm for finding a maximum partition is to search nodes that are reachable from different instances of dominators, and then unify the sets they stem from. A union-find algorithm will be the basis.

Definition 8.2 (Union-Find)
For a set of entities A and a disjoint partition $A = \bigcup A_i$, union-find has two operations:

- $\mathit{find}(a) = A_i$, where $a \in A_i$
  I. e., this operation finds the set that a is contained in. (In practice, this operation usually finds a representative for that set.)

- $\mathit{union}(a, b)$ modifies the partition in such a way that $\mathit{find}(a) = \mathit{find}(b)$.
  Note that *union* is commutative and transitive.

Our algorithm works on the call graph only, since contexts only change at call nodes, so nodes can only be reached from two edges if also the start node of their routine is reached from these edges.

For simplicity, we will perform union-find on all nodes contained in the loop, so we gather nodes that are reachable from the same instance of a dominator.

Algorithm Figure 8.6 shows an example of this algorithm.

1. Make an initial singleton partition: $\mathit{find}(v) := \{v\}$ for each node v contained in a loop l.

2. Perform depth first search (DFS) from each instance of a dominator v_0. For each node v reached during DFS, unify the sets v and v_0 belong to:
   $\mathit{union}(v_0, v)$.

Because there are no return edges in our call graphs, nodes contained in a loop are those that are reachable from the header. Furthermore, missing return edges prevent that during DFS, loops can be left and the re-entered via a different entry edge. So the algorithm never leaves a loop that is once entered.

For the algorithm it is not vital to use DFS. Breadth-first-search or anything else that finds reachable nodes is suitable, too.

```
routine a
    f()
    f()

routine f
    while ... do – loop 1
        ...
```

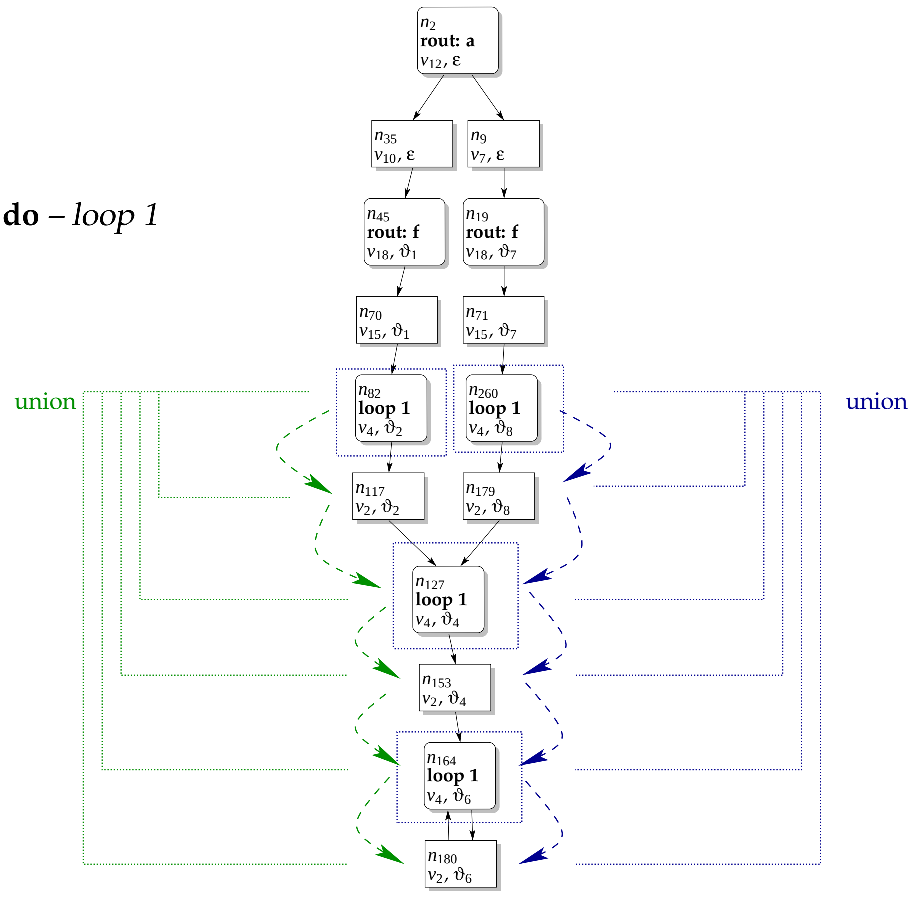
n_2 rout: a v_{12}, ε
n_{35} v_{10}, ε
n_9 v_7, ε
n_{45} rout: f v_{18}, ϑ_1
n_{19} rout: f v_{18}, ϑ_7
n_{70} v_{15}, ϑ_1
n_{71} v_{15}, ϑ_7
union
n_{82} loop 1 v_4, ϑ_2
n_{260} loop 1 v_4, ϑ_8
union
n_{117} v_2, ϑ_2
n_{179} v_2, ϑ_8
n_{127} loop 1 v_4, ϑ_4
n_{153} v_2, ϑ_4
n_{164} loop 1 v_4, ϑ_6
n_{180} v_2, ϑ_6

Figure 8.6: Union-Find loop bound algorithm depicted for two instances of header nodes for a CG* with CallString(2). DFS steps are shown by dashed arrows. Union operations are shown as dotted lines. Dotted rectangles mark instances of the dominator v_4. Union operations from node v_4, ϑ_4 and v_4, ϑ_6 are not shown for simplicity reasons. An optimisation of the algorithm will be shown soon.

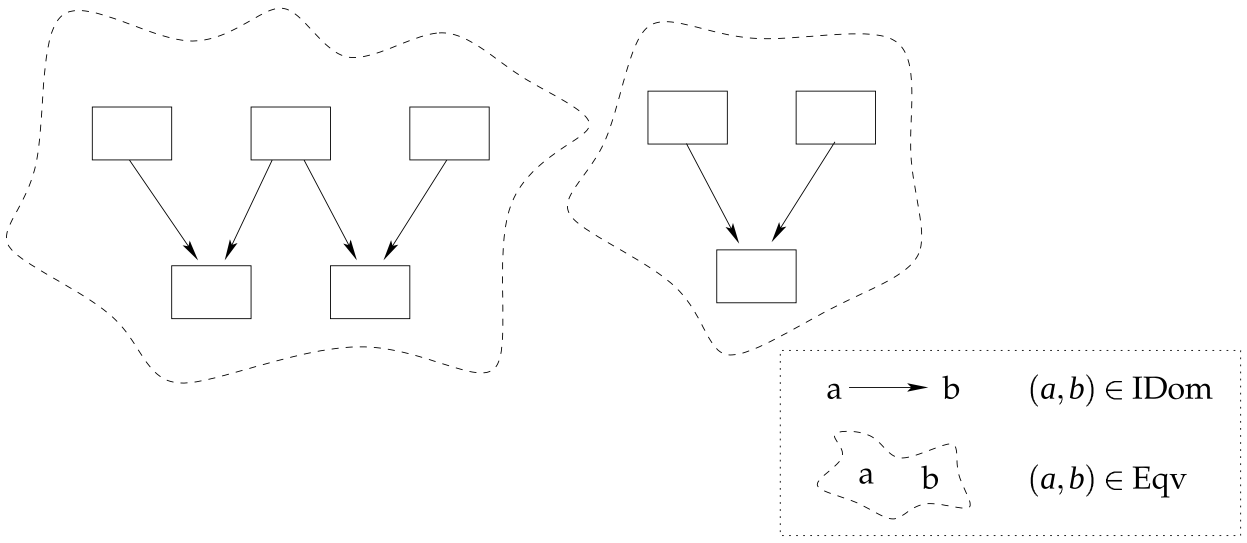

Figure 8.7: The equivalence relation for the *find* operation, Eqv, and the IDom relation. We prove that Eqv is the least equivalence relation such that IDom ⊆ Eqv.

Claim 8.3
The algorithm computes a partition such that the following conditions hold:

- Correctness: if node v is reached from an instance of a dominator v_0, then $\mathit{find}(v) = \mathit{find}(v_0)$.
- Minimality:
$$\text{Eqv} := \{(v_1, v_2) \mid \mathit{find}(v_1) = \mathit{find}(v_2)\}$$
is the least equivalence relation such that
$$\text{IDom} := \{(v_0, v_1) \mid v_0 \text{ is an instance of a dominator and } v_1 \text{ is reachable from } v_0\} \subseteq \text{Eqv}.$$
Figure 8.7 on page 130 depicts this situation.

Proof
Correctness is easy to prove: since DFS finds reachable nodes, $\mathit{union}(v, v_0)$ is eventually performed. By definition of *union*, it then holds that $\mathit{find}(v) = \mathit{find}(v_0)$.

Minimality: Assume the contrary, namely that there exists $(v, v') \in \text{Eqv}$, such that for an equivalence relation Eqv' with $(v, v') \notin \text{Eqv}'$ it holds that $\text{IDom} \subseteq \text{Eqv}'$.

This means that a union operation was performed by the algorithm, but need not be performed for $\text{IDom} \subseteq \text{Eqv}'$ to hold.

Let $\mathit{union}(v, v_1), \mathit{union}(v_1, v_2), \ldots, \mathit{union}(v_{n-1}, v_n), \mathit{union}(v_n, v')$ be a sequence of union operations that the algorithm performed that led to $\mathit{find}(v) = \mathit{find}(v')$. For convenience, we will define $v = v_0$ and $v' = v_{n+1}$.

One operand of the *union* operations the algorithm performs is always an instance of a dominator of the other operand. This holds for each pair $(v_i, v_{i+1}), i \in \{0, \ldots, n\}$. For each i, without loss of generality, let v_i be an instance of a dominator. So by definition of IDom : $(v_i, v_{i+1}) \in \text{IDom}$. And because we assumed $\text{IDom} \subseteq \text{Eqv}'$, it follows that $\forall i \in \{0, \ldots, n\} : (v_i, v_{i+1}) \in \text{Eqv}'$.

Because Eqv′ is an equivalence relation, and equivalence is transitive: $(v_0, v_{n+1}) \in \text{Eqv}'$. This is a contradiction. ▭

So we proved that the sets in the partition are minimal, meaning that the partition contains the maximum number of sets.

Constraints

After the partition of contexts of instances of header nodes is found, constraints can easily be generated.

Let l be a loop and $v_0 := \text{header}(l)$ be its loop header node (in the CG). Recall that $\Theta(v_0)$ is defined to be the set of contexts of v_0.

Let $\Theta_1, \ldots, \Theta_n$ be the partition of $\Theta(v_0)$ found by the algorithm in the previous section. Let the set of entry edges $\hat{E}_0^\star$ contain those edges in CG⋆ that enter v_0 in one of these contexts.

$$\hat{E}_0^\star := \{(v, (v_0, \vartheta)) \in \hat{E}^\star\}$$

Then a loop bound constraint is generated for each Θ_i.

$$\sum_{\vartheta \in \Theta_i} \text{cnt}(v_0, \vartheta) \leq \sum_{e \in \hat{E}_0^\star} n_{\max}(e) \cdot \text{trav}(e)$$

The involved nodes and the constraint itself are depicted in Figure 8.8 on the next page.

In Appendix A, examples of loop bound constraints are shown for different programs and different mappings.

Speed Optimisation

The above algorithm can be sped up a bit by checking the effect of union-operations. Consider Figure 8.9 on page 133.

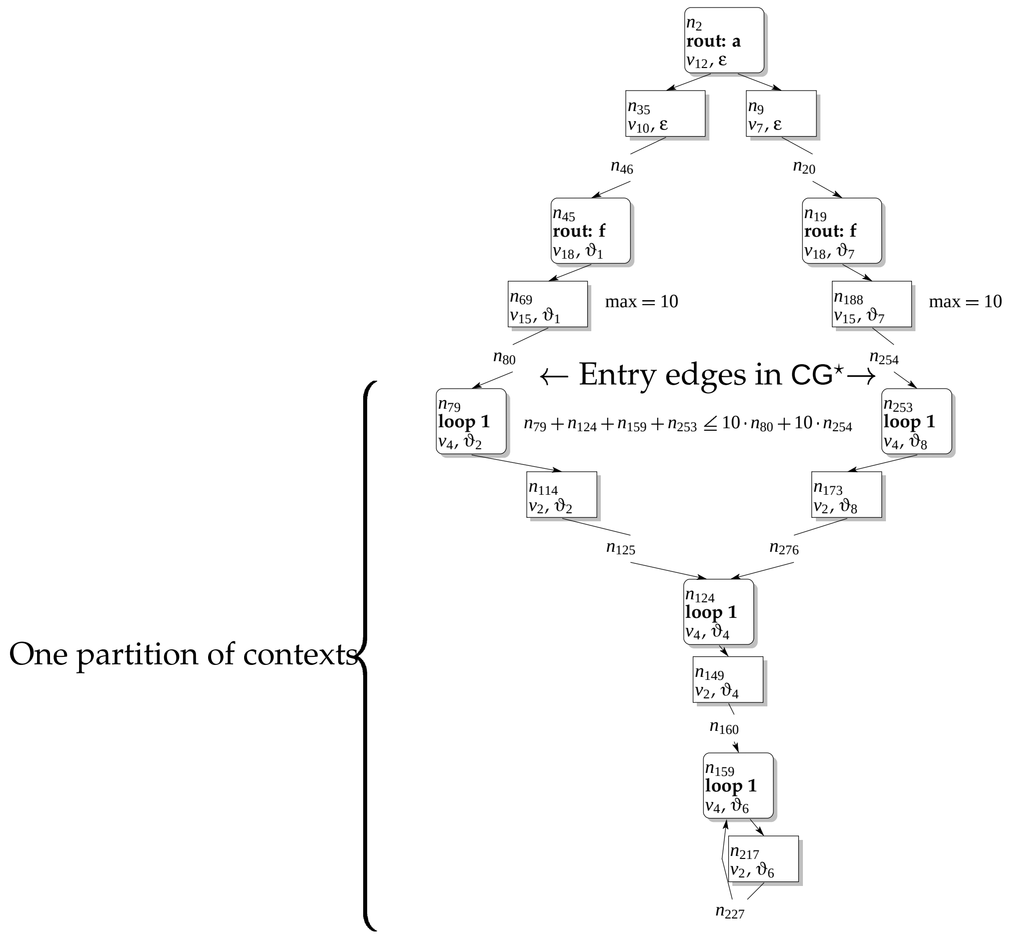
n_2 **rout: a** v_{12}, ε
n_{35} v_{10}, ε
n_9 v_7, ε
n_{46}
n_{20}
n_{45} **rout: f** v_{18}, ϑ_1
n_{19} **rout: f** v_{18}, ϑ_7
n_{69} v_{15}, ϑ_1
max = 10
n_{188} v_{15}, ϑ_7
max = 10
n_{80}
← Entry edges in CG⋆→
n_{254}
n_{79} **loop 1** v_4, ϑ_2
$n_{79} + n_{124} + n_{159} + n_{253} \leq 10 \cdot n_{80} + 10 \cdot n_{254}$
n_{253} **loop 1** v_4, ϑ_8
n_{114} v_2, ϑ_2
n_{173} v_2, ϑ_8
n_{125}
n_{276}
n_{124} **loop 1** v_4, ϑ_4
One partition of contexts
n_{149} v_2, ϑ_4
n_{160}
n_{159} **loop 1** v_4, ϑ_6
n_{217} v_2, ϑ_6
n_{227}

Figure 8.8: The computed partition and the entry edges of that partition for a simple CG⋆ with the generated constraint.

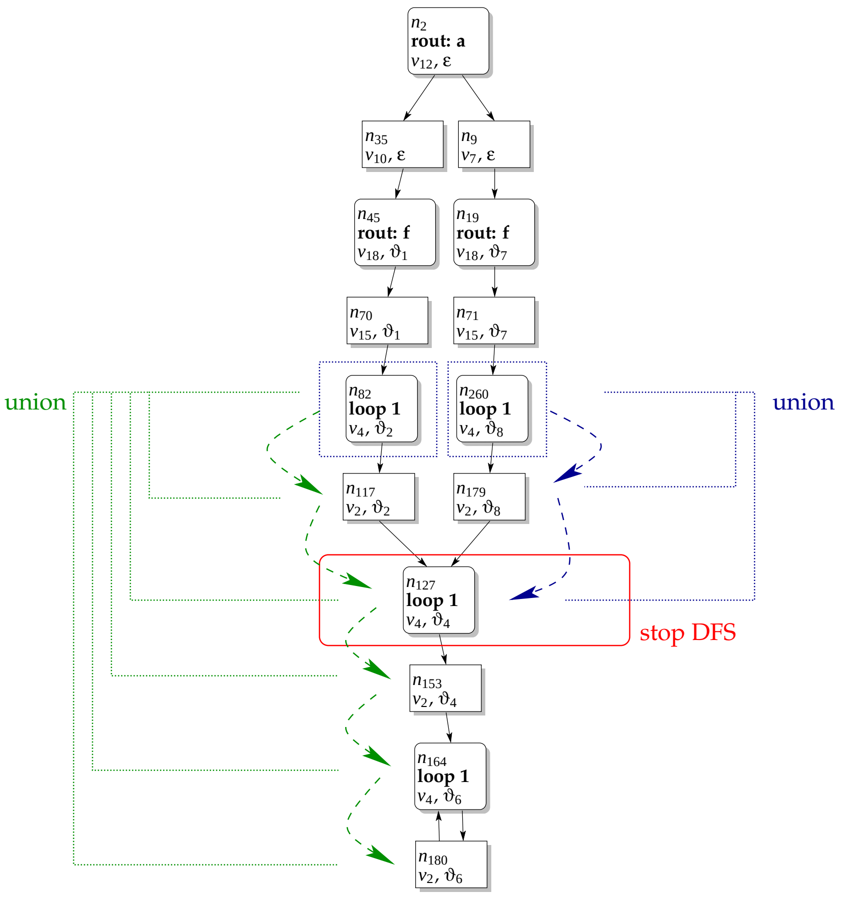
n_2 rout: a v_{12}, ε
n_{35} v_{10}, ε
n_9 v_7, ε
n_{45} rout: f v_{18}, ϑ_1
n_{19} rout: f v_{18}, ϑ_7
n_{70} v_{15}, ϑ_1
n_{71} v_{15}, ϑ_7
union
n_{82} loop 1 v_4, ϑ_2
n_{260} loop 1 v_4, ϑ_8
union
n_{117} v_2, ϑ_2
n_{179} v_2, ϑ_8
n_{127} loop 1 v_4, ϑ_4
stop DFS
n_{153} v_2, ϑ_4
n_{164} loop 1 v_4, ϑ_6
n_{180} v_2, ϑ_6

Figure 8.9: Optimisation of algorithm. Instances of the dominator v_4 that have entry edges are marked by dotted rectangles. When these instances of dominators are united in one set, the current DFS can be stopped since all subsequent nodes are known to be reached by a previous DFS already.

Important nodes are those instances of dominators that have an incoming edge that is an entry edge. DFS needs to be performed only starting at these nodes. Further, when a union-operation unites the current starting point of the DFS with another of these instances of dominators (a previously reached one), the DFS can stop, since a previous DFS has already found all subsequent nodes.

8.3 User Added Constraints

Fortunately, user added constraints are rare. For most application, the automatically generated constraints give very good analysis results.

With the presence of contexts, user added constraints become extremely hard to understand for users that do not know anything about contexts at all.

So the framework should hide the actual context mapping from the user, since otherwise, they would need to know it in order to state constraints, which is unlikely to work for unexperienced users. For experienced users, it would be a lot of work to state constraints for the current mapping.

Instead, the most probable way this is going to be implemented is to allow the user to specify an arbitrary piece of invocation history that led to a routine, i. e. to let them specify a suffix of the concrete call string. The framework can then use this to find all the contexts this suffix applies to and combine these in one constraint.

This briefly described technique is very flexible but would require a lot of additional code in the analyser, so it is not implemented yet but will be implemented as soon as it is urgently needed.

Currently, user added constraints are added for all contexts. In our applications, this was always enough precision since the users did not know anything about invocation history anyway.

Part IV

Evaluation

Chapter 9

Experimental Results

9.1 Implementation

Here is a list of programs that were implemented as part of this thesis.

exec2crl. This is the tool that reconstructs ICFGs for use with our framework's analyses. It consists of many modules for executable formats, machine decoders, and output formats. The total implementation consists of approx. 37 000 lines of C++ code.

NET library. This library is used by exec2crl for generic description of different machine architectures. Each description file contains information about machine code layout, instruction operands etc.. The implementation with all the machine descriptions totals approx. 46 000 lines in C++ and specification files.

pathan. This is the implementation of the path analysis. It consists of a library with all the algorithms and a frontend implementing a user interface. The implementation totals approx. 6400+2600 lines of C++ code.

9.2 Decision Trees

The algorithm was implemented in our analysis framework for real-time systems (*see* [Ferdinand et al., 1999a; Ferdinand et al., 2001]).

We have written machine descriptions for the IBM PowerPC (*see* [PowerPC, 1997])[1], the Motorola ColdFire (*see* [ColdFire, 1997]) architecture and the ARM 5 architecture (*see* [ARM, 2001]).

Moreover, with the help of a small script (only 194 lines of Perl) we could automatically convert a PDF manual (*see* [Infineon, 1997]) for the Infineon C166 architecture into a specification with all the processor's bit patterns. The result is a template file where the command classifications can be filled in. We included this file in our tests of the decision tree building algorithm. Writing this script only took a few hours.

The time for tree generation was negligible for all test inputs. For the ColdFire specification it took less than 0.2 seconds on a Pentium III with 650 MHz. The specification has 908 instruction patterns, because the ColdFire is quite a complex processor due to its CISC history.

Self-evident by the construction of the selecting mask, but still not uninteresting, is the fact that our algorithm generates a root node that tests exactly for the primary opcode for both the PowerPC and the ColdFire processor.

The generated decision tree for the ColdFire architecture has a maximal leaf node depth of 5 (including the root node). The average depth is 2.76, i. e., this is the average number of decisions needed to decode one instruction at the front of a bit string, which is very little.

To compare the algorithm to one that is limited to testing adjacent bit groups instead of arbitrary ones, we explicitly forced it to select only adjacent bits for testing. The generated tree then has a maximal depth of 7 and an average depth of 3.13.

The PowerPC 403 specification has 210 instruction patterns and the time to generate the decision tree is below the precision limits of measurement. The maximal leaf node depth is 3 including the root node. The average depth of the PowerPC decision tree is 2.2. The PowerPC is a RISC architecture, so these 3 levels are explained very easily: the root node tests opcode 1, the next node tests opcode 2 and some commands are distinguished by either setting the condition code bits or not, thus another bit is tested for those commands in the third node. And because of the layout of the bits of the opcode 1 and 2, the decision tree always tests adjacent bit groups in this tree already.

The C166 specification is 230 instruction patterns and again, the time to generate the decision tree is below the precision limits of measurement. The maximal leaf node depth is 4, the average depth is 2.41. The tree with bit group tests of adjacent bits is a maximal depth of 6, and the average depth increases marginally to 2.48, because only very few commands have longer decoding paths.

The feature of default nodes for instructions that are subsumed by others is needed sev-

[1]The PowerPC architecture standard was developed together with Motorola and Apple. IBM currently manufactures processors that are compliant with this standard.

eral times in the machine code specification of the ColdFire architecture. Some examples are two sorts of branch commands, which have different sizes if the displacement constant of the shorter variant has a value of 0. Another example are the divide and remainder instructions which share the same opcodes but are distinguished by whether two of the three operands are identical.

The experiments show that writing a decoder for machine code of a new processor has become much easier and less time-consuming, less error-prone and, therefore, much safer.

9.3 CFG Reconstruction

To maximise reconstruction speed, the decision trees are compiled into ANSI C++ by generating a nested `switch` statement, i. e., for each decision node, one `switch` statement is generated. The decision trees can be compiled for little and big endian code, if the processors support both. This makes the following CFG reconstruction experiments even faster, because the trees are not interpreted, but compiled.

To evaluate our algorithm, we used Infineon TriCore Rider B and IBM PowerPC 755 and 403GCX ELF executables, counted the number of uncertainties and examined how many of them could be resolved. Because we had real-time systems in mind, only statically linked executables were used for evaluation. However, several dynamically linked executables where screened to ensure that external routine calls are analysed correctly.

For the PowerPC architecture we used the MetaWare High C/C++ Compiler 3.50D to compile our test programs. For the TriCore architecture, the HighTec C/C++ Compiler was used, which is based on the GNU C Compiler. We used the maximum available optimisation level.

The sizes of the executables ranged from a small program with only 300 instructions to Livermore loop benchmarks which contained around 15000 instructions (TriCore architecture, 45000 bytes). Additionally, we analysed the unused parts of a bigger executable (which were parts of its standard C library) in order to analyse optimised library code. This totalled 13000 instructions (PowerPC architecture, 54000 bytes).

Figure 9.1 shows some results. Almost all computed branches could be predicted. The ones that were left unpredictable occurred in highly optimised library code. In the TriCore library, a frequently used address was kept in a register throughout several routines. The address of the switch table depended on it. In the PowerPC code, the targets of the computed branch were written into the jump table at run-time and depended on the caller of the routine.

Apart from these specific tests, we reconstructed the ICFG of numerous other programs that where analysed during commercial usage of exec2crl. These all worked without

Program	Arch.	#Instr.	#Bytes	#Comp.	#Unres.	%Recogn.
Fast Fourier Transform	TriCore	5563	17488	1	0	100.0%
AVL Trees	TriCore	5577	16786	2	0	100.0%
Livermore Loops	TriCore	14692	46644	8	1	87.5%
LCD Panel Control	PowerPC	360	1440	12	0	100.0%
LCD Jumping Ball	PowerPC	3163	12652	80	0	100.0%
LCD Jumping Ball*	PowerPC	13484	53932	275	2	99.3%
Commercial RTS	PowerPC	21505	86020	3	3	100.0%

Figure 9.1: Some results of our disambiguation algorithm during ICFG reconstruction. The program sizes, number of computed jumps and the number of unresolved computed jumps are given. In the example marked with *, all the unreachable library code was analysed, too.

Program	Arch.	#Instr.	#Bytes	Reconstruction Time [s]
Fast Fourier Transform	TriCore	5563	17488	0.5
AVL Trees	TriCore	5577	16786	0.6
Livermore Loops	TriCore	14692	46644	1.6
LCD Panel Control	PowerPC	360	1440	0.2
LCD Jumping Ball	PowerPC	3163	12652	1.2
LCD Jumping Ball*	PowerPC	13484	53932	3.9
Commercial RTS 1	PowerPC	21505	86020	5.5
Commercial RTS 2	ColdFire	9457	43890	1.8
Commercial RTS 3	ColdFire	10811	49900	2.1
Commercial RTS 4	ARM/Thumb	13487	29058	4.5

Figure 9.2: Run-time of exec2crl for different input programs for different architectures. The table compares the extracted amount of code to the time needed to produce a resulting CRL file on an Athlon XP1900+ processor (a 32 bit, 80x86 compatible processor clocked with 1600 MHz) with 512 MB of main memory.

any flaw, and with a prediction of 100% for computed branches for the PowerPC architecture.

To see how fast our algorithm works, we used Infineon TriCore Rider B, IBM PowerPC 755 and 403GCX, Motorola ColdFire MCF 5307 and ARM 5 executables in ELF (*see* [ELF]) and COFF2 format. Figure 9.2 shows reconstruction times. We used executables from various architectures and reconstructed the ICFG for several test programs and some commercial real-time applications. As can be seen from the table, exec2crl performs very well for all programs. Note that the times include compressing (with gzip) the resulting CRL file and writing it to disk.

9.4 Path Analysis

Our approach was implemented mainly in order to improve the analysis time of large executables. W.r.t. the path analysis, the standard examples that are widely used for experiments (e. g. Fast-Fourier Transform, Bubblesort, Matrix Multiplication, Circle Drawing Algorithm, Prime Test) all resulted in an optimal 100% precise WCET path prediction.

We also ran tests of real-life programs from safety critical embedded hard real-time systems for the Motorola ColdFire MCF 5307 (*see* [ColdFire, 1997]) architecture. Due to the complex nature of these programs, the real WCET is not known.

Because of this, the most interesting measure is the analysis speed for real-life executables.

The path analysis is implemented in a hardware independent way. The framework (*see* [Ferdinand et al., 2001]) we used for finding the run-time of the path analysis comes with microarchitecture analyses for value analysis (*see* [Sicks, 1997; Ferdinand et al., 1999a]), (instruction and data) cache analysis (*see* [Ferdinand, 1997; Theiling et al., 2000]), and pipeline and memory bus analysis (*see* [Schneider and Ferdinand, 1999; Ferdinand et al., 2001]). All these can be parameterised (at least) with a specific mapping. Loops are transformed at the beginning of the analysis suite, just after the executable's CFG has been reconstructed (*see* [Theiling, 2000; Theiling, 2001]). The loop transformation also computes the sets $\mathsf{Entries}(l)$ and $\mathsf{Backs}(l)$ for each loop l.

The pipeline and memory bus analysis, which runs just before the path analysis, yields execution times for each basic block/context pair. The path analysis then reads these results and also the loop-transformed control flow graph, has the needed $\mathsf{CG}^\star$ computed by the given mapping and then generates constraints. In the last step of this generation, loop bound constraints are generated using the algorithm described above. After the ILP has been generated, `lp_solve`[2] is used to solve the ILP.

For us, it was most interesting to see how fast the ILP-generator is, and also how long the ILP takes to be solved. The solving step has quite a high theoretical worst-case run-time, namely exponential, due to the used branch-and-bound technique[3]. For our tests, we used twelve test programs from a real-life hard real-time application that all had a size in the order of about 50kB. The target architecture was the Motorola ColdFire MCF 5307 processor (*see* [ColdFire, 1997]). The programs contain several loops and were analysed with a few user added constraints.

[2] `lp_solve` was written by Michel Berkelaar and is freely available at `ftp://ftp.es.ele.tue.nl/pub/lp_solve`.

[3] It could be reduced to polynomial run-time, if the ILP was relaxed to an LP. In this case, the resulting execution counts might become non-integer, making them quite unusable for propositions and reasoning about control flow. However, the value of the objective function is still usable, since it is guaranteed to be only larger than the one of the ILP, so a WCET prediction is still useful, although maybe less precise.

Mapping	#Nodes	#Edges	gen. time [s]	#vars	#constraints	solv. time [s]
CallString(0)	7173	4728	4	833	816	0
CallString(1)	21145	16139	12	7457	6512	14
CallString(2)	22039	16872	13	7709	6760	15
CallString(6)	25367	19432	15	8733	7784	20
VIVU(1,1)	21054	16069	12	7429	6470	13
VIVU(2,1)	21145	16139	13	7457	6512	14
VIVU(5,1)	21418	16349	13	7541	6596	18
VIVU(10,1)	21873	16699	13	7681	6736	15
VIVU(∞,1)	22899	17499	14	8001	7049	16
VIVU(1,2)	21857	16732	13	7653	6918	15
VIVU(2,2)	22689	17372	14	7909	7174	18
VIVU(5,2)	25185	19292	15	8677	7942	23
VIVU(10,2)	29345	22492	17	9957	9222	32
VIVU(∞,3)	39513	30412	23	13125	12326	48
VIVU(1,∞)	21857	16732	13	7653	6918	15
VIVU(2,∞)	22689	17372	14	7909	7174	18
VIVU(5,∞)	25185	19292	15	8677	7942	23
VIVU(10,∞)	29345	22492	17	9957	9222	32
VIVU(∞,∞)	39513	30412	23	13125	12326	48

Figure 9.3: This table shows the generation and solving times for a fixed input program for different mappings. Columns two and three show the size of the CFG* for this program with the given mapping. The time for generation of the ILP is shown, the size of that ILP, and the time to solve the ILP.

We used 59 different mappings for testing (CallString and VIVU mappings with different parameters), including our most precise mapping, namely VIVU(∞,∞) (where every loop is unrolled by its maximal iteration count), which resulted in the largest ILPs. Figure 9.3 on the next page shows the results for selected mappings for one of the programs.

The ILP generation for any of our test executables never took longer than 25 seconds on an Athlon processor with 1600 MHz and 512 MB main memory, so the algorithm can be said to perform very well.

As can be seen from the table, the largest resulting ILPs had some 13000 non-trivial variables (plus over 50000 pairs of variables that are not shown in the table, since they were automatically collapsed due to trivial constraints of the form $x = y$) and also some thousand constraints (more than 12000). Still, solving took less than 50 seconds for this program even for our most precise mappings. So this also shows very good performance.

With respect to its theoretical worst case solving time, an ILP with some thousand variables and constraints is quite threatening. Relievingly, the generated ILPs have a structure similar to a network flow problem due to the localised generation of most kinds of constraints and are, therefore, quickly solvable.

However, the ILP structure cannot be guaranteed to be easily solvable. Loop bound constraints are not as local as the other constraints. Further, users may add arbitrary constraints. But we found no settings where the solving time for the ILPs behaved badly even with user added constraints and many different mappings.

In our tests, we found that all our solving times were polynomial in the number of variables in the ILP with a seemingly small exponent $\leqq 2$ (though, as mentioned before, no guarantees can be given, of course). So the potential exponential worst case solving time of `lp_solve` was by far not reached. Figure 9.4 on the next page shows this for the twelve example programs when analysed for 59 different mappings.

In order to check the presumption that the good solving time was reached because the relaxed LP was integer by nature, we compared the results with another run of the same 420 tests with relaxed LPs. The solving times were the same, so no branch-and-bound step was necessary in `lp_solve`, showing that the first solution of its simplex algorithm is already integer for all tests. Figure 9.5 on page 145 shows a comparison between solving times for the original ILPs and the corresponding relaxed LPs. There is no difference.

We also did a lot of tests to check that the loop bound constraints are generated in the correct way. Because the printed CFGs take up a lot of space, and because these tests are only checks that the algorithm is programmed correctly, but not tests for other interesting properties, the results were moved to an Appendix, Section A.1 on page 161.

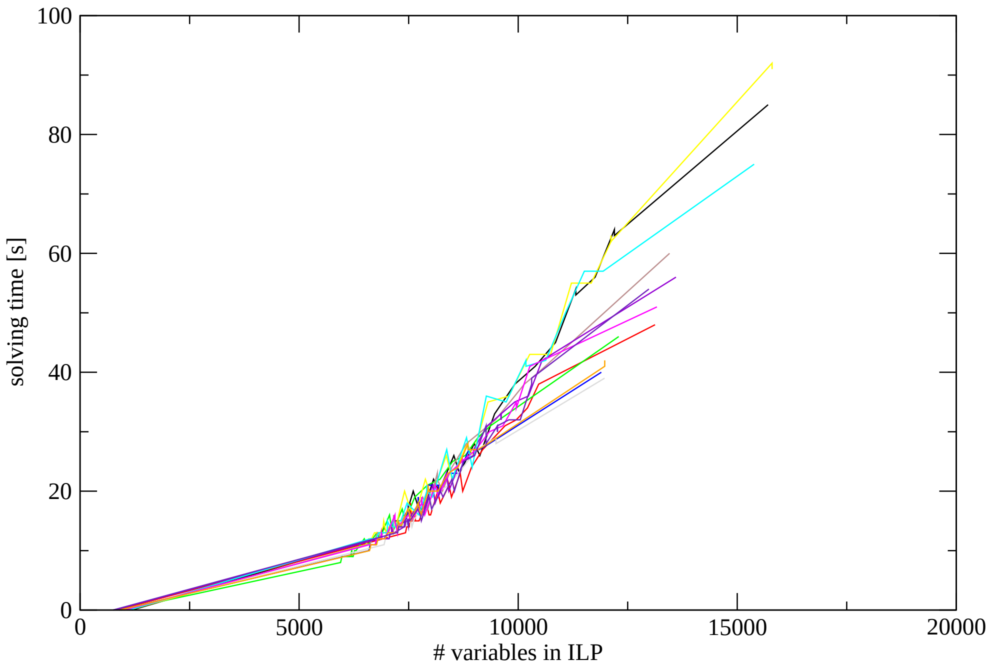

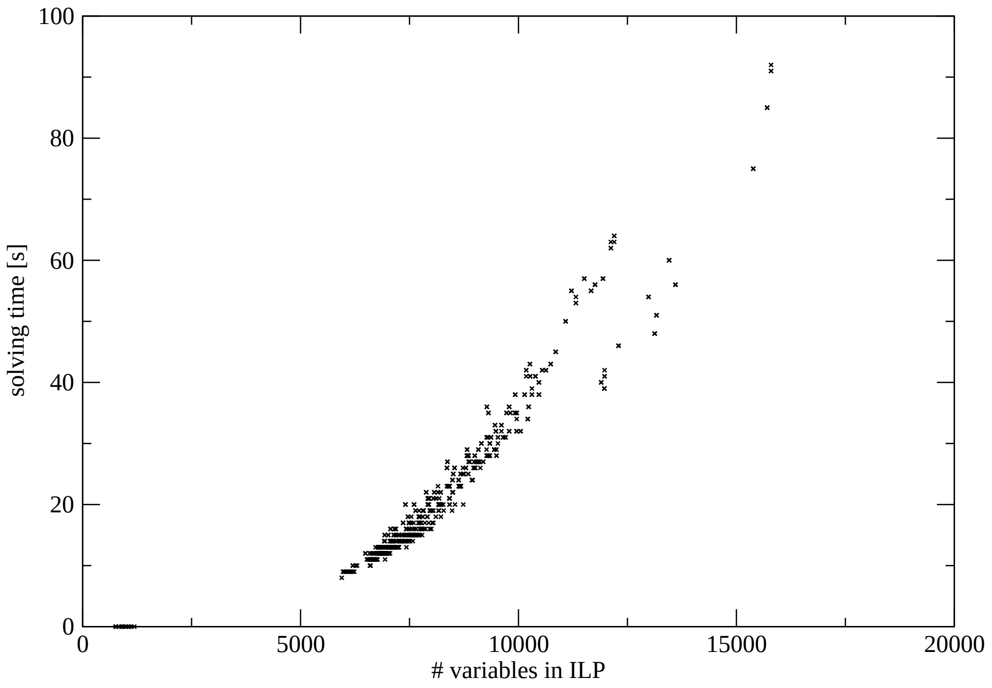

Figure 9.4: Solving times of the ILPs for different mappings and different input programs. Depending on the mapping, differently sized ILPs result. The ILP size is shown on the x-axis as the number of variables. Each line in the upper graph shows a different program. The lower graph shows the same results as independent points.

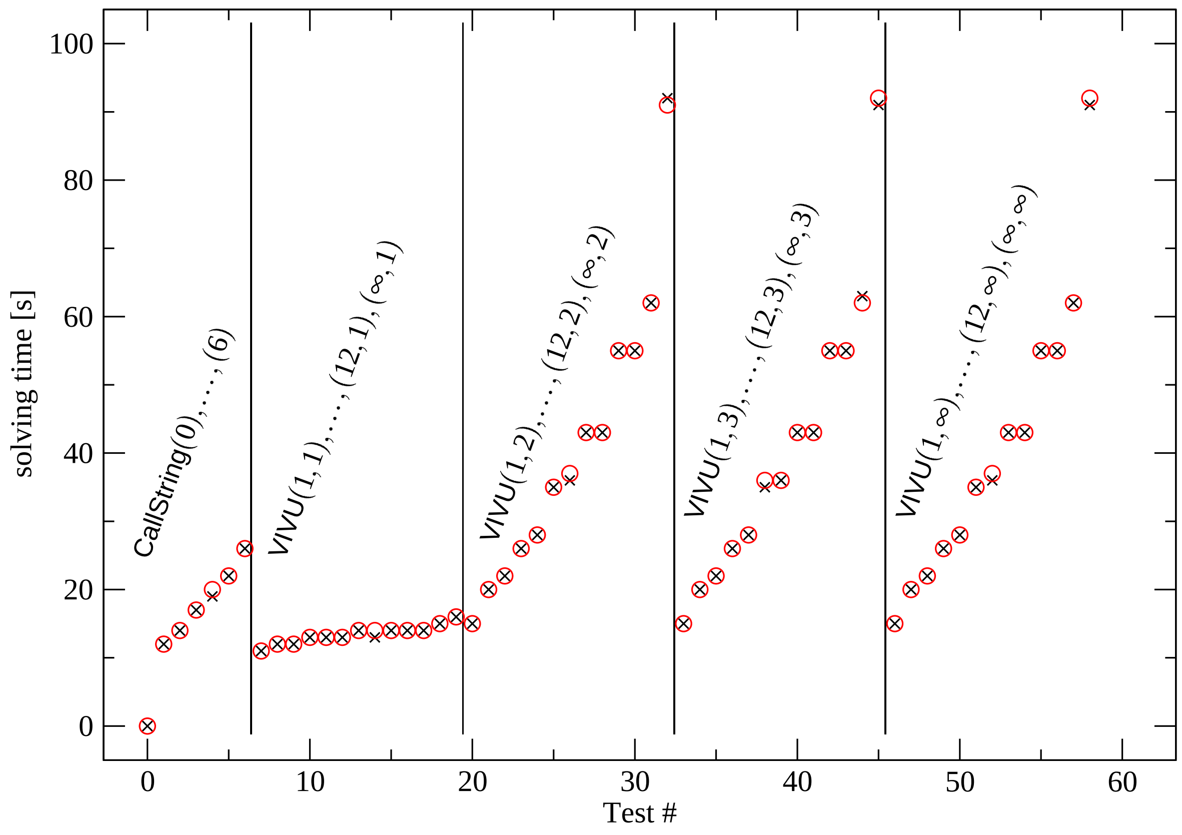

Figure 9.5: Solving time comparison for a fixed program and different mappings. Crosses: solving times of ILPs, circles: solving times of relaxed LPs. The two are virtually identical (apart from measurement imprecision), so no branch-and-bound branching was necessary to solve the ILPs.

Chapter 10
Related Work

This chapter is organised in four sections. The first section deals with related work concerning WCET analysis for real-time systems and its history.

Each following part will show related work w.r.t. a different part of this thesis. This structure was chosen since the work about decision trees, ICFG reconstruction and path analysis is from very different areas and quite incomparable. Certain work might be mentioned in more than one section if appropriate.

10.1 History of WCET Analysis

10.1.1 Abstract Interpretation

Abstract Interpretation (AI) is a widely used technique for static analysis of programs, usually used in compilers (*see* [Wilhelm and Maurer, 1995; Aho et al., 1986]) but also in other analysis tools, e. g. for WCET analysis (*see* [Ferdinand et al., 1999a; Ferdinand et al., 2001]). Our framework uses AI for value, pipeline and cache analysis.

AI has its roots in publications by Cousot and Cousot (*see* [Cousot and Cousot, 1977a]). Nielson et al. wrote a text book about that topic (*see* [Nielson et al., 1999]). Examples of typical analyses using AI can be found in [Wilhelm and Maurer, 1995].

Florian Martin implemented the analysis tool PAG as described in his Ph. D. thesis (*see* [Martin, 1995a; Martin, 1998; Martin, 1999b]). PAG is a program analysis generator that allows the specification of an analysis in a functional language. The PAG framework then translates such a specification into a C program that implements a program analyser. This analyser uses a fixed-point algorithm together with the user-defined specification to analyse programs. Many language frontends are available, including one for performing analyses on machine code level, which is used in our WCET framework. PAG incorporates approaches to interprocedural analysis (*see* [Martin et al., 1998; Martin, 1999a]).

10.1.2 Worst-Case Execution Time Analysis

One of the earliest approaches to WCET analysis is presented in [Puschner and Koza, 1989]. It combines execution times of basic blocks according to the structure of a program using *timing schemata* for different program constructs. Their method, due to the state of computers at that time, does not deal with pipelines or caches or other sophisticated hardware features. Hardware was so simple that a source code analysis was feasible for retrieving good WCETs.

In [Park and Shaw, 1991], a timing tool for retrieving WCETs from source level is presented. This paper also uses timing schemata to compute the WCET. The work group has modified these timing schemata to allow for analysis of more complex architectural features (*see* [Hur et al., 1995; Lim et al., 1995; Kim et al., 1996; Lim et al., 1998]). Although this work group has shown that their approach is applicable to many different hardware features (pipelines, caches, multiple issue), there was no work that showed how these features can be analysed together; each paper focuses on only one aspect.

Timing schemata are still used by some recent work (*see* [Colin and Puaut, 2001]) although the precision on modern architectures is not satisfying due to complex behaviour of hardware.

In 1995, the technique of ILP-based path analysis was presented to overcome the problems of tree-based approaches in combination with complex hardware. The first publications about this were [Li et al., 1995b; Li and Malik, 1995a; Li and Malik, 1995b]. In the same year, Puschner and Koza compiled a technical report about this topic (*see* [Puschner and Koza, 1995]). The advantage of the ILP-based approach has been mentioned in previous chapters: there is no need for an extensive path search since the paths are considered implicitly by re-formulating the WCET computation (*see* Section 7.3 on page 112). Li et al. published more work to handle different hardware features (*see* [Li et al., 1995a; Li et al., 1996]). Their approach of combining microarchitecture analysis and path analysis in one ILP (*see* [Li et al., 1996]) showed complexity problems with highly associative caches, so we follow a split approach, first published in [Theiling and Ferdinand, 1998] and in full detail in [Theiling et al., 2000] (and in German in [Theiling, 1998]).

After the basic techniques for microarchitecture analysis had been established, a lot of specialised work was published that deals with hardware features of modern architectures.

Before 1994, real-time systems usually did not use caches. An overview of analysis techniques up to that date is given in (*see* [Basumallick and Nilsen, 1994]). Analysis of caches was then published, gradually improving the precision and adapting to data caches. Work about caches includes [Liu and Lee, 1994; Mueller et al., 1994; Mueller, 1994; Ferdinand et al., 1997; Ferdinand, 1997; Ferdinand and Wilhelm, 1999; Ferdinand et al., 1999b; Theiling and Ferdinand, 1998; Theiling et al., 2000; Li et al., 1996; Lim et al., 1995; Blieberger et al., 2000]. The most sophisticated techniques can be considered to be [Ferdinand, 1997] and [Blieberger et al., 2000]. However, the latter computes formulae that describe the cache behaviour for different situations, which makes the approach too complex for large programs.

Work about pipeline behaviour prediction was published in [Zhang et al., 1993; Schneider and Ferdinand, 1999; Engblom and Ermedahl, 1999; Stappert et al., 2001; Ferdinand et al., 2001; Engblom, 2002; Langenbach et al., 2002]. From those, the most sophisticated work can be considered to be [Ferdinand et al., 2001] and [Langenbach et al., 2002], where a modern processor is analysed in a real-life commercial environment in full interaction with caches and memory busses.

A value analysis for address prediction has been published in [Sicks, 1997]. It is based on interval analysis as described e. g. in [Moore, 1966; Alefeld and Herzberger, 1983]. An extended and generic version of the value analysis is used in our framework (*see* [Ferdinand et al., 2001]).

There is also work about trying to exclude infeasible paths from the WCET calculation. An automatic, very precise but unfortunately complex and slow analysis was proposed in [Gustafsson, 2000]. This analysis is also based on Abstract Interpretation. The method even iterates loops to find infeasible paths per iteration. Exclusion of paths by annotations was proposed in [Kirner and Puschner, 2000; Stappert et al., 2001]. Our framework also allows annotations for this purpose by adding constraints to the generated ILP.

A combined, fully static approach to WCET analysis, considering all hardware components of by splitting microarchitecture and path analyses was published in [Ferdinand et al., 2001].

Due to the complex nature of static WCET prediction, several work groups have proposed approaches that try to use measurements (*see* [Petters and Färber, 1999; Petters, 2000; Bernat et al., 2000; Bate et al., 2000; Lindgren et al., 2000]). or simulation along program traces (*see* [Nilsen and Rygg, 1995; Engblom and Ermedahl, 1999; Huang, 1997]) to predict the WCET. Those approaches must clearly be considered unsafe and, therefore, dangerous for hard real-time system analysis, because measurements are never exhaustive and in the same way, program traces only cover certain paths. These techniques are only usable for soft real-time systems in no safety-critical environments. Those approaches cannot be compared to the methods in our framework.

The following sections compare related work to parts of this thesis, describe the differences and show the contribution of this work.

10.2 Decision Trees

There is a lot of work on decision trees in many different areas of Computer Science (*see* [Moret, 1982; Russell and Norvig, 1995]). A survey of decision tree building methods is given by Sreerama K. Murthy in [Murthy, 1998]. The basic principles of recursive partitioning and finding a splitting method are introduced there. Methods of compiling lazy pattern matching can be found in [Laville, 1991].

[Hadjiyiannis et al., 1999] present an algorithm for disassembling that searches linearly for the given bit patterns, thus not using a decision tree and involving $O(n)$ decoding runtime where n is the number of instruction patterns.

The contribution of the novel algorithm presented in Chapter 5 is the splitting function for bit patterns given as machine words. They form a special class of multiple boolean attributes, which this algorithm handles in parallel. To the best of our knowledge, no solution to this problem has been published before ours (*see* [Theiling, 2001]).

Other approaches to real-time system analysis often do not read machine code, so the problem of decoding bit strings does not occur there. Either assembly (*see* [Lim et al., 1995; Lim et al., 1998]) or source code (*see* [Puschner and Koza, 1989; Gustafsson, 2000]) are used as input. For modern processors, the precise analysis of low-level effects of caches and pipelines needs precise location information. This is only available with machine code for most machines (not even on assembly level, because linking is not performed), so our framework reads machine code from linked executables.

Another algorithm that tries to solve the same problem as ours is found in the New Jersey Machine-Code Toolkit (*see* [Ramsey and Fernandez, 1996; Ramsey and Fernandez, 1995]). The decision tree building algorithm used in that framework, however, it is not described in publications. Looking at the documentation in the source code, it can be seen that it uses opcode fields of the machine code defined by the user to compute the decision tree, so the nodes in the decision tree are quite obviously available from the user's specification (each opcode field with its possible values becomes one node in the decoding tree). Our approach is much more flexible by allowing a flat list of bit patterns as input and finding the decision nodes automatically.

Another widely used way of decoding machine code is the GNU Binutils package (*see* [Binutils]). One tool that uses Binutils is the Wisconsin Architectural Research Tool Set (*see* [Cinderella; Li et al., 1996]). In Binutils, decoders are written manually for each processor. E. g. for the Motorola 68xxx processor, the decoding is done by linearly searching the bit patterns and limiting the search algorithm to partitions by sorting the patterns by their 4-bit primary opcode. In contrast to this, that partitioning is done automatically and in a generic way by our novel algorithm.

10.3 ICFG Reconstruction

First of all, this work of ICFG reconstruction is not comparable to that of the problem occurring in object-oriented and functional language compilers of finding a call graph (*see* [Grove and Chambers, 2001]). That problem is rather a compilation problem to find a good mapping of the object-oriented or functional source program to machine or byte code. In contrast to that, our problem is to read binaries and reconstruct a ICFG from these.

In the Wisconsin Architectural Research Tool Set (WARTS), the control flow is reconstructed using program slices. As mentioned before, the framework incorporated in the Cinderella tools (*see* [Cinderella]) relies on GNU Binutils (*see* [Binutils]). Our early prototype tools for the SPARC architecture used their EEL library (*see* [Larus, 1996; Larus and Schnarr, 1995]) via a special frontend (*see* [Ramrath, 1997]), but genericity and safety with real-time systems in mind made a new approach necessary in order to cope with more complex architectures and compiler techniques.

One of the more recent works concerning ICFG reconstruction is [De Sutter et al., 2000]. The paper addresses the next step of the ICFG reconstruction, i. e. disambiguating uncertainties by constant propagation, and shows how it can be used to analyse the DEC Alpha architecture. We focused more on the basic step, because we found it was complicated to obtain even a conservative ICFG approximation due to ambiguous usage of machine instructions. Some problems [De Sutter et al., 2000] solves by an additional analysis step are solved in our bottom-up algorithm, too, because some disambiguation takes place during the reconstruction of the ICFG. We think, however, that for other architectures than the ones evaluated so far, constant propagation using abstract interpretation will be needed.

Much work was done in order to restructure CFGs of optimised code for debugging purposes (*see* [Brooks et al., 1992; Cifuentes and Gough, 1995; Adl-Tabatabai and Gross, 1996; Tice and Graham, 1998]). All work either assumes that instructions are easily recognisable (e. g. Intel 80x86 (*see* [Brooks et al., 1992; Cifuentes and Gough, 1995])), or that a basic ICFG is already known. The reconstruction usually uses a top-down approach, assuming that a basic CFG exists.

A related problem is the reconstruction of control flow from assembly code. Recently, our work group has extended its research to this problem and published [Kästner and Wilhelm, 2002]. However, the problem is quite different from ICFG reconstruction from binaries. Most importantly, top-down algorithms work very well for assembly code since control structures (routines and branch targets) are clearly marked. Hence, a top-down algorithm is used in the above paper.

Nevertheless, due to some similarities of the two problems, for instance w.r.t. to disambiguation of instructions' influence on control flow, there will certainly be communication inside our work group about cooperation and exchange.

10.4 Path Analysis

Work about ILP-based path analysis was first published by Li et al. in [Li et al., 1995a; Li et al., 1995b; Li and Malik, 1995a]. In the same year, Puschner and Koza compiled a technical report (*see* [Puschner and Koza, 1995]) dealing with the same topic. Li et al. extended their work to include non-direct-mapped cache analysis in [Li et al., 1996]. For caches with high associativity, a pure ILP-approach is not feasible using that technique due to complexity problems.

In [Theiling and Ferdinand, 1998] an alternative approach was presented that split off the microarchitecture modelling from the path analysis by ILP. This approach overcame complexity problems Li et al. suffered as a tribute to a combined cache and path analysis in one pass.

The method in [Theiling and Ferdinand, 1998] is usable for some simple mappings without context length restriction. Strongly extending that work, this thesis presents how ILPs can be generated for any statically computed mapping. Analysis techniques using contexts are described in detail in [Martin et al., 1998; Martin, 1999b].

Ottoson and Sjödin also used constraint-based path analysis with a different objective function weighting the edges instead of the nodes (*see* [Ottoson and Sjödin, 1997]), something we also do in this work. However, their approach uses non-linear constraints, making the analysis very slow. They report that their approach is not usable in practice yet.

In total, the basic technique can be said to be well-established. However, to our best knowledge, no other work group yet published the use of basic block contexts for precision improvement of ILP-based path analysis.

Lim et al. have proposed a method of WCET computation called extended timing schema (*see* [Lim et al., 1995; Lim et al., 1998]). The approach also does not handle contexts.

Another technique of path search was proposed by Stappert et al. (*see* [Stappert et al., 2001]) where instead of extensive path search or implicit path enumeration by ILP, an approach based on acyclic directed graphs (DAGs) is described. The result is a fast way of computing the WCET using a well-known graph algorithm (Dijkstra). The worst-case run-time of their approach is better than that of ILP solving, whereas the precision of our approach is higher because of the ability to include long-distance constraints. Furthermore, our approach is now much more flexible w.r.t. using different context mappings. Also, the real-life analysis speed of our approach has turned out to be very good even for large problems.

Moreover, the work uses simulation to predict microarchitecture behaviour, which is not applicable to architectures like the ColdFire MCF 5307 whose timing behaviour depends very much on execution history. Using precise techniques, however, seems to be possible for their approach as well, since the analysis phases for microarchitecture behaviour prediction and for path analysis are decoupled just as in our approach.

Jan Gustafsson examines in [Gustafsson, 2000] how infeasible paths can be removed from the worst case execution time analysis. He uses Abstract Interpretation. The approach is very precise, he even traces loops, and the results seem to be combinable with our approach by automatically adding constraints about infeasible paths found by his analysis. However, the analysis is very complex and, therefore, quite slow for larger input programs, so it is not suited for our needs.

Chapter 11
Conclusion

This work described the successful generation and usage of control flow graphs that were especially designed to be suitable for real-time system analysis. It was shown in detail in Chapter 3 what requirements real-time systems have w.r.t. WCET analysis and what the consequent requirements are for the underlying control flow graph.

The extraction of control flow graphs with these special requirements can be done from binary executables without the help of any compiler generated additional meta-information about the structure of the program. The description of this extraction in this thesis is structured into two parts: the usage of decision trees for very convenient classification of single instructions, and the central control flow reconstruction algorithm. The first two sections of this chapter will summarise these two aspects.

Our novel approach to path analysis as part of our WCET framework also uses the generated control flow graphs. Chapters 7 and 8 describe this ILP-based path analysis. We presented how constraints can be generated for arbitrary static context mappings used for interprocedural analysis. The last section of this chapter will summarise that path analysis.

11.1 Decision Trees

In this work, a novel algorithm for decision tree generation from bit patterns was presented. The algorithm does not need any user-provided selection of bit fields, so no classification of opcodes and sub-opcodes is needed. All this error-prone work is done automatically now.

Our algorithm can handle specialised instructions (those that are subsumed by others) by default nodes. It is generic and can be applied to various specification formats.

By handling non-adjacent groups of bits in one step, the decision tree is kept more shallow than with opcode or single bit-oriented approaches, improving decoding speed.

We also mentioned that the decision trees together with their interpreting selection algorithm can be compiled by exec2crl into ANSI C in order to facilitate compilation for maximum speed of instruction classification.

By its degree of automatism, the algorithm makes porting to new architectures much easier and safer than doing it manually. We even succeeded in converting an architecture manual in PDF format into a specification skeleton automatically.

The implementation is very fast by using $O(1)$ machine word operations and has proven in practice to be integrable into existing frameworks.

We have stressed here that the safety properties of the algorithm make it suitable for safety-critical applications like real-time system analysis, which was the most important design goal for all algorithms throughout this thesis.

11.2 CFG Reconstruction

In this work, an algorithm for ICFG approximation from binary executables was presented. It provides real-time system analysers with a safe ICFG. The algorithm is designed for modern processors, and involves concepts like uncertainty in the very low-level reconstruction from streams of bytes, thereby making it possible to generate a conservative ICFG approximation with most uncertainties disambiguated.

The bottom-up approach of ICFG reconstruction makes fine-grained instruction classifications available to the core of the algorithm, resulting in safer and more precise ICFGs than those produced by top-down algorithms. It can cope with interlocked and overlapping routines and it skips data portions even if located inside routines.

Further, the algorithm can handle different instruction sets that may be switched dynamically in the code. The switches are automatically recognised.

We presented the idealised formal version of the bottom-up approach as well as our implementation of the algorithm, which follows a generic approach by using a module interface and showed that CFG edges can be disambiguated for the supported architectures.

11.3 Path Analysis

An extension to the established technique of implicit path enumeration using ILP for WCET prediction was presented in Chapter 8.

Our approach makes it possible to add a very fine-grained tuning mechanism for analysis precision and speed by allowing context mappings for interprocedural analyses that are parameterised for various aspects, e. g. maximal context length or the amount of loop unrolling.

The method of using contexts for distinguishing basic blocks by execution history was used already for microarchitecture behaviour prediction (value analysis, cache and pipeline analyses) as these use the PAG framework where the interprocedural methods are integrated. This thesis now makes sophisticated context mappings available to the urgently needed precise ILP-based path analysis.

We showed how well-known and very efficient methods of ILP-based path analysis can be extended to be interprocedural. The great problem of precise loop bounds was solved and shown to be optimally precise for all statically given context mappings.

The algorithms that are used for generating the ILP are very fast so that the path analysis is even one of the fastest parts of our WCET framework.

And finally, the ILP solving was shown to be feasible for ILPs generated from graphs with contexts as well.

Generally, this shows that our approach of splitting microarchitecture and path analyses is faster, more flexible than and still equally precise as combined analyses.

11.4 History & Development

All parts that are described in this work are widely used in many projects now. These include commercial ones by AbsInt Angewandte Informatik GmbH. It is also used for research at our work group at Universität des Saarlandes.

exec2crl has become *the* universal tool for all of our projects that rely on ICFGs that have to be extracted from binaries. These not only include our WCET tools but also ICFG visualisation tools and stack analyses. exec2crl was developed during the time of our research project TF14 (Transferbereich 14) in the years 1999 to 2001. Possible further extensions will be done by AbsInt.

pathan is used in our WCET framework for different architectures. Most notably, it is used in Coldfire and PowerPC WCET analysis tools developed in our research project DAEDALUS starting in 1999. Soon it will be used for an ARM WCET tool developed

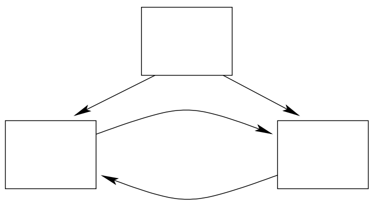

Figure 11.1: A simple irreducible loop. The problem is that it is impossible to identify a unique loop header due to two entry edges.

by AbsInt.

During my work at our work group's WCET framework, I also re-implemented the instruction cache analysis presented in [Ferdinand, 1997] for usage in that framework. The description of this implementation is beyond the scope of this work, since the major goal was to create a retargetable tool for industrial applications. For the sake of completeness, I want to report here that the reconstructed ICFGs are also very well suited for the cache analysis. Additional to a standalone tool, the cache analysis is now available as a library in order to also allow for a combined pipeline and cache analysis that can handle instruction and data cache accesses.

11.5 Outlook

11.5.1 Cycles

An interesting extension is the support for cycles that cannot be reduced to natural loops. The standard example is shown in Figure 11.1.

The technique presented here allows for these kind of cycles to be handled, i. e., constraints can be generated.

One open problem is finding and classifying arbitrary cycles. A possible technique would be to use algorithms for finding strongly connected components of the graphs with cycles and to try to reason about the structures found.

In this work arbitrary cycles did not play an important role, because they are rare in practice and due to their diversity, user interaction is likely to be required to handle all cases. Irreducible cycles can currently be handled easily by user defined constraints provided by the framework, so for these rare cases, there was no need to implement automatic handling.

One example occurred in a piece of library code of a commercial real-time operating system. As expected, it was easy to handle this special case by user defined constraints.

11.5.2 CFG Reconstruction

A constant propagation to refine the approximated initial ICFG could be thought of the future. Because exec2crl already has very good recognition ratios, it is currently not needed. Other architectures, especially those with guarded code, possibly make this extension necessary.

Nevertheless, we expect our algorithms to work for other architectures very well, too. E. g. examination of guarded code of the Philips Trimedia processor revealed that the guard is a trivial 'true' for relevant parts of the ICFG.

11.5.3 Architectures

In the future, our framework will support more architectures. Currently, the WCET framework is being extended to the ARM processor. A decoder module is already built into exec2crland is currently tested.

Other architectures will certainly follow for research or due to commercial needs.

Appendix A
Experiments in Tables and Figures

A.1 Path Analysis

For several test programs, this section lists analysis times and results of the path analysis. Different context mappings were used for each test program.

The crucial point about interprocedural path analysis are loop bound constraints. Therefore, selected test programs show how pathan generates them. In the scope of this work, it is infeasible to print large graphs of commercially sided applications. Therefore, some selected programs show the principles.

All call graphs shown in this section are loop-converted, i. e., the loop is represented by an own routine. Further recall that the $\mathsf{CG}^{\star}$ with $\mathsf{CallString}(0)$ is isomorphic to the CG of a program.

A.1.1 One Loop, One Invocation

```
routine a
    while ... do – loop 1
        ...
```

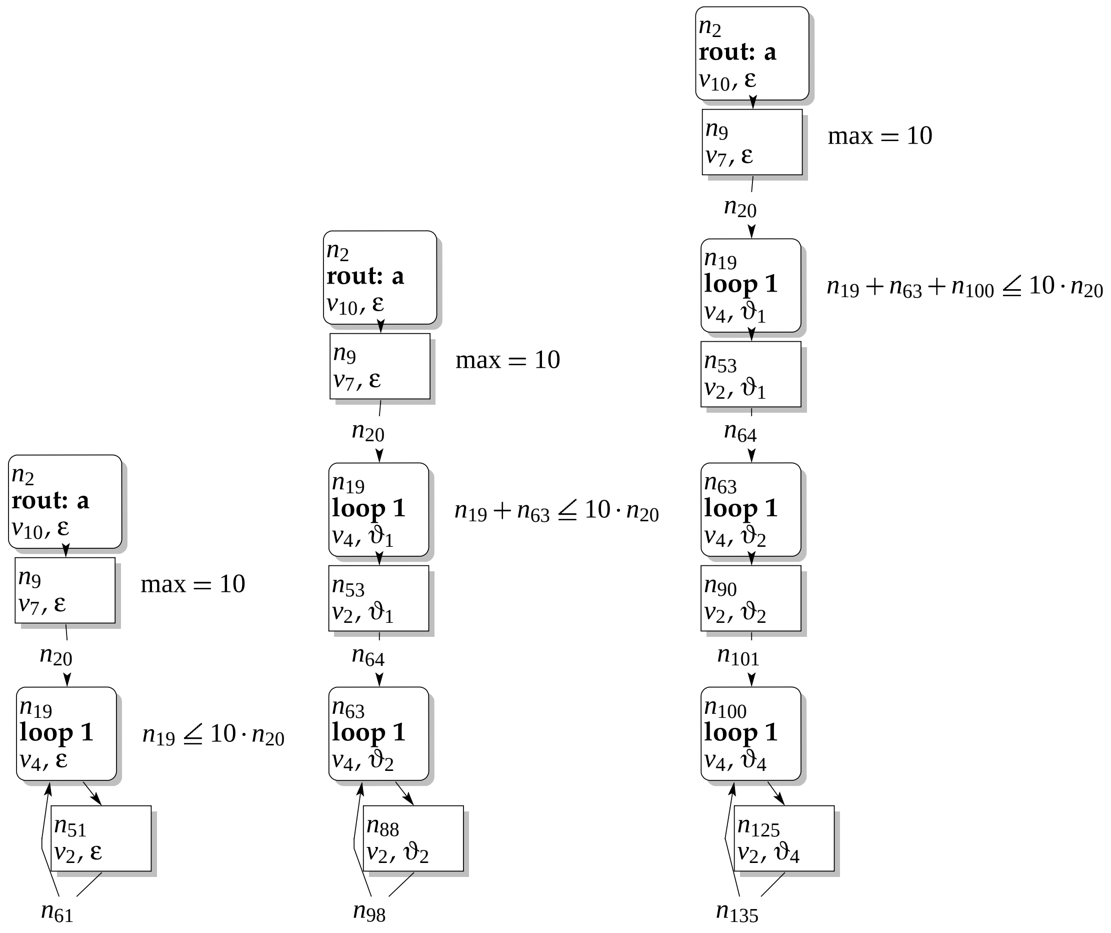

Figure A.1: CG*. Left: CallString(0), Middle: CallString(1), Right: CallString(2)

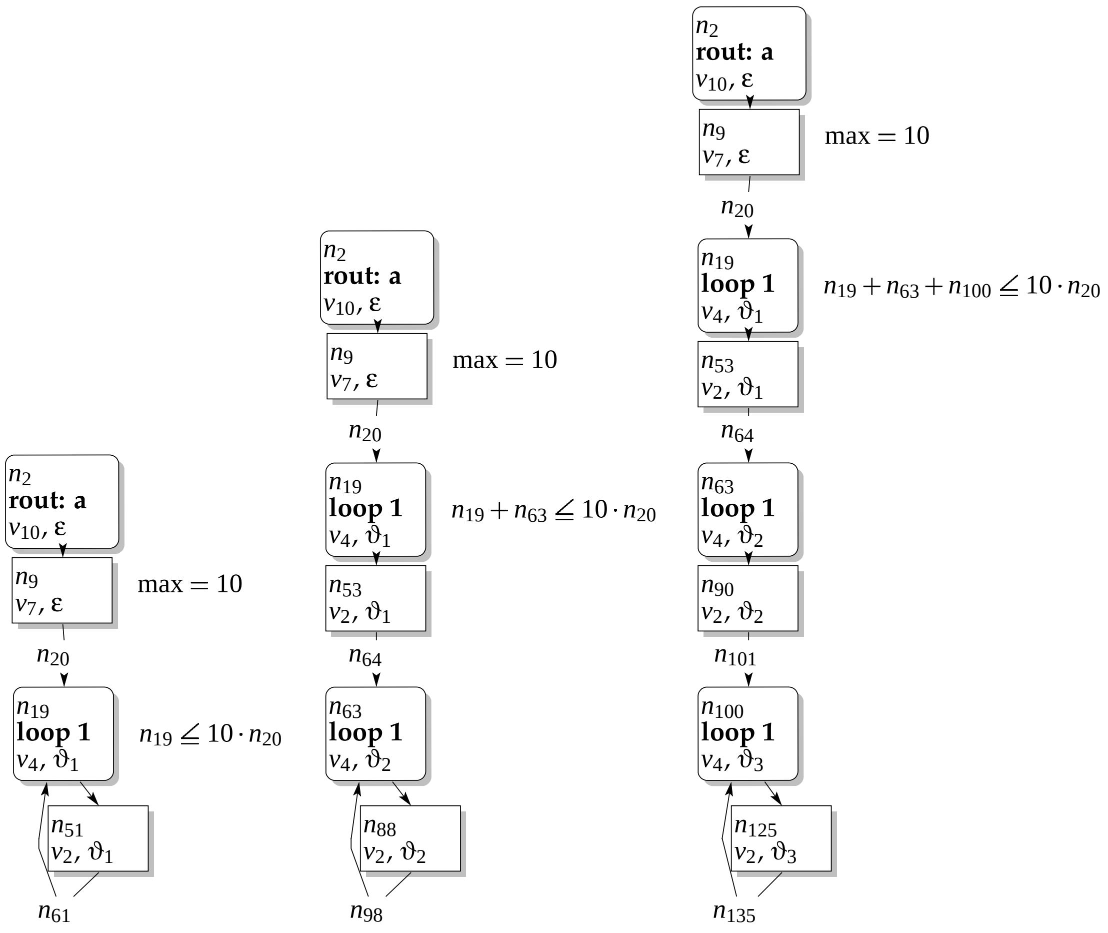

Figure A.2: $\mathsf{CG}^\star$. Left: $\mathsf{VIVU}(1,\infty)$, Middle: $\mathsf{VIVU}(1,\infty)$, Right: $\mathsf{VIVU}(3,\infty)$

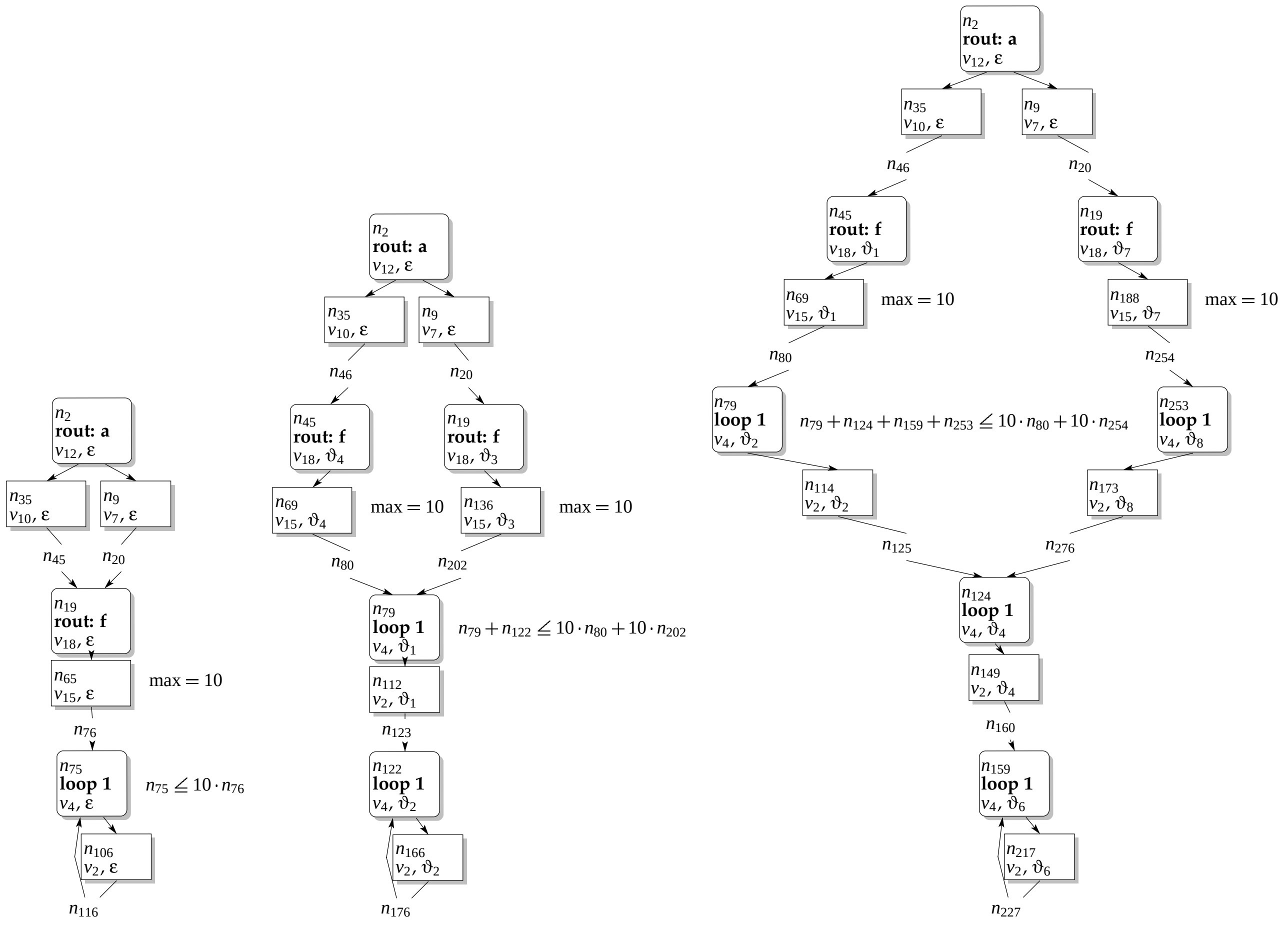
n_2 rout: a v_{12}, ε
n_{35} v_{10}, ε
n_9 v_7, ε
n_{45}
n_{20}
n_{19} rout: f v_{18}, ε
n_{65} v_{15}, ε
max = 10
n_{76}
n_{75} loop 1 v_4, ε
$n_{75} \leqq 10 \cdot n_{76}$
n_{106} v_2, ε
n_{116}
n_2 rout: a v_{12}, ε
n_{35} v_{10}, ε
n_9 v_7, ε
n_{46}
n_{20}
n_{45} rout: f v_{18}, ϑ_4
n_{19} rout: f v_{18}, ϑ_3
n_{69} v_{15}, ϑ_4
max = 10
n_{136} v_{15}, ϑ_3
max = 10
n_{80}
n_{202}
n_{79} loop 1 v_4, ϑ_1
$n_{79} + n_{122} \leqq 10 \cdot n_{80} + 10 \cdot n_{202}$
n_{112} v_2, ϑ_1
n_{123}
n_{122} loop 1 v_4, ϑ_2
n_{166} v_2, ϑ_2
n_{176}
n_2 rout: a v_{12}, ε
n_{35} v_{10}, ε
n_9 v_7, ε
n_{46}
n_{20}
n_{45} rout: f v_{18}, ϑ_1
n_{19} rout: f v_{18}, ϑ_7
n_{69} v_{15}, ϑ_1
max = 10
n_{188} v_{15}, ϑ_7
max = 10
n_{80}
n_{254}
n_{79} loop 1 v_4, ϑ_2
$n_{79} + n_{124} + n_{159} + n_{253} \leqq 10 \cdot n_{80} + 10 \cdot n_{254}$
n_{253} loop 1 v_4, ϑ_8
n_{114} v_2, ϑ_2
n_{173} v_2, ϑ_8
n_{125}
n_{276}
n_{124} loop 1 v_4, ϑ_4
n_{149} v_2, ϑ_4
n_{160}
n_{159} loop 1 v_4, ϑ_6
n_{217} v_2, ϑ_6
n_{227}

Figure A.3: CG*. Left: CallString(0), Middle: CallString(1), Right: CallString(2)

A.1.2 One Loop, Two Invocations

```
routine a
    f()
    f()

routine f
    while … do – loop 1
        …
```

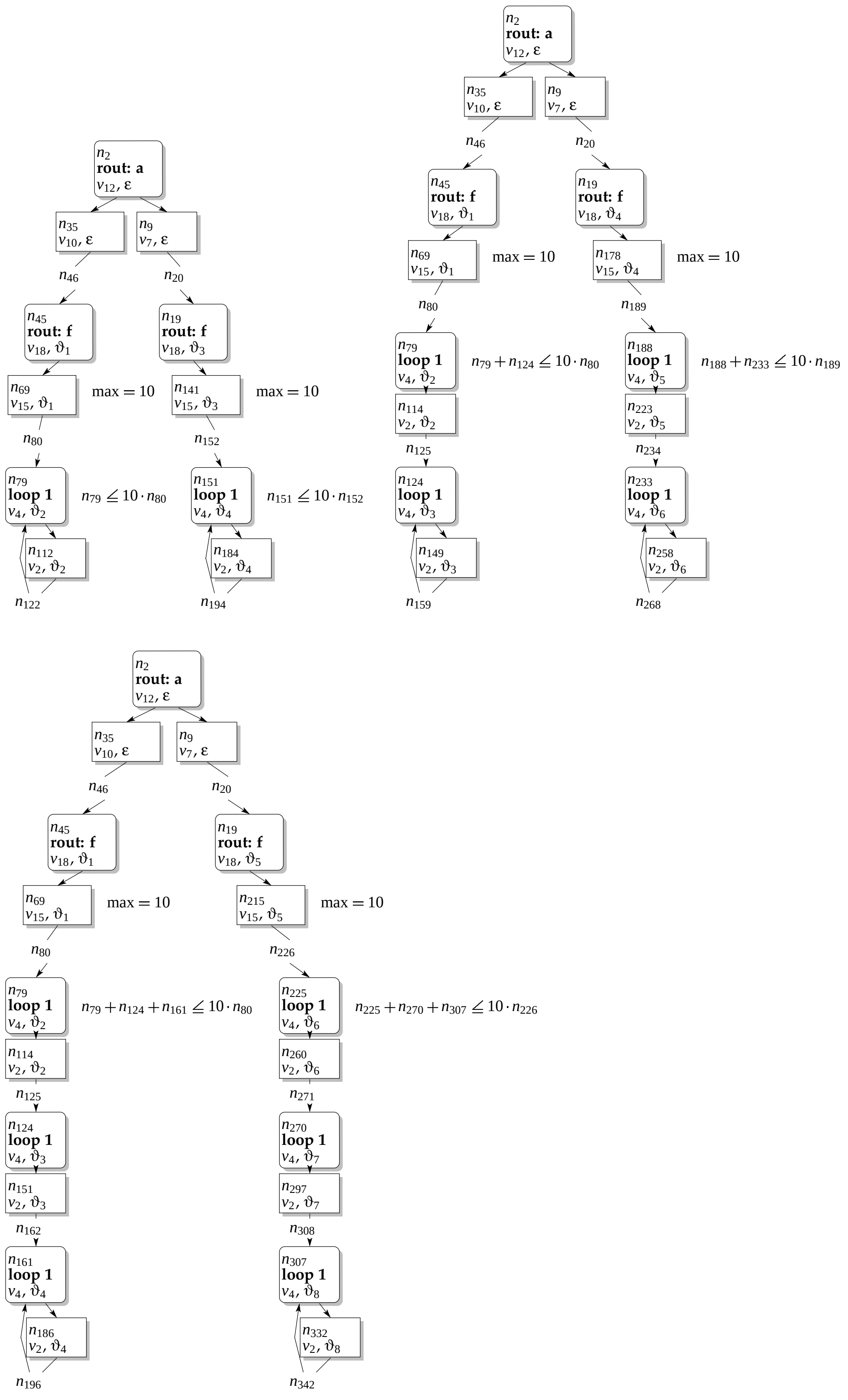
n_2 **rout: a** v_{12}, ε
n_{35} v_{10}, ε
n_9 v_7, ε
n_{46}
n_{20}
n_{45} **rout: f** v_{18}, ϑ_1
n_{19} **rout: f** v_{18}, ϑ_3
n_{69} v_{15}, ϑ_1
max = 10
n_{141} v_{15}, ϑ_3
max = 10
n_{80}
n_{152}
n_{79} **loop 1** v_4, ϑ_2
$n_{79} \leqq 10 \cdot n_{80}$
n_{151} **loop 1** v_4, ϑ_4
$n_{151} \leqq 10 \cdot n_{152}$
n_{112} v_2, ϑ_2
n_{122}
n_{184} v_2, ϑ_4
n_{194}
n_2 **rout: a** v_{12}, ε
n_{35} v_{10}, ε
n_9 v_7, ε
n_{46}
n_{20}
n_{45} **rout: f** v_{18}, ϑ_1
n_{19} **rout: f** v_{18}, ϑ_4
n_{69} v_{15}, ϑ_1
max = 10
n_{178} v_{15}, ϑ_4
max = 10
n_{80}
n_{189}
n_{79} **loop 1** v_4, ϑ_2
$n_{79} + n_{124} \leqq 10 \cdot n_{80}$
n_{188} **loop 1** v_4, ϑ_5
$n_{188} + n_{233} \leqq 10 \cdot n_{189}$
n_{114} v_2, ϑ_2
n_{223} v_2, ϑ_5
n_{125}
n_{234}
n_{124} **loop 1** v_4, ϑ_3
n_{233} **loop 1** v_4, ϑ_6
n_{149} v_2, ϑ_3
n_{258} v_2, ϑ_6
n_{159}
n_{268}
n_2 **rout: a** v_{12}, ε
n_{35} v_{10}, ε
n_9 v_7, ε
n_{46}
n_{20}
n_{45} **rout: f** v_{18}, ϑ_1
n_{19} **rout: f** v_{18}, ϑ_5
n_{69} v_{15}, ϑ_1
max = 10
n_{215} v_{15}, ϑ_5
max = 10
n_{80}
n_{226}
n_{79} **loop 1** v_4, ϑ_2
$n_{79} + n_{124} + n_{161} \leqq 10 \cdot n_{80}$
n_{225} **loop 1** v_4, ϑ_6
$n_{225} + n_{270} + n_{307} \leqq 10 \cdot n_{226}$
n_{114} v_2, ϑ_2
n_{260} v_2, ϑ_6
n_{125}
n_{271}
n_{124} **loop 1** v_4, ϑ_3
n_{270} **loop 1** v_4, ϑ_7
n_{151} v_2, ϑ_3
n_{297} v_2, ϑ_7
n_{162}
n_{308}
n_{161} **loop 1** v_4, ϑ_4
n_{307} **loop 1** v_4, ϑ_8
n_{186} v_2, ϑ_4
n_{196}
n_{332} v_2, ϑ_8
n_{342}

Figure A.4: CG*. Top Left: VIVU$(1, \infty)$, Top Right: VIVU$(2, \infty)$, Bottom: VIVU$(3, \infty)$

A.1.3 Two Loops

```
routine a
    f()
    g()

routine f
    while ... do – loop 2
        ...

routine g
    while ... do – loop 1
        ...
```

The purpose of this test program is to make explicit the split of a loop into two contexts by simply programming the loop twice. Many of the mappings will, therefore, lead to the same CG* as for the previous program.

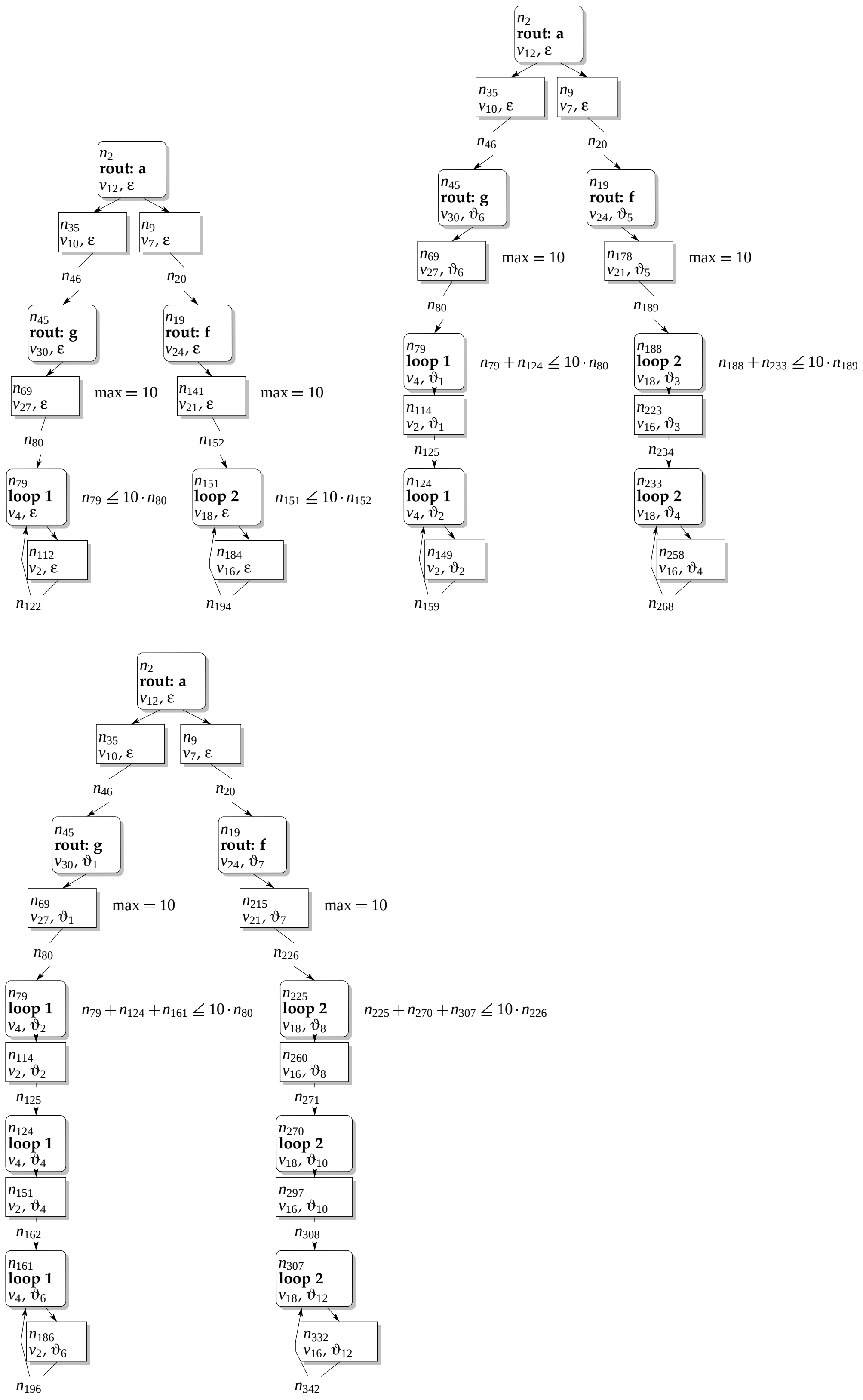

Figure A.5: CG*. Top Left: CallString(0), Top Right: CallString(1), Bottom: CallString(2)

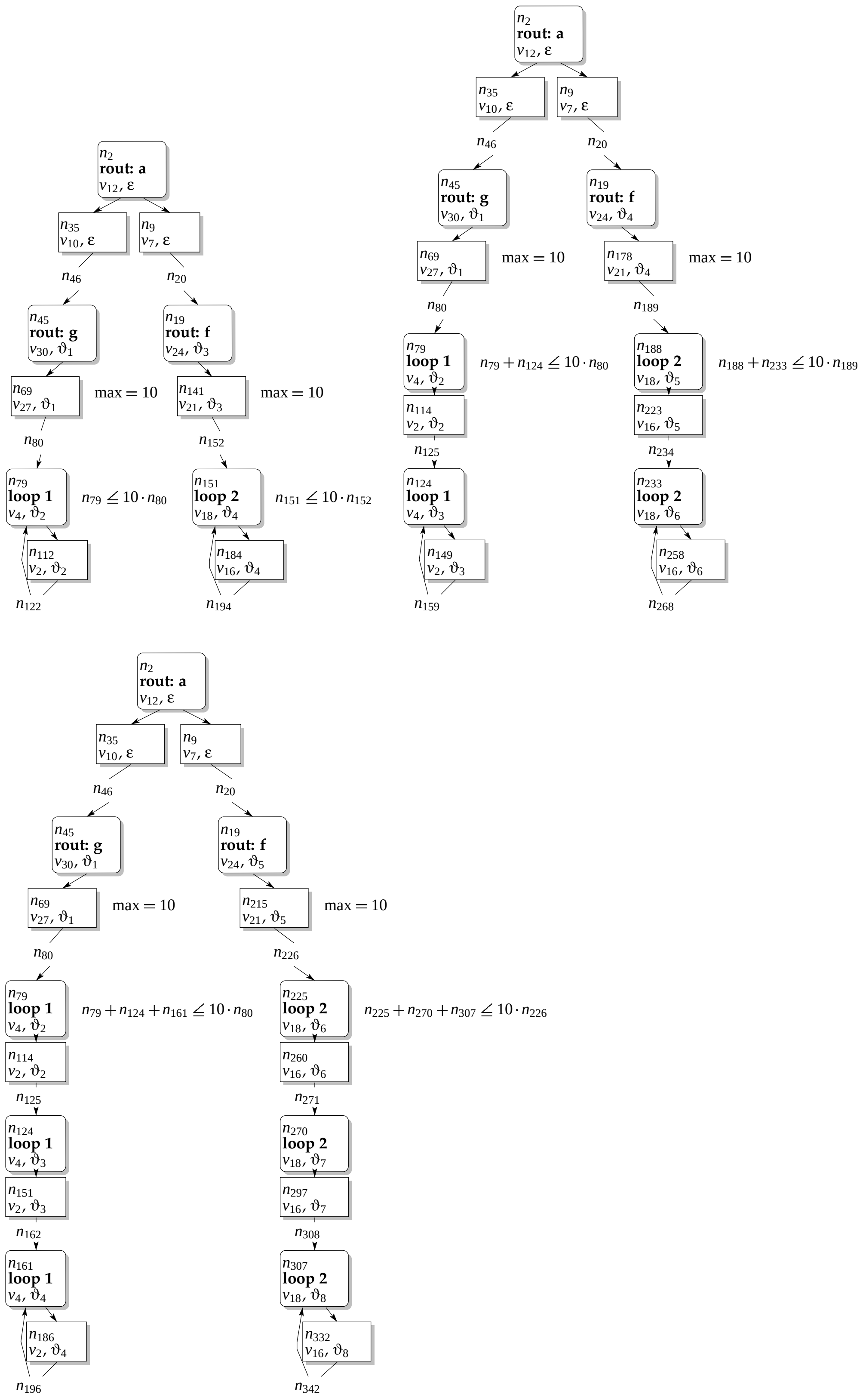

n_2 rout: a v_{12}, ε
n_{35} v_{10}, ε
n_9 v_7, ε
n_{46}
n_{20}
n_{45} rout: g v_{30}, ϑ_1
n_{19} rout: f v_{24}, ϑ_3
n_{69} v_{27}, ϑ_1
max = 10
n_{141} v_{21}, ϑ_3
max = 10
n_{80}
n_{152}
n_{79} loop 1 v_4, ϑ_2
$n_{79} \leq 10 \cdot n_{80}$
n_{151} loop 2 v_{18}, ϑ_4
$n_{151} \leq 10 \cdot n_{152}$
n_{112} v_2, ϑ_2
n_{184} v_{16}, ϑ_4
n_{122}
n_{194}
n_2 rout: a v_{12}, ε
n_{35} v_{10}, ε
n_9 v_7, ε
n_{46}
n_{20}
n_{45} rout: g v_{30}, ϑ_1
n_{19} rout: f v_{24}, ϑ_4
n_{69} v_{27}, ϑ_1
max = 10
n_{178} v_{21}, ϑ_4
max = 10
n_{80}
n_{189}
n_{79} loop 1 v_4, ϑ_2
$n_{79} + n_{124} \leq 10 \cdot n_{80}$
n_{188} loop 2 v_{18}, ϑ_5
$n_{188} + n_{233} \leq 10 \cdot n_{189}$
n_{114} v_2, ϑ_2
n_{223} v_{16}, ϑ_5
n_{125}
n_{234}
n_{124} loop 1 v_4, ϑ_3
n_{233} loop 2 v_{18}, ϑ_6
n_{149} v_2, ϑ_3
n_{258} v_{16}, ϑ_6
n_{159}
n_{268}
n_2 rout: a v_{12}, ε
n_{35} v_{10}, ε
n_9 v_7, ε
n_{46}
n_{20}
n_{45} rout: g v_{30}, ϑ_1
n_{19} rout: f v_{24}, ϑ_5
n_{69} v_{27}, ϑ_1
max = 10
n_{215} v_{21}, ϑ_5
max = 10
n_{80}
n_{226}
n_{79} loop 1 v_4, ϑ_2
$n_{79} + n_{124} + n_{161} \leq 10 \cdot n_{80}$
n_{225} loop 2 v_{18}, ϑ_6
$n_{225} + n_{270} + n_{307} \leq 10 \cdot n_{226}$
n_{114} v_2, ϑ_2
n_{260} v_{16}, ϑ_6
n_{125}
n_{271}
n_{124} loop 1 v_4, ϑ_3
n_{270} loop 2 v_{18}, ϑ_7
n_{151} v_2, ϑ_3
n_{297} v_{16}, ϑ_7
n_{162}
n_{308}
n_{161} loop 1 v_4, ϑ_4
n_{307} loop 2 v_{18}, ϑ_8
n_{186} v_2, ϑ_4
n_{332} v_{16}, ϑ_8
n_{196}
n_{342}

Figure A.6: CG*. Top Left: VIVU$(1,\infty)$, Top Right: VIVU$(2,\infty)$, Bottom: VIVU$(3,\infty)$

A.1.4 Recursion with Two Loop Entries

```
routine a
    x = if ... then b else c
    x() – computed call

routine b
    b()

routine c
    b()
```

Additionally, this example show how the framework handles general user loop bounds and special loop bounds for a given edge.

The user specified that the default maximum for the recursion is 5 iterations and that the invocation from routine a iterates maximally 6 times and from c maximally 10 times. With this input, the framework automatically uses the maximum found for each entry edge.

The graphs shows the two given maximums at the entry call node.

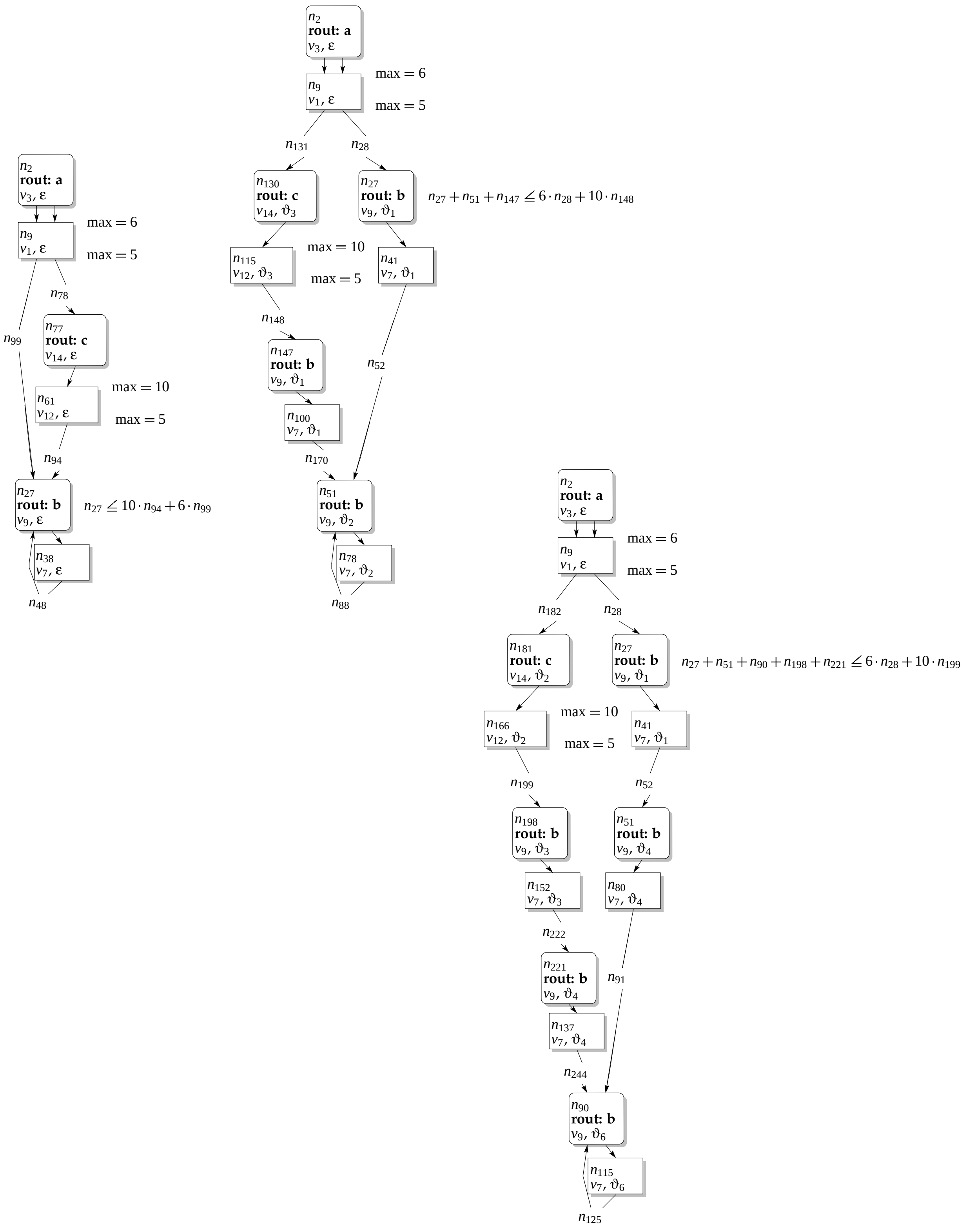

Figure A.7: CG*. Top Left: CallString(0), Top Right: CallString(1), Bottom: CallString(2)

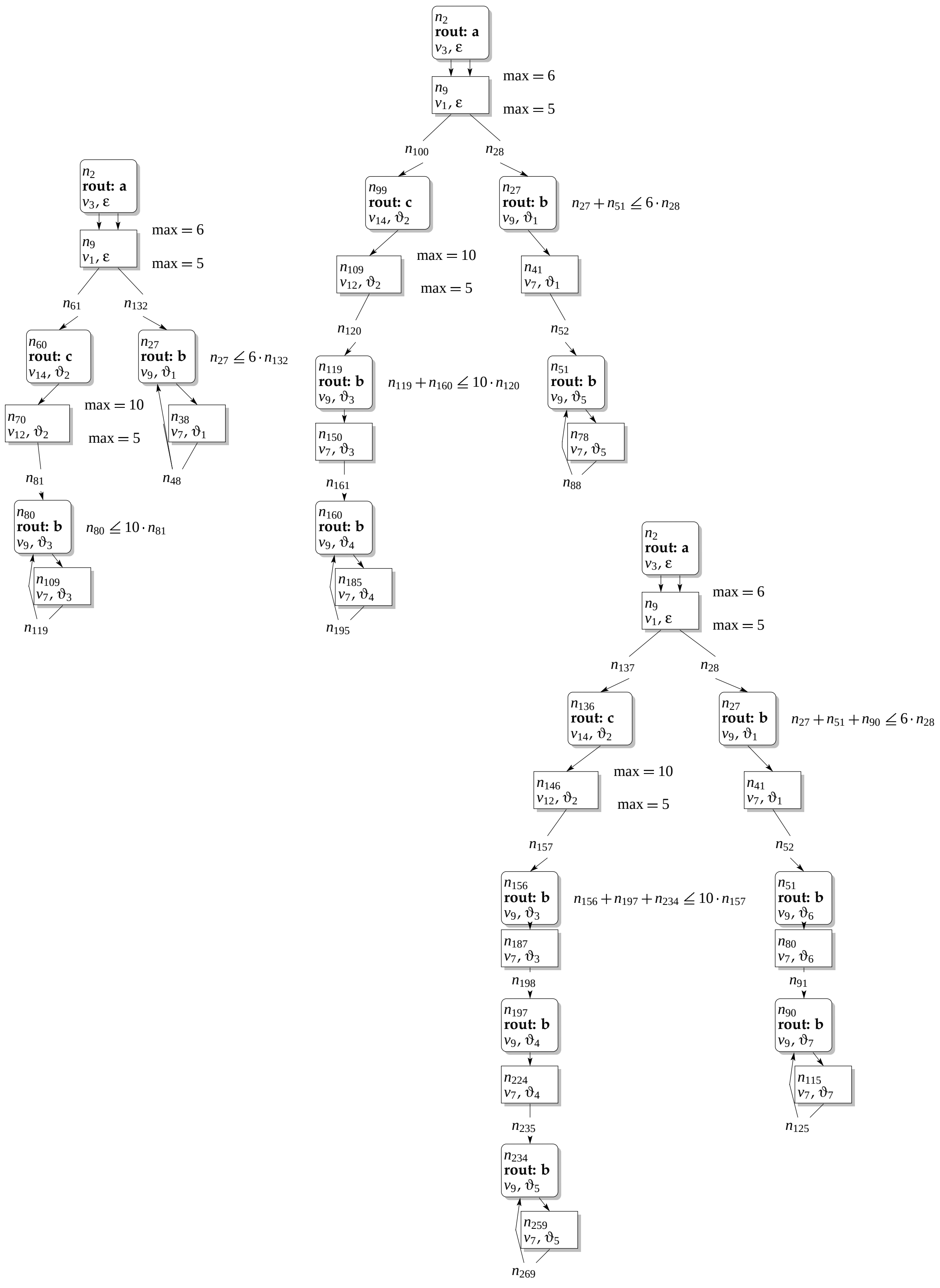

n_2 **rout: a** v_3, ε
n_9 v_1, ε
max = 6
max = 5
n_{61}
n_{132}
n_{60} **rout: c** v_{14}, ϑ_2
n_{27} **rout: b** v_9, ϑ_1
$n_{27} \leqq 6 \cdot n_{132}$
n_{70} v_{12}, ϑ_2
max = 10
max = 5
n_{38} v_7, ϑ_1
n_{81}
n_{48}
n_{80} **rout: b** v_9, ϑ_3
$n_{80} \leqq 10 \cdot n_{81}$
n_{109} v_7, ϑ_3
n_{119}
n_2 **rout: a** v_3, ε
n_9 v_1, ε
max = 6
max = 5
n_{100}
n_{28}
n_{99} **rout: c** v_{14}, ϑ_2
n_{27} **rout: b** v_9, ϑ_1
$n_{27} + n_{51} \leqq 6 \cdot n_{28}$
n_{109} v_{12}, ϑ_2
max = 10
max = 5
n_{41} v_7, ϑ_1
n_{120}
n_{52}
n_{119} **rout: b** v_9, ϑ_3
$n_{119} + n_{160} \leqq 10 \cdot n_{120}$
n_{51} **rout: b** v_9, ϑ_5
n_{150} v_7, ϑ_3
n_{78} v_7, ϑ_5
n_{161}
n_{88}
n_{160} **rout: b** v_9, ϑ_4
n_{185} v_7, ϑ_4
n_{195}
n_2 **rout: a** v_3, ε
n_9 v_1, ε
max = 6
max = 5
n_{137}
n_{28}
n_{136} **rout: c** v_{14}, ϑ_2
n_{27} **rout: b** v_9, ϑ_1
$n_{27} + n_{51} + n_{90} \leqq 6 \cdot n_{28}$
n_{146} v_{12}, ϑ_2
max = 10
max = 5
n_{41} v_7, ϑ_1
n_{157}
n_{52}
n_{156} **rout: b** v_9, ϑ_3
$n_{156} + n_{197} + n_{234} \leqq 10 \cdot n_{157}$
n_{51} **rout: b** v_9, ϑ_6
n_{187} v_7, ϑ_3
n_{80} v_7, ϑ_6
n_{198}
n_{91}
n_{197} **rout: b** v_9, ϑ_4
n_{90} **rout: b** v_9, ϑ_7
n_{224} v_7, ϑ_4
n_{115} v_7, ϑ_7
n_{235}
n_{125}
n_{234} **rout: b** v_9, ϑ_5
n_{259} v_7, ϑ_5
n_{269}

Figure A.8: CG*. Top Left: VIVU$(1,\infty)$, Top Right: VIVU$(2,\infty)$, Bottom: VIVU$(3,\infty)$

Bibliography

Ali-Reza Adl-Tabatabai and Thomas Gross (1996). Source-Level Debugging of Scalar Optimized Code. In *Proceedings of the ACM SIGPLAN '96 Conference on Programming Language Design and Implementation (PLDI)*, May 1996, Philadephia, Pennsylvania, USA, *SIGPLAN Notices*, 31(5):33–43. ACM.

Alfred V. Aho, Ravi Sethi, and Jeffrey D. Ullman (1986). *Compilers: Principles, Techniques, and Tools*. Addison Wesley.

Götz Alefeld and Jürgen Herzberger (1983). *Introduction to Interval Computations*. Academic Press, New York City, New York, USA.

ARM (2001). *ARM Architecture Reference Manual*.

Swagato Basumallick and Kelvin Nilsen (1994). Cache Issues in Real-Time Systems. In *Proceedings of the ACM SIGPLAN 1994 Workshop on Languages, Compilers, & Tool Support for Real-Time Systems (LCT-RTS)*, June 1994, Orlando, Florida, USA.

Iain Bate, Guillem Bernat, Greg Murphy, and Peter Puschner (2000). Low-Level Analysis of a Portable Java Byte Code WCET Analysis Framework. In *Proceedings of the 7th International Conference on Real-Time Computing Systems and Applications (RTCSA)*, December 2000, Cheju Island, South Korea.

Guillem Bernat, Alan Burns, and Andy J. Wellings (2000). Portable Worst-Case Execution Time Analysis Using Java Byte Code. In *Proceedings of the 12th Euromicro Workshop on Real-Time Systems*, June 2000, Stockholm, Sweden.

Binutils. *GNU Binutils*. http://www.gnu.org.

Johann Blieberger, Thomas Fahringer, and Bernhard Scholz (2000). Symbolic Cache Analysis for Real-Time Systems. *Real-Time Systems*, 18(2/3):181–215.

Gary Brooks, Gilbert J. Hansen, and Steve Simmons (1992). A New Approach to Debugging Optimized Code. In *Proceedings of the ACM SIGPLAN '92 Conference on Programming Language Design and Implementation (PLDI)*, June 1992, San Francisco, California, USA, *SIGPLAN Notices*, 27(7):1–11. ACM.

Vašek Chvátal (1983). *Linear Programming*. W. H. Freeman and Company.

Christina Cifuentes and K. John Gough (1995). Decompilation of Binary Programs. *Software – Practice and Experience*, 25(7):811–829.

Cinderella. *Cinderella 3.0 Home Page*. http://www.ee.princeton.edu/˜yauli/cinderella-3.0/.

ColdFire (1997). *ColdFire Microprocessor Family Programmer's Reference Manual*. Motorola.

Antoine Colin and Isabelle Puaut (2001). Worst-Case Execution Time Analysis of the RTEMS Real-Time Operating System. In *Proceedings of the 13th Euromicro Workshop on Real-Time Systems*, June 2001, Delft, The Netherlands.

Patrick Cousot and Radhia Cousot (1976). Static Determination of Dynamic Properties of Programs. In *Proceedings of the Second International Symposium on Programming*, Dunod, Paris, France.

Patrick Cousot and Radhia Cousot (1977a). Abstract Interpretation: A Unified Lattice Model for Static Analysis of Programs by Construction or Approximation of Fixpoints. In *Proceedings of the 4th ACM Symposium on Principles of Programming Languages*, Los Angeles, California, USA.

Patrick Cousot and Radhia Cousot (1977b). Static Determination of Dynamic Properties of Generalized Type Unions. In *Proceedings of an ACM Conference on Language Design for Reliable Software*, Raleigh, North Carolina, USA, *SIGPLAN Notices*, 12(3). ACM.

Patrick Cousot and Radhia Cousot (1978). Static Determination of Dynamic Properties of Recursive Procedures. *Formal Description of Programming Concepts*.

Patrick Cousot and Radhia Cousot (1979). Systematic Design of Program Analysis Frameworks. In *Proceedings of the 6th ACM Symposium on Principles of Programming Languages*, San Antonio, Texas, USA.

Patrick Cousot and Radhia Cousot (1992). Abstract Interpretation and Application to Logic Programs. *Journal of Logic Programming*, 13(2).

Bjorn De Sutter, Bruno De Bus, Koenraad De Bosschere, Peter Keyngnaert, and Bart Demoen (2000). On the Static Analysis of Indirect Control Transfers in Binaries. In *Proceedings of the International Conference on Parallel and Distributed Processing Techniques and Applications (PDPTA)*, June 2000, Las Vegas, Nevada, USA.

ELF. *Executable and Linking Format (ELF).*

Jakob Engblom (2002). Processor Pipelines and Static Worst-Case Execution Time Analysis. Ph. D. Thesis, Acta Universitatis Upsaliensis.

Jakob Engblom and Andreas Ermedahl (1999). Pipeline Timing Analysis Using a Trace-Driven Simulator. In *Proceedings of the 6th International Conference on Real-Time Computing Systems and Applications (RTCSA)*, December 1999.

Christian Ferdinand (1997). Cache Behavior Prediction for Real-Time Systems. Ph. D. Thesis, Universität des Saarlandes.

Christian Ferdinand, Reinhold Heckmann, Marc Langenbach, Florian Martin, Michael Schmidt, Henrik Theiling, Stephan Thesing, and Reinhard Wilhelm (2001). Reliable and Precise WCET Determination for a Real-Life Processor. In *Proceedings of EMSOFT 2001, First Workshop on Embedded Software, Lecture Notes in Computer Science*, 2211.

Christian Ferdinand, Daniel Kästner, Marc Langenbach, Florian Martin, Michael Schmidt, Jörn Schneider, Henrik Theiling, Stephan Thesing, and Reinhard Wilhelm (1999a). Run-Time Guarantees for Real-Time Systems – The USES Approach. In *Proceedings of Informatik '99 – Arbeitstagung Programmiersprachen*, Paderborn, Germany.

Christian Ferdinand, Florian Martin, and Reinhard Wilhelm (1997). Applying Compiler Techniques to Cache Behavior Prediction. In *Proceedings of the ACM SIGPLAN Workshop on Language, Compiler & Tool Support for Real-Time Systems (LCT-RTS).*

Christian Ferdinand, Florian Martin, and Reinhard Wilhelm (1999b). Cache Behavior Prediction by Abstract Interpretation. *Science of Computer Programming*, 35(2–3):163–189. Selected for special issue SAS'96.

Christian Ferdinand and Reinhard Wilhelm (1999). Efficient and precise cache behavior prediction for real-time systems. *Real-Time Systems*, 17(2–3):131–181.

Mary Fernández and Norman Ramsey (1997). Automatic Checking of Instruction Specifications. In *Proceedings of the 19th International Conference on Software Engineering*. ACM Press.

David Grove and Craig Chambers (2001). A Framework for Call Graph Construction Algorithms. *ACM Transactions on Programming Languages and Systems (TOPLAS)*, 23(6):685–746.

Jan Gustafsson (2000). Analyzing Execution-Time of Object-Oriented Programs Using Abstract Interpretation. Ph. D. Thesis, Uppsala University, Mälardalens Högskola.

George Hadjiyiannis, Pietro Russo, and Srinivas Devadas (1999). A Methodology for Accurate Performance Evaluation in Architecture Exploration. In *Proceedings of the 36th Design Automation Conference (DAC'99)*, pages 927–932.

John L. Hennessy and David A. Patterson (1990). *Computer Architecture: A Quantitative Approach*. Morgan Kaufmann.

Tai-Yi Huang (1997). Worst-Case Timing Analysis of Concurrently Executing DMA I/O and Programs. Ph. D. Thesis, University of Illinois.

Yerang Hur, Young Hyun Bae, Sung-Soo Lim, Byung-Do Rhee, Sang Lyul Min, Chang Yun Park, Minsuk Lee, Heonshik Shin, and Chong Sang Kim (1995). Worst Case Timing Analysis of RISC Processors: R3000/R3010 Case Study. In *Proceedings of the 16th IEEE Real-Time Systems Symposium (RTSS)*.

Infineon (1997). *Instruction Set Manual for the C16x Family of Siemens 16-Bit CMOS Single-Chip Microcontrollers*. Infineon.

Neil D. Jones and Flemming Nielson (1995). Abstract Interpretation: a Semantics-Based Tool for Program Analysis. In *Handbook of Logic in Computer Science*. Oxford University Press.

Daniel Kästner and Stephan Wilhelm (2002). Generic Control Flow Reconstruction from Assembly Code. In *Proceedings of the ACM SIGPLAN 2002 Joined Conference on Languages, Compilers, and Tools for Embedded Systems (LCTES) and Software and Compilers for Embedded Systems (SCOPES)*, June 2002, Berlin, Germany.

Sung-Kwam Kim, Sang Lyul Min, and Rhan Ha (1996). Efficient Worst Case Timing Analysis of Data Caching. In *Proceedings of the 1996 IEEE Real-Time Technology and Applications Symposium*.

Raimund Kirner and Peter Puschner (2000). Supporting Control-Flow Dependent Execution Times on WCET Calculation. In *Proceedings of WCET-Tagung at C-Lab*, October 2000, Paderborn, Germany.

Marc Langenbach (1998). CRL – A Uniform Representation for Control Flow. Technical report, Universität des Saarlandes.

Marc Langenbach, Stephan Thesing, and Reinhold Heckmann (2002). Pipeline Modeling for Timing Analysis. In *Proceedings of the 9th International Static Analysis Symposium (SAS)*, September 2002, Madrid, Spain, *Lecture Notes in Computer Science*. Springer. To appear.

James Larus (1996). *EEL Guts: Using the EEL Executable Editing Library*. Computer Science Department, University of Wisconsin-Madison.

James R. Larus and Eric Schnarr (1995). EEL: Machine-Independent Executable Editing. In *Proceedings of the ACM SIGPLAN '95 Conference on Programming Language Design and Implementation (PLDI)*, June 1995, La Jolla, California, USA, *SIGPLAN Notices*, 30(5):291–300. ACM.

A. Laville (1991). Comparison of Priority Rules in Pattern Matching and Term Rewriting. *Journal of Symbolic Computations*, 11(4):321–348.

Thomas Lengauer and Robert Endre Tarjan (1979). A Fast Algorithm for Finding Dominators in Flowgraphs. *ACM Transactions on Programming Languages and Systems (TOPLAS)*, 1(1):121–141.

Yau-Tsun Steven Li and Sharad Malik (1995a). Performance Analysis of Embedded Software Using Implicit Path Enumeration. In *Proceedings of the 32nd ACM/IEEE Design Automation Conference*.

Yau-Tsun Steven Li and Sharad Malik (1995b). Performance Analysis of Embedded Software Using Implicit Path Enumeration. In *Proceedings of the ACM SIGPLAN 1995 Workshop on Languages, Compilers, & Tools for Real-Time Systems (LCT-RTS)*, June 1995, La Jolla, California, USA, *SIGPLAN Notices*, 30(11):88–98. ACM.

Yau-Tsun Steven Li, Sharad Malik, and Andrew Wolfe (1995a). Efficient Microarchitecture Modeling and Path Analysis for Real-Time Software. In *Proceedings of the 16th IEEE Real-Time Systems Symposium (RTSS)*, December 1995, Pisa, Italy, pages 298–307. IEEE Computer Society Press.

Yau-Tsun Steven Li, Sharad Malik, and Andrew Wolfe (1995b). Performance Estimation of Embedded Software with Instruction Cache Modeling. In *Proceedings of the IEEE/ACM International Conference on Computer-Aided Design*.

Yau-Tsun Steven Li, Sharad Malik, and Andrew Wolfe (1996). Cache Modeling for Real-Time Software: Beyond Direct Mapped Instruction Caches. In *Proceedings of the 17th IEEE Real-Time Systems Symposium (RTSS)*, December 1996, Washington, District of Columbia, USA. IEEE Computer Society Press.

Sung-Soo Lim, Young Hyun Bae, Gye Tae Jang, Byung-Do Rhee, Sang Lyul Min, Chang Yun Park, Heonshik Shin, Kunsoo Park, Soo-Mook Moon, and Chong Sang Kim (1995). An Accurate Worst Case Timing Analysis for RISC Processors. *IEEE Transactions on Software Engineering*, 21(7).

Sung-Soo Lim, Jung Hee Han, Jihong Kim, and Sang Lyul Min (1998). A Worst Case Timing Analysis Technique for Multiple Issue Machines. In *Proceedings of the 19th IEEE Real-Time Systems Symposium (RTSS)*, December 1998, Madrid, Spain, pages 334–345. IEEE Computer Society Press.

Markus Lindgren, Hans Hansson, and Henrik Thane (2000). Using Measurements to Derive the Worst-Case Execution Time. In *Proceedings of the 7th International Conference on Real-Time Computing Systems and Applications (RTCSA)*, December 2000, Cheju Island, South Korea.

C. L. Liu and James W. Layland. (1973). Scheduling algorithms for multiprogramming in a hard-real-time environment. *Journal of the ACM*, 20(1):46–61.

Jyh-Charn Liu and Hung-Ju Lee (1994). Deterministic Upperbounds of the Worst-Case Execution Time of Cached Programs. In *Proceedings of the 15th IEEE Real-Time Systems Symposium (RTSS)*.

Florian Martin (1995a). Die Generierung von Datenflußanalysatoren. Diploma Thesis, Universität des Saarlandes.

Florian Martin (1995b). *PAG Reference Manual*. Universität des Saarlandes.

Florian Martin (1998). PAG – an efficient program analyzer generator. *International Journal on Software Tools for Technology Transfer*, 2(1).

Florian Martin (1999a). Experimental Comparison of *call string* and *functional* Approaches to Interprocedural Analysis. In Stephan Jähnichen, editor, *Proceedings of the 8th International Conference on Compiler Construction, Lecture Notes in Computer Science*. Springer.

Florian Martin (1999b). *Generation of Program Analyzers*. PhD thesis, Universität des Saarlandes.

Florian Martin, Martin Alt, Reinhard Wilhelm, and Christian Ferdinand (1998). Analysis of Loops. In Kai Koskimies, editor, *Proceedings of the 7th International Conference on Compiler Construction, Lecture Notes in Computer Science*, 1383. Springer.

David Melski and Tom W. Reps (2000). Interconvertibility of a Class of Set Constraints and Context-Free Language Reachability. *In Theoretical Computer Science*, 248(1–2):29–98.

Ramon E. Moore (1966). *Interval Analysis*. Prentice Hall, Englewood Cliffs, New Jersey, USA.

Bernard M. E. Moret (1982). Decision Trees and Diagrams. *Computing Surveys*, 14(4).

Frank Mueller (1994). Static Cache Simulation and its Applications. Ph. D. Thesis, Florida State University.

Frank Mueller, David B. Whalley, and Marion Harmon (1994). Predicting Instruction Cache Behavior. In *Proceedings of the ACM SIGPLAN 1994 Workshop on Languages, Compilers, & Tool Support for Real-Time Systems (LCT-RTS)*, June 1994, Orlando, Florida, USA.

Sreerama K. Murthy (1998). Automatic Construction of Decision Trees from Data: A Multi-Disciplinary Survey. *Data Mining and Knowledge Discovery*, 2(4).

George L. Nemhauser and Laurence A. Wolsey (1988). *Integer and Combinatorial Optimization*. John Wiley & Sons Ltd., New York City, New York, USA.

Flemming Nielson, Hanne Riis Nielson, and Chris Hankin (1999). *Principles of Program Analysis*. Springer.

Kelvin D. Nilsen and Bernt Rygg (1995). Worst-Case Execution Time Analysis on Modern Processors. In *Proceedings of the ACM SIGPLAN 1995 Workshop on Languages, Compilers, & Tools for Real-Time Systems (LCT-RTS)*, June 1995, La Jolla, California, USA, *SIGPLAN Notices*, 30(11):20–30. ACM.

Greger Ottoson and Mikael Sjödin (1997). Worst-Case Execution Time Analysis for Modern Hardware Architectures. In *Proceedings of the ACM SIGPLAN Workshop on Language, Compiler & Tool Support for Real-Time Systems (LCT-RTS)*.

Chang Yun Park and Alan C. Shaw (1991). Experiments with a Program Timing Tool Based on Source-Level Timing Schema. *IEEE Computer*, 24(5).

David A. Patterson and John L. Hennessy (1994). *Computer Organization & Design: The Hardware/Software Interface*. Morgan Kaufmann.

Stefan M. Petters (2000). Bounding the Execution Time of Real-Time Tasks on Modern Processors. In *Proceedings of the 7th International Conference on Real-Time Computing Systems and Applications (RTCSA)*, December 2000, Cheju Island, South Korea.

Stefan M. Petters and Georg Färber (1999). Making Worst Case Execution Time Analysis for Hard Real-Time Tasks on State of the Art Processors Feasible. In *Proceedings of the 6th International Conference on Real-Time Computing Systems and Applications (RTCSA)*, December 1999, Hong Kong, People's Republik of China.

PowerPC (1997). *PPC403GCX Embedded Controller, User's Manual*. IBM.

Peter Puschner and Christian Koza (1989). Calculating the Maximum Execution Time of Real-Time Programs. *Real-Time Systems*, 1.

Peter Puschner and Christian Koza (1995). Computing Maximum Task Execution Times with Linear Programming Techniques. Technical Report, Technische Universität Wien, Institut für Technische Informatik, Vienna, Austria.

Ganesan Ramalingam (2000). On Loops, Dominators, and Dominance Frontier. In *Proceedings of the ACM SIGPLAN '00 Conference on Programming Language Design and Implementation (PLDI)*, June 2000, Vancouver B.C., Canada, *SIGPLAN Notices*, 36(5):233–241. ACM.

Thomas Ramrath (1997). Entwurf und Implementierung eines Frontends für Analysen zur Vorhersage des Cache- und Pipelining-Verhaltens. Diploma Thesis, Universität des Saarlandes.

Norman Ramsey and Mary Fernandez (1995). The New Jersey Machine-Code Toolkit. In *Usenix Technical Conference*, New Orleans, Louisiana, USA.

Norman Ramsey and Mary Fernandez (1996). *The New Jersey Machine-Code Toolkit, Reference Manual*.

Stuart Russell and Peter Norvig (1995). *Artificial Intelligence, A Modern Approach*. Prentice Hall.

Georg Sander (1994). Graph Layout through the VCG tool. In *Proceedings of the DIMACS International Workshop on Graph Drawing, Lecture Notes in Computer Science*, 894. Springer.

Jörn Schneider and Christian Ferdinand (1999). Pipeline Behaviour Prediction for Superscalar Processors by Abstract Interpretation. In *Proceedings of the ACM SIGPLAN '99 Workshop on Language, Compiler and Tools for Embedded Systems (LCTES)*, May 1999, Atlanta, Georgia, USA, *SIGPLAN Notices*, 34(7):35–44. ACM.

Alexander Schrijver (1996). *Theory of Linear and Integer Programming*. John Wiley & Sons Ltd..

Micha Sharir and Amir Pnueli (1981). Two Approaches to Interprocedural Data Flow Analysis. In Steven S. Muchnick and Neil D. Jones, editors, *Program Flow Analysis: Theory and Applications*, chapter 7. Prentice-Hall.

Martin Sicks (1997). Adreßbestimmung zur Vorhersage des Verhaltens von Daten-Caches. Diploma Thesis, Universität des Saarlandes.

Vugranam C. Sreedhar, Guang R. Gao, and Yong-Fong Lee (1996). Identifying Loops Using DJ Graphs. *ACM Transactions on Programming Languages and Systems (TOPLAS)*, 18(6).

John A. Stankovic (1996). *Real-Time and Embedded Systems*. ACM 50th Anniversary Report on Real-Time Computing Research. http://www-ccs.cs.umass.edu/sdcr/rt.ps.

Friedhelm Stappert, Andreas Ermedahl, and Jakob Engblom (2001). Efficient Longest Executable Path Search for Programs with Complex Flows and Pipeline Effects. In *Proceedings of the 4th International Conference on Compilers, Architectures, and Synthesis for Embedded Systems (CASES)*, November 2001, Atlanta, Georgia, USA.

Henrik Theiling (1998). Über die Verwendung ganzzahliger linearer Programmierung zur Suche nach längsten Programmpfaden. Diploma Thesis, Universität des Saarlandes.

Henrik Theiling (2000). Extracting Safe and Precise Control Flow from Binaries. In *Proceedings of the 7th International Conference on Real-Time Computing Systems and Applications (RTCSA)*, December 2000, Cheju Island, South Korea.

Henrik Theiling (2001). Generating Decision Trees for Decoding Binaries. In *Proceedings of the ACM SIGPLAN 2001 Workshop on Language, Compiler and Tools for Embedded Systems (LCTES)*, June 2001, Snowbird, Utah, USA, *SIGPLAN Notices*, 36(8):112–120. ACM.

Henrik Theiling (2002). ILP-based Interprocedural Path Analysis. In *Proceedings of EMSOFT 2002, Second Workshop on Embedded Software*, October 2002, Grenoble, France.

Henrik Theiling and Christian Ferdinand (1998). Combining Abstract Interpretation and ILP for Microarchitecture Modelling and Program Path Analysis. In *Proceedings of the 19th IEEE Real-Time Systems Symposium (RTSS)*, December 1998, Madrid, Spain, pages 144–153. IEEE Computer Society Press.

Henrik Theiling, Christian Ferdinand, and Reinhard Wilhelm (2000). Fast and Precise WCET Prediction by Separated Cache and Path Analyses. *Real-Time Systems*, 18(2/3).

Caroline Tice and Susan L. Graham (1998). OPTVIEW: A New Approach for Examining Optimized Code. In *Proceedings of the SIGPLAN/SIGSOFT 1998 Workshop on Program Analysis for Software Tools and Engineering (PASTE)*, June 1998, Montreal, Canada, *SIGPLAN Notices*, 33(7). ACM.

Reinhard Wilhelm and Dieter Maurer (1995). *Compiler Design*. International Computer Science Series. Addison Wesley. Second Printing.

Ning Zhang, Alan Burns, and Mark Nicholson (1993). Pipelined Processors and Worst Case Execution Times. *Real-Time Systems*, 5.